New players controlling multidrug resistance and biofilm formation in *C. glabrata*: the important role of *Rpn4*

Mónica da Luz Galocha

Thesis to obtain the Master of Science Degree in
Biotechnology

Supervisor: Prof. Dr. Miguel Nobre Parreira Cacho Teixeira

Co-Supervisor: Dr. Ana Catarina da Silva Portinha e Costa

Examination Committee

Chairperson: Prof. Dr. Isabel Maria de Sá-Correia Leite Almeida

Supervisor: Prof. Dr. Miguel Nobre Parreira Cacho Teixeira

Member of the Committee: Prof. Dr. Nuno Gonçalo Pereira Mira

October 2017

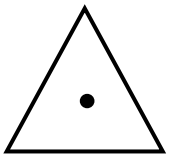

For those I love the most

Acknowledgements

The development of a master project is a challenging and most of the times extensive process, for I would like to acknowledge some personalities who have helped me to accomplish this goal.

First of all, I would like to thank my supervisor, Professor Miguel Teixeira, for the opportunity given by accepting me in his team and in this project. His inexhaustible support, guidance and motivation, as well as the patience showed, were crucial for the success of the work developed in this master thesis. Also, I tank to my co-supervisor, Dr. Ana Catarina Costa, who was always supportive and available regarding the work developed herein.

I would like to thank Professor Isabel Sá-Correia for giving me the chance to join the Biological Sciences Research Group to develop my master thesis work.

My gratitude should also be expressed towards my colleague Pedro Pais, who helped in several steps of my work. His availability and patience were crucial so that I could accomplish this work. Also, I thank my colleague Mafalda Cavalheiro for her inexhaustible support in the lab as well as to all my other lab partners.

The achievement of this thesis required an indispensable help from several parts, which deserve my recognition. For the collaboration in the transcriptomic analysis herein accomplished, I thank Professor Geraldine Butler and her team, from University College of Dublin. For the supply of *Candida glabrata* mutants used in this work, I should thank Professor Hiroji Chibana, from University of Chiba, Japan.

For all the friendship, laughs, study nights and naites, I leave a big thanks to all my friends, in special to Filipe Bica, Mariana Jerónimo, Joana Aldeias, Inês Gonçalves, Carlota Miranda, André Costa and Carolina Gonçalves, that were always present during this important stage of my life.

To my girls, my mates for life, Ana Tavares, Inês Vintém, Catarina Chaparro and Catarina Trindade, a big thank you for your support not now but always.

Without enough words, I thank my boyfriend, André, for his love, patience, support and for always having faith in me. Thank you for always stay by my side.

Most of all, I would like to express my gratitude to my family, specially to my parents, not only for supporting me financially during my studies, but also for all the love and support throughout the course of my life. My lil bro, André, I hope to be always an example for him to follow and a sister he will always be proud of. You all are everything to me, and for that I have no words to say how much I love you.

This work was financially supported by Fundação para a Ciência e Tecnologia (FCT), contract PTDC/BBB-BIO/4004/2014 and UID/BIO/04565/2013.

Abstract

Candida glabrata is the second most common pathogenic *Candida* species and has emerged as a leading cause of nosocomial fungal infections. Its reduced susceptibility to antifungal drugs and unusual ability to sustain proliferate within the human host make it an interesting research focus. However, little is known about the mechanisms underlying the transcriptional control of multidrug resistance and biofilm formation in this pathogen. Herein, a phenotypic study on seventeen uncharacterized *C. glabrata* ORFs, selected based on their amino acid similarity to *S. cerevisiae* or *C. albicans* known transcription factors was carried out in an attempt to identify new players in these processes. Antifungal susceptibility assays and biofilm formation assessment showed that *CgRPN4*, a predicted stimulator of proteasomal genes, is involved in both azole drug resistance and biofilm formation mechanisms. Its subcellular localization assessment through fluorescence microscopy demonstrated nuclear localization of the transcription factor in both cells under control conditions and cells undergoing fluconazole or ketoconazole exposure. The effect of the deletion of *CgRPN4* in *C. glabrata* transcriptome-wide response to fluconazole was also assessed using RNA-seq. CgRpn4 was found to activate the expression of genes involved, for instance, in amino acid metabolism, while repressing, probably indirectly, the expression of genes involved in ribosomal biogenesis and translation. These genes are promising candidates as new players in the context of azole resistance. The analysis of the promoter regions of the Rpn4 activated target genes enabled the identification of two possible parts of the binding site for this transcription factor: GAAGCA and AGTCTA.

Altogether, this study highlights the complexity of the transcription regulatory networks that govern pathogenesis related phenotypes, reinforcing the need to obtain a complete picture of these processes to design more suitable tools to fight fungal infections.

Keywords: *Candida glabrata*, antifungal drug resistance, biofilm formation, *CgRPN4*, RNA-seq approach.

Resumo

Candida glabrata é a segunda espécie patogénica de *Candida* mais comum e emergiu como uma das principais causas de infeções fúngicas nosocomiais. A sua reduzida suscetibilidade a antifúngicos e a capacidade incomum de conseguir proliferar dentro do hospedeiro humano tornam esta espécie um foco de pesquisa interessante. No entanto, pouco se sabe acerca dos mecanismos de regulação transcricional da resistência a múltiplos fármacos e da formação de biofilme neste patógeno. Neste estudo, foi realizada uma análise fenotípica a dezassete genes não caracterizados de *C. glabrata* no âmbito de identificar novos intervenientes nestes dois processos importantes para a virulência. Os genes foram selecionados com base na sua similaridade de aminoácidos com fatores de transcrição conhecidos de S*. cerevisiae* ou *C. albicans*. Os ensaios de suscetibilidade a antifúngicos e a quantificação de biofilme revelaram o envolvimento do gene *CgRPN4*, previsto como ativador de genes proteossómicos, nos mecanismos de resistência a azóis e formação de biofilme. Através de microscopia de fluorescência, constatou-se que CgRpn4p tem localização nuclear tanto em células em condições controlo como em células expostas a fluconazole ou ketoconazole. O efeito da deleção do gene *CgRPN4* no transcriptoma de *C. glabrata* em resposta ao fluconazole também foi avaliado, através de RNA-seq. Os dados mostraram que este gene está envolvido na ativação de genes associados a diferentes grupos funcionais, por exemplo no metabolismo de aminoácidos, e na repressão, provavelmente indireta, de outros, por exemplo envolvidos na biogénese do ribossoma e tradução. Este conjunto de genes são candidatos promissores no contexto do mecanismo de resistência azóis. A análise das regiões promotoras dos genes alvo ativados pelo CgRpn4 permitiu a identificação de duas possíveis partes de locais de ligação para este fator de transcrição: GAAGCA e AGTCTA.

Em suma, este estudo destaca a complexidade das redes regulatórias de transcrição que controlam os fenótipos relacionados à patogénese, reforçando a necessidade de obter uma imagem completa desses processos para projetar ferramentas mais adequadas para combater infeções fúngicas.

Palavras-chave: *Candida glabrata*, resistência a antifúngicos, formação de biofilme, *CgRPN4*, RNA-seq.

Contents

List of figures

Figure 4. 2. | Model of *CgRPN4* regulation and action in *C. glabrata*. Azole drug exposure activates the pleiotropic drug resistance regulator *CgPDR1*, which besides regulates its own expression induces the expression of drug transporters such as ABC transporters (black arrows). Recently, it was demonstrated that *CgYAP1* also induce the expression of multidrug transporters, besides being the major known oxidative stress response regulator in *C. glabrata.* These two drug responsive genes, activates the expression of the predicted transcription factor *CgRPN4* (black arrows) which is predicted to activate proteasomal genes, such as in *S. cerevisiae*. In turn, the assembled proteasome degrades CgRpn4, in order to maintain a negative feedback loop (dark blue dashed line) to control proteome homeostasis and expression of Rpn4 target genes. Herein, a screening to analyse CgRpn4 targets in response to fluconazole was performed for the first time, through RNA-seq approach. Several genes belonging to different functional clusters involved in different cellular processes were found to be regulated by CgRpn4 (light blue bracket) in response to fluconazole. This represents the first step to unveil the mechanism through which CgRpn4 expression influences *C. glabrata* resistance toward azole antifungals. 62

List of tables

Acronyms

5-FU – 5-fluoruacil;

ABC - ATP-binding cassette;

AIDS – Immunodeficiency syndrome;

ARE – Azole-responsive enhancer;

CDR – *Candida* drug resistance genes;

CGD – *Candida* Genome Database;

CHS – Chitin synthase;

DRE – Drug responsive element;

ECM - Extracellular Matrix;

GOF – Gain-of-function;

HOG – High-osmolarity glycerol pathway;

MAPK - Mitogen-activated protein kinase;

MDR – Multidrug resistance genes;

MFS – Major facilitator superfamily;

MIC – Minimal Inhibitory Concentration;

MMB – Minimal Medium. Contains (per liter): 1.7 g of yeast nitrogen base without amino acids or NH4+ (Difco), 5 g of glucose (Merck), 1 g of galactose (Sigma) and 2.7 g of (NH4)2SO4 (Merck);

MMB-U – Minimal Medium supplemented with 20 mg/L histidine, 20 mg/L methionine and 60 mg/L leucine;

MMG-U – Minimal Medium supplemented with 60 mg/L leucine;

MTL – Mating-type-like;

NAC - Non-*albicans Candida*;

OPC – Oropharyngeal candidiasis;

PACE – Proteasome Associated Control Element;

PDRE – Pdr Responsive Elements;

PKC – Protein kinase C;

ROS – Reactive Oxygen Species;

RPMI 1640 – Roswell Park Memorial Institute Medium. Contains (per 300 mL): 6.24 g RPMI 1640 (Sigma), 20.72 g MOPs (Sigma) and 10.8 g glucose (Merck);

SDB - Sabouraud Dextrose Broth Medium. Contains (per liter): 80 g glucose (Merck) and 20 g meat peptone (Merck);

SIR – Silent information regulator;

SGD – *Saccharomyces* Genome Database;

TF – Transcription Factor;

YPD - Yeast extract –Peptone–Dextrose medium. Contains (per liter): 20 g of glucose (Merck), 20 g of bacterial peptone (Dickson) and 10 g of yeast extract (Merck);

YRE – Yap Responsive Element;

Introduction

1.1. Thesis outline

This dissertation is organized in five chapters. The first chapter offers an overview on the increasing relevance of the opportunistic pathogenic yeast *Candida glabrata*, followed by some insight into the currently used families of antifungal drugs in clinical practice, together with their modes of action. Special attention is given to azoles and echinocandins, two of the main families of drugs presently used, with information concerning modes of action and resistance mechanisms. The importance of biofilm formation for *Candida's* virulence is also addressed, along with the transcriptional control underlying this phenomenon unveiled until now. Lastly, the role and regulation of *RPN4* transcription factor in the closely related yeast *S. cerevisiae* is overviewed. In *C. glabrata*, little is known about this putative transcription factor function. However, concerning the prelaminar results obtained in the phenotypic study, its functional analysis was undertaken further on.

The second chapter contains all the materials and methods used during the fulfillment of this work.

The third chapter describes the results attained with this study, comprising the phenotypic screening on seventeen *C. glabrata* ORFs predicted to be transcription factors based on amino acid similarity with *S. cerevisiae* and *C. albicans* known transcription factors involved in these organisms' multidrug resistance and oxidative stress response, and multidrug resistance and biofilm formation, respectively. In order to assess the function of the seventeen predicted transcription factors on *C. glabrata* multidrug resistance and biofilm formation parameters, single deletion mutants for each ORF were analysed. Based on these results, the functional characterization of the predicted proteasomal activator, CgRpn4, and its role in resistance to azoles, fluconazole and ketoconazole, is described. The results achieved include study the effect of the deletion of this predicted transcription factor, as well as its overexpression in *C. glabrata* azole drug susceptibility, as well as its capability to complement the absence of its *S. cerevisiae* homolog, *ScRPN4*, in BY4741_*Δrpn4* mutant cells. Additionally, its subcellular localization was assessed. This chapter also includes a RNA-seq analysis of the *CgRPN4* deletion effect on the transcriptome-wide response toward mild fluconazole-induced stress conditions.

In the fourth chapter, the results obtained with this project are discussed and compared with the current knowledge. A model of CgRpn4 activation and action is hypothesized.

In the fifth and last chapter, final remarks considering the work developed and future perspectives are made, together with references to what contributions this work offered in the comprehension of acquired resistance mechanisms in *C. glabrata*.

1.2. Candidiasis

Infections caused by fungal pathogens have become a relevant threat to human health as their prevalence has continuously increased over the past decades [1]. *Candida* species are the most common opportunistic fungal pathogens in humans, causing an infection, called candidiasis, that may be mucosal or systemic. Mucosal candidiasis is very frequent and occurs chiefly in oral, gastrointestinal and vaginal mucosae. Systemic candidiasis is not so common, but it is associated to a high mortality rate [2].

The cause of infection relies in several aspects. However, the health of the patient is often an important issue to consider. *Candida* is present in the mouth of up to 60% of healthy people, but oropharyngeal candidiasis (OPC) may arise associated with immunosuppression, diabetes, broad-spectrum antibiotics, corticosteroid use, haematinic deficiencies, and denture wear [3]. This infection is characterized by a burning pain and odynophagia [1], and 80 to 90% of patients with Immunodeficiency Syndrome (AIDS) develop OPC [2].

In immunocompromised patients, esophageal candidiasis is more common than OPC. The esophageal candidiasis has as symptoms dysphagia, odynophagia and retrosternal chest pain within the patients [4].

Vulvovaginal candidiasis is another type of mucosal candidiasis which corresponds to the second most frequent vaginal infection after bacterial vaginosis. Development of symptomatic vulvovaginal candidiasis probably represents increased growth of yeast that previously colonized the vagina without causing symptoms. Risk factors for vulvovaginal candidiasis include pregnancy, diabetes mellitus, and systemic antibiotics with *Candida albicans* accounting for 85% to 90% of cases [5].

Another niche of infection is the urinary tract. *Candida* species cause urinary tract infection by either the hematogenous or ascending routes. Most kidney infection occurs by hematogenous seeding during an episode of candidemia, but this event is usually asymptomatic regarding urinary tract symptoms [6].

The chronic infections of candidiasis frequently result from the overuse of antifungal agents and repeated antifungal therapies that result in increased resistance of the strains responsible for the infection [7].

Unlike infections in the mouth, throat or vagina, which are localized to one part of the body, systemic or invasive candidiasis can affect the blood, heart, brain, eyes, bones, or other parts of the body. *Candida* normally lives in the gastrointestinal tract and on skin without causing any problems [8]. However, in certain patients who are at risk, *Candida* can enter the bloodstream and cause an infection leading to diverse clinical manifestations, from low-grade fever to fulminant septic shock. Thus, candidemia translates into high mortality rates, those promoted by the lack of fast and precise diagnostic tools or inefficient antifungal therapies [2]. Additionally, the development of systemic infection usually occurs due to the presence of medical devices. *Candida spp*. systemic infections arise mostly from implantable cardioverter defibrillators, vascular catheters, cardiac devices, prosthetic valves and urinary catheters [9]. This type of devices enhances biofilm formation which increases cells resistance to

administered antimicrobial agents, since the formed extracellular matrix (ECM) interfere with their diffusion.

The large variety of sites of possible *Candida* infections - including vaginal, oral, urinary tract or disseminated infections – appears to correlate with its ability to sustain long-term carbon and iron starvation upon phagocytosis by macrophages, as well as to proliferate in a low-pH environment in the vaginal mucosa or in phagolysosomes, to tolerate nitrosative and oxidative stresses, and relatively hypoxic conditions, encountered by this pathogen in some of the host niches it occupies, such as the periodontal space or intestine [10].

Candida albicans remains the predominant causative agent of all forms of candidiasis [3]. Epidemiological data, however, indicate the growing role of non-*albicans Candida* (NAC) species as causative agents of nosocomial invasive candidaemias, altogether surpassing *C. albicans* [4], [5]. Most infections attributed to NAC are caused by *Candida glabrata*, *Candida parapsilosis* and *Candida tropicalis*. This changing epidemiology and shift towards species characterized by elevated minimal inhibitory concentrations (MIC) of azoles, as compared with *C. albicans*, reflects their widespread use and prolonged prophylaxis in the growing population of high-risk patients [6]. The evolved antifungal drug resistance and virulence factors characteristic of fungal pathogens, combined with their great potential to develop antifungal resistance, account for the observed epidemiology [3].

1.3. *Candida glabrata*

Candida glabrata, formerly named as *Cryptococcus glabratus*, was described in 1917 as a component of the human gut microbiota ([11]; reviewed in [12]). Years later, it started to be identified as the source of several infections either named as *Cryptococcus glabratus* [13], or as *Torulopsis glabrata* [14], due to its lack of pseudohyphae. In the late 1980's, already renamed as *Candida glabrata*, it began to be commonly identified as the etiological agent of candidaemia in immunocompromised patients, and later on was recognized as an emergent pathogen [15].

The genome of *C. glabrata* (CBS138/American Type Culture Collection, ATCC2001) was sequenced, showing that this species shares a common ancestor with *Saccharomyces cerevisiae* [16] (Figure 1.1.). The first has lost many more genes than *S. cerevisiae* upon the Whole Genome Duplication event, decreasing traces of duplication to a minimum and leading to the complete loss of some metabolic pathways [2]. Although it has reserved homology with the *S. cerevisiae* mating pathway genes, several deficiencies having been identified and *C. glabrata* is strictly haploid [17]. Additionally, *C. glabrata* has lost some genes required for galactose (*GAL1, GAL7, GAL10*), phosphate (*PHO3, PHO5, PHO11, PHO12*), allantoin (*DAL1, DAL2*), sulfur (*SAM4*), and pyridoxine metabolism (*SNO1, SNO2, SNO3*) [18, 19]. The natural auxotrophy of *C. glabrata*, such as the inability to synthesize nicotinic acid, pyridoxine, and thiamine, and the inability to use galactose [18], is generally compensated by the mammalian host environment. Moreover, expansion of genes involved in cell wall organization occurred in *C. glabrata*, possibly facilitating adherence to a broad spectrum of surfaces.

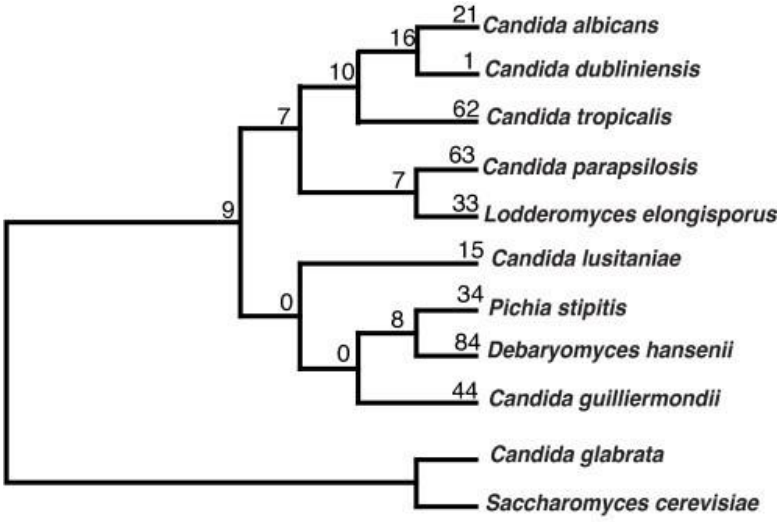

Figure 1. 1. | Phylogenetic supertree of *Candida* species represented in CGOB. *Candida glabrata* and *Saccharomyces cerevisiae* have been selected as outgroups. Numbers on branches represent tandem duplications gained along each lineage. Adapted from Fitzpatrick *et al.* (2010) [20].

Candida glabrata general features are displayed in Table 1.1.. It contrasts with other *Candida* species in its nondimorphic blastoconidial morphology and haploid genome, but, although this yeast does not exhibit a sexual stage, it has several genes associated to mating and meiosis. Chromosomal alterations, such as chromosome loss, translocations and aneuploidy, have been reported in *C. glabrata,* which suggests that this yeast, although lacking a sexual cycle, can have an impressive clonal population diversity [15].

C. glabrata live as commensals on mucosal surfaces, where they are a constituent of the normal microbiome [7], [8]. However, under suitable conditions it may turn into an opportunistic pathogen. This pathogen affects mostly immunocompromised individuals, including HIV-infected people, transplant recipients, patients undergoing chemotherapy for cancer, very old people or very young children, as well as diabetics.

Despite the lack of hyphae development and of fully characterized virulence factors, mortality rates associated to candidaemia are higher in *C. glabrata* than in *C. albicans* infections, with an average mortality rate of 50% (30%-80%) [21]. Indeed, switching to hyphal growth is a known virulence mechanism in *C. albicans*, which enables it to be more invasive and escape macrophage engulfment [22]. But notably, it has been demonstrated that *C. glabrata* lets itself to be taken up by macrophages, where it can persist for long periods of time and even divide [23]. It is capable of detoxifying radical oxidative species and seems to be able to disrupt normal phagosomal maturation, leading to the inhibition of phagolysosome formation and phagosome acidification [24]. Additionally, *C. glabrata* genome encodes a large group of putative glycosylphosphatidylinositol (GPI)-anchored cell wall proteins, such as those of the epithelial adhesin (EPA) and yapsins (YPS) families, which play a crucial role in the process of interaction with host tissues [25]. The overall structure of EPA proteins is similar to that of the ALS (agglutinin-like sequence) proteins of *C. albicans.*

According to the MetaPhOrs orthology database [26], 1557 (29.5%) *C. glabrata* protein-coding genes lack an ortholog in *C. albicans*, and the reverse is true for 2257 (36.3%) *C. albicans* genes. Thus,

large physiological differences are expected simply due to the intrinsically different genetic background of both species.

Table 1. 1. | Characterization of *Candida glabrata* general features. Adapted from Rodrigues *et al.* (2014) [27].

Feature	*C. glabrata* characteristics
Ploidy	Haploid
Hyphae/pseudohyphae	Absent
Cell size	1-4 µm
Biochemical reactions	Ferments and assimilates glucose and trehalose
Major sites of infection	Vaginal, oral, disseminated
Biofilm formation	Yes
Major adhesins	Lectins
Mating genes	Present
Auxotrophy	Niacin, thiamine, pyridoxine
Epidemiology of infection	Mainly nosocomial (except vaginal); Immunocompromised or debilitated host; Specific risk factors: prolonged hospitalization, prior antibiotic use, use of fluconazole, patient exposure.

In addition, even if corresponding orthologs are present, their function may have diverged to an extent that it may affect its role in virulence. This may be especially true for versatile proteins such as transcription factors and other regulators than can easily rewire its network of targets. An exemplary such case is provided by the finding that null mutants in the transcription factor Ace2, that is known to be involved in cell separation and adherence [28], had slightly attenuated virulence in *C. albicans*, whereas they are hypervirulent in *C. glabrata* [29]. All these considerations underscore the fact that *C. glabrata* seems to use quite different mechanisms for virulence.

Given the large differences between *C. albicans* and *C. glabrata*, it was soon realized that the closer relative model yeast *S. cerevisiae* would be a much better source of information (Figure 1.1.). Indeed, the number of *C. glabrata* genes without ortholog in *S. cerevisiae* is more limited (446 genes, representing 8.6% of the gene repertoire) and thus the physiology of these two species is expected to be more conserved [30]. Grossly, the main differences between *C. glabrata* and *S. cerevisiae* that were interpreted as adaptation to the human host in the former are: (i) the optimal growth temperature close to 37°C, (ii) higher stress resistance and enhanced ability to sustain prolonged starvation as compared to *S. cerevisiae*, (iii) its genome has remodeled the cell-wall components, resulting in a higher adherence, (iv) it has lost more genes than *S. cerevisiae* from its common ancestor, meaning that it may have a higher dependence on the host (Table 1.2.) Genome reduction is a general consequence of commensal and pathogenic lifestyles [31]. In *C. glabrata*, the 5202 protein-coding gene collection is 'only' 688 genes smaller than that of *S. cerevisiae*, which represents a relative size reduction of 11.7%. Nevertheless, the nature of some of the losses points to a possible higher dependence on the host to overcome auxotrophies such as those of pyridoxine, thiamine and nicotinic acid [19].

Table 1. 2. | Relevant virulence traits in *C. glabrata*. Adapted from Gabaldón & Carreté (2016) [30].

Trait of *C. glabrata*	**Relevance for virulence**
Growth at 37℃	Standard body temperature
High stress resistance	Response to stresses present in human tissues and related to immune system
Resistance to starvation	Allows survival within macrophages
Drug resistance	Resistant to commonly used azole drugs
High adherence	Adhesion to human tissues, clinical material, formation of biofilms
Presence of several auxotrophies	May be related to a higher dependence on the host

C. glabrata is responsible for 7 to 20% of all the infections caused by *Candida* species, depending on the geographical locations, which makes it the second most prevalent [32]. Indeed, cases of systemic and superficial candidiasis have been found to increase mostly due to *C. glabrata*. This increase has been associated with the resistance of this species to the antifungal agents administered as a treatment for candidiasis, particularly to azoles [33] which are very effective in eradicating infections caused by other *Candida* species. Thus, the treatment of *C. glabrata* infections often requires the use of echinocandins [34], which have recently become the first option in the treatment of invasive candidiasis caused by *C. glabrata*, being especially important in the case of the harder-to-treat biofilm-derived infections [35].

Given the increasing number of immunocompromised patients and increasing antifungal drug resistance, especially exhibited by *C. glabrata*, there is an urgent need for the development of new effective treatments. Better understanding of basic fungal biology and pharmacotherapy adaptation mechanisms, are facilitated by progress in new technologies. Nonetheless, the regulation of transcriptional networks is complex and presents significant variations among different fungal pathogens, either in terms of regulators themselves or their regulatory targets [36]. The study of regulatory circuits should therefore be a prime strategy in the fight against fungal infections, allowing to develop better diagnostic and treatment approaches according to each pathogen's conserved or specific pathways. In order to overcome drug resistance, it is essential to understand the structure of the transcription networks regulating this phenomenon, as it implies a complex regulatory circuit in order to activate the most appropriate response according to distinct stimuli.

1.4. Antifungal drugs

Antifungals are drugs used to treat infections caused by fungi which can be divided in two groups according to their effects: fungicidal or fungistatic agents. Fungicides are substances that are able to kill fungi or fungal spores, whereas fungistatic agents are capable of inhibiting the growth and reproduction of fungi without destroying them [37].

There are 5 major classes of antifungal agents developed until today, they include: polyenes, fluorinated pyrimidines, azoles, allylamines, and echinocandins [38]. These compounds have different

mechanisms of action, targeting different molecules and disrupting different processes inside the cells (Figure 1.2. and Table 1.3.).

Mechanisms of antifungal resistance can be primary (intrinsic) or secondary (acquired). Primary or intrinsic resistance is found naturally among certain fungi without prior exposure to the drug. Resistance of *Candida krusei* to azole drugs is an example of intrinsic resistance [39]. On the other hand, secondary or acquired resistance develops among previously susceptible strains after exposure to the antifungal agent and is many times dependent on altered gene expression. The development of fluconazole resistance among *Candida albicans* and *C. neoformans* strains illustrates this type of resistance [32].

Antifungal resistance is both complex and multifaceted. It can be inducible in response to a compound or be an irreversible genetic change resulting from prolonged exposure. In detail, these include alterations or even an overexpression of target molecules, active extrusion through efflux pumps, limited diffusion, tolerance, and cell density, which are all characterized mechanisms utilized by fungi to combat the effects of antifungal treatments [40]. Planktonic cells generally rely on irreversible genetic changes to maintain a resistant phenotype, whereas biofilm cells are able to persist due to their physical presence and the density of the population, which provides an almost inducible resistant phenotype irrespective of defined genetic alterations.

C. glabrata presents higher levels of intrinsic resistance to azoles than *C. albicans* and develops further resistance during prolonged azole therapy. In fact, previous studies reported that the average fluconazole MIC for *C. glabrata* was 32-fold higher than for *C. albicans* [41]. Since *C. glabrata* grows only as yeast form *in vivo* and its adhesion is relatively weak [42], it is believed that the increase of infections caused by this pathogen is due to its intrinsically low susceptibility to azoles, as well as polyenes, echinocandins [33].

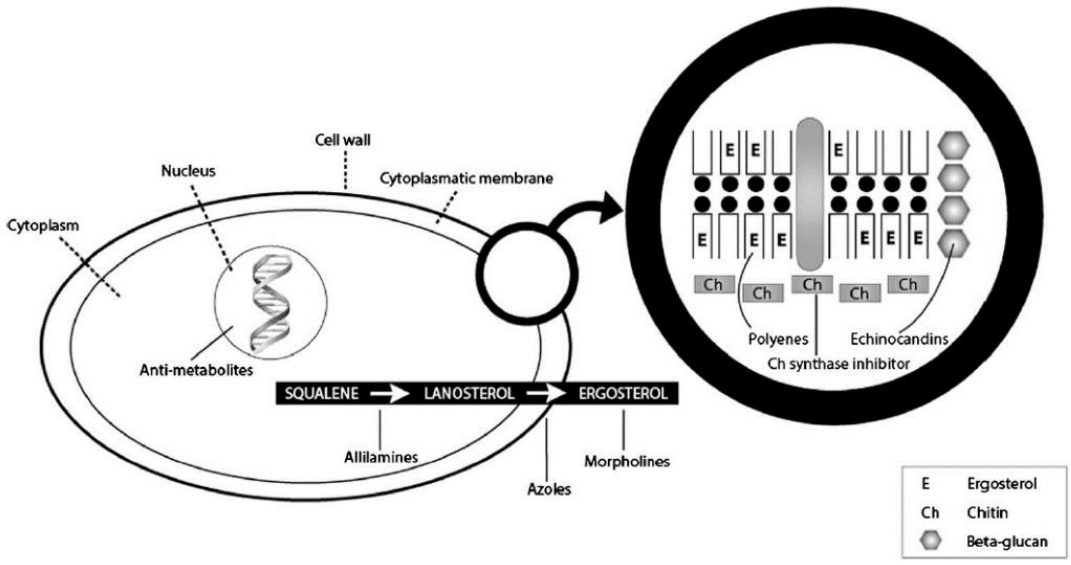

Figure 1. 2. | Mechanisms and sites of action of antifungal drugs. Adapted from Rodrigues *et al.* (2014) [27].

Table 1. 3. | Mechanisms of action and resistance of different antifungal drugs. From: www.basicmedicalkey.com.

Drug	Mechanism of action	Mechanism of resistance
Amphotericin B (polyene)	Binds to ergosterol in fungi membranes to form pores and increase membrane permeability.	Replacement of ergosterol with precursor sterols.
Flucytosine (fluorinate pyrimidine)	Converted in fungi to 5-fluorouracil (5-FU), which is incorporated into RNA and inhibits nucleic acid synthesis resulting in cell death.	Loss of the fungal permease necessary for cytosine transport or decrease in fungal cytosine deaminase activity.
Imidazoles and Triazoles	Perturbation of fungal membrane through the impaired ergosterol synthesis due to inhibition of 14-α-sterol demethylase, leading to the accumulation of lanosterol.	Mutation in *ERG11*, the gene coding for the 14-α-sterol demethylase.
Allylamines	Inhibition of fungal squalene epoxidase, blocking ergosterol biosynthesis, leading to disruption of fungal cell membrane.	Mutations in squalene epoxidase.
Echinocandins	Inhibition of 1,3-β-D-glucan synthesis in fungal cell wall resulting in loss of structural integrity, osmotic instability, and cell death.	Mutations in glucan synthase complex genes.

1.4.1. Azoles

Azoles are a group of fungistatic agents with broad-spectrum activity. They are classified into two groups: the triazoles (fluconazole, itraconazole, voriconazole and posaconazole) and the imidazoles (clotrimazole, miconazole, tioconazole, econazole and ketoconazole). These drugs belong to a class of five-membered heterocyclic compounds containing a nitrogen atom and at least one other non-carbon atom (i.e. nitrogen, sulphur, or oxygen) as part of the ring (Figure 1.3.) [43]. Azoles inhibit fungal growth by binding to the cytochrome P450 dependent enzyme lanosterol 14-α-sterol-demethylase encoded by *ERG11* gene in yeasts, which coverts lanosterol to ergosterol, the main sterol in fungal cell membranes (Figure 1.4.). Depletion of ergosterol damages the cell membrane resulting in defective structural properties, loss of fluidity and

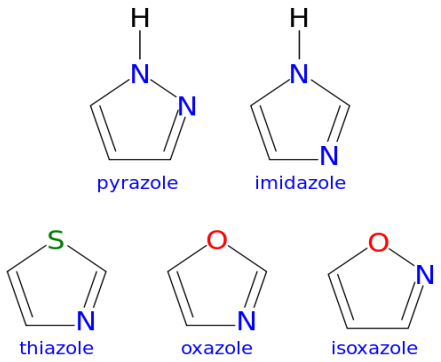

Figure 1. 3. | Basic azole compounds structure. Adapted from en.citizendium.org.

altered functions such as signalling, transport, exocytosis and endocytosis. Moreover, inhibition of Erg11p activity leads to the accumulation of a toxic sterol produced by *ERG3* [39], [44].

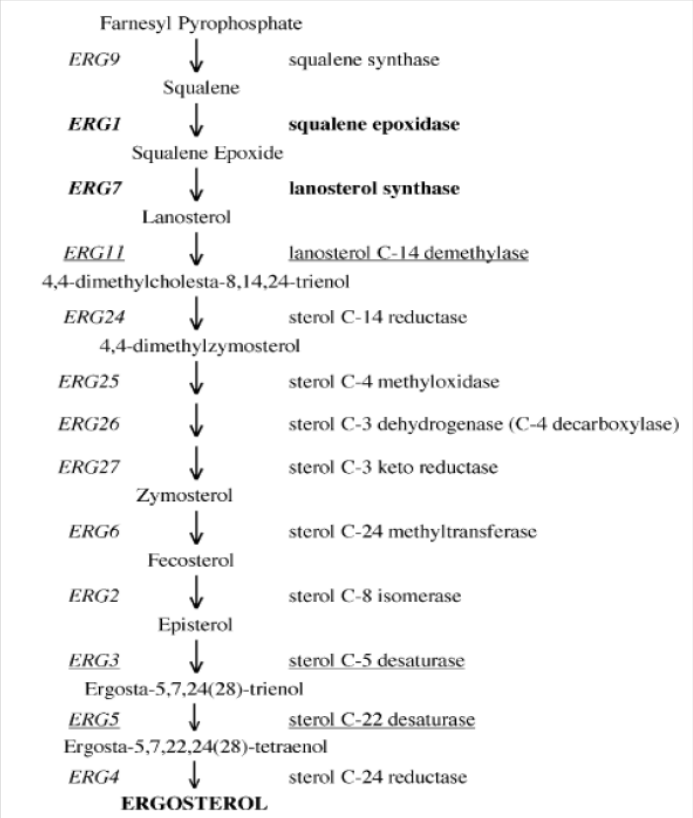

Figure 1. 4. | Ergosterol biosynthesis pathway. Adapted from M. Brad *et al.* (2005) [45].

Azoles differ in their affinities to their target, which may account for differences in their spectrum of activity. It is known that the long side chain of posaconazole and itraconazole results in tighter affinities to their target-protein by making extensive hydrophobic contacts along their entire lengths, suggesting that side chain has a significant role concerning the drug activity. On the contrary, compact azoles without extended side chains, such as fluconazole or voriconazole, display less affinity to their target and consequently they have the tendency to be less effective and more easily affected by acquired resistance strategies [46].

In recent decades, the increasing frequency of life-threatening fungal infections has been accompanied by an increase in the prophylactic use of azoles for high-risk individuals due to concerns of developing fungal infections or to treat patients who have already acquired fungal disease [47]. This widespread deployment of azoles coupled with the fungistatic nature of these drugs has led to the emergence of azole resistance in clinical isolates [48]. Canonical mechanisms of azole resistance in *Candida* species, identified in clinical isolates and experimental populations, include alterations of the drug target Erg11p, overexpression of multidrug transporters, and the development of bypass pathways (Figure 1.5.).

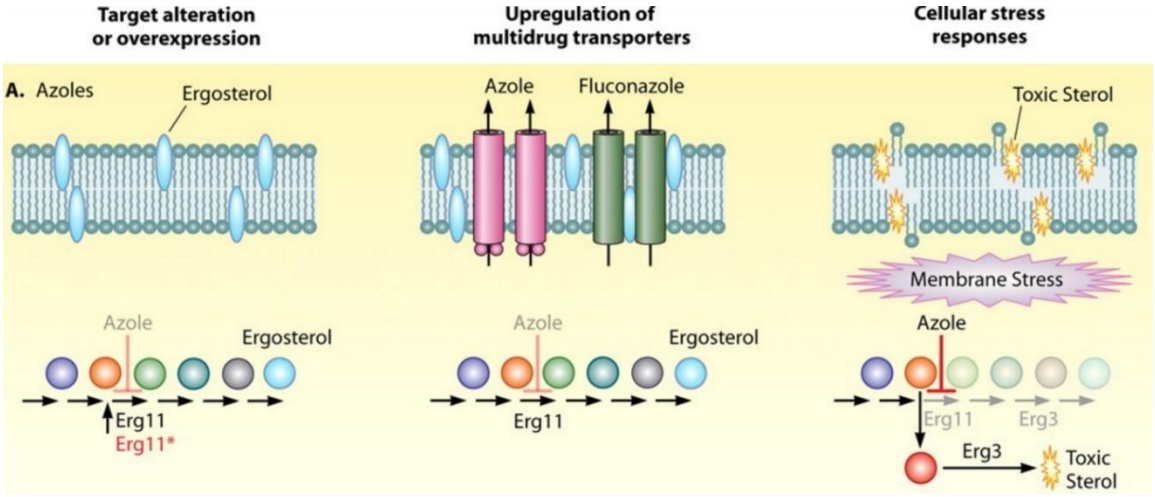

Figure 1. 5. | Candida drug resistance mechanisms. Acquired resistance to azoles through upregulation or alteration of the drug target Erg11p; upregulation of multidrug transporters; or induction of numerous cellular responses. Adapted from Shapiro *et al.* (2011) [47].

1.4.1.1 Azole resistance mechanisms in *C. albicans* and *C. glabrata*

1.4.1.1.1 Alteration of drug target

The alteration of the drug target can be achieved through mutation or overexpression. The three-dimensional structure of *C. albicans* Erg11p was previously modelled and residues that are important for its interaction with azoles were predicted [49]. In fact, more than 80 amino acid substitutions in Erg11p have been detected in azole resistant *C. albicans* clinical isolates [50], meaning that individual mutations in *ERG11* gene can confer azole resistance by decreasing drug binding affinity.

On the other hand, the overexpression of *ERG11* has also been documented for *C. albicans* clinical isolates, although it is often accompanied by other alterations [51]. In populations of *C. albicans* evolved in the presence of fluconazole, resistance was found to be acquired by distinct overexpression patterns of four genes which are important for fluconazole resistance, including *ERG11* [52]. Higher intracellular concentration of Erg11p results in reduced susceptibility to azoles since, as result of the increased number of target molecules, the antifungal agent can no longer be effective in inhibiting ergosterol synthesis when administrated in routine therapeutic concentration. *ERG11* overexpression can be achieved through mutations in the transcription factor regulating its expression, Upc2p. This transcription factor upregulates *ERG11* expression in response to azoles by binding to the azole-responsive enhancer element (ARE), a region localized to two distinct 7-bp sequences at positions −224 to −251 in the *ERG11* promoter [53, 54], thus contributing to azole resistance. Additionally, it also binds to two distinct regions in its own promoter to autoregulates its own expression during azole exposure [55]. Furthermore, G648D and G643A point mutations in *UPC2* gene cause hyperactivation of the transcription factor, resulting in the overexpression of ergosterol biosynthesis genes and increased fluconazole resistance. These mutations have been identified in *C. albicans* clinical isolates [56].

1.4.1.1.2 Overexpression of multidrug transporters

Overexpression of multidrug transporters results in a decrease of drug concentration inside the cell, leading to a decrease in susceptibility. Efflux pumps in *C. albicans* are encoded by *Candida* Drug Resistance (CDR) genes of the ATP-binding Cassette (ABC) family and by Multidrug Resistance (MDR) genes of the Major Facilitator Superfamily (MFS). While *CDR* genes upregulation confers resistance to all azoles, MFS-encoded transporters were described to have a narrower spectrum of activity [39].

CDR1 and *CDR2*, from the ABC transporter superfamily, contain two membrane-spanning domains and two nucleotide binding domains that utilize ATP to drive substrates across the membrane [57]. It was shown that *C. albicans CDR1* homozygous deletion mutant was hypersensitive to azoles, whereas *CDR2* homozygous deletion mutants were not [58, 59]. However, the combined deletion of both *CDR1* and *CDR2* resulted in an increased hypersensitivity compared to the deletion of *CDR1* alone, suggesting that *CDR2* contributes to azole resistance too [58]. Furthermore, many azole-resistant clinical isolates have up to a 10-fold increase in *CDR1* expression as well as an increase in *CDR2* expression [60].

In *C. albicans*, the expression of *CDR1* and *CDR2* is regulated by the transcription factor *TAC1*, which binds to a distinct *cis* sequence, termed the drug response element (DRE), found in their promoters (Table 1.4.) [61]. *TAC1* is located on chromosome 5 along with *ERG11* and the *MTL* (*mating-type-like*) locus, and homozygosity at the *TAC1* locus is often associated with homozygosity at the *MTL* and *ERG11* loci [62]. It was recently proposed, based on five groups of related isolates containing azole-susceptible and azole-resistant counterparts, that isolates acquired mutations conferring azole resistance in a predictable, sequential order: a gain-of-function mutation at *TAC1* along with mutations in *ERG11*, followed by a loss of heterozygosity of *TAC1* and *ERG11* and, finally, by the formation of [i(5L)] (left arm of chromosome 5), resulting in an increased copy number of azole resistance genes [63]. Additionally, genome-wide studies were recently conducted to identify other Tac1p-dependent genes in addition to *CDR1* and *CDR2*. Eight genes whose expression was modulated in a Tac1p-dependent manner and whose promoters were bound by *TAC1* were identified [64]. Among these genes were *GPX1*, encoding a putative glutathione peroxidase; *LCB4*, encoding a putative sphingosine kinase; and *RTA3*, encoding a putative phospholipid flippase. This suggests that the regulation of genes involved in other signalling pathways, such as oxidative stress responses and lipid metabolism, may play important roles in Tac1p-mediated azole resistance.

The second main class of multidrug transporters that plays an important role in azole resistance is the MFS. These drug pumps have no nucleotide binding domain but instead use the proton motive force of the membrane as energy source [57]. In *C. albicans*, *MDR1* is a MFS gene involved specifically in resistance to fluconazole rather than other azoles, being overexpressed in fluconazole-resistant isolates [60]. The multidrug resistance regulator (encoded by *MRR1*) is the transcription factor that controls the expression of *MDR1* and is also upregulated in drug-resistant clinical isolates (Table 1.4.) [65]. In fact, in clinical and *in vitro*-generated *C. albicans* strains that are fluconazole resistant due to increased levels of *MDR1* expression, gain-of-function mutations in *MDR1* are also present (Figure 1.6.) [66]. Much like Tac1p, Mrr1p appears to have other targets besides drug efflux pumps, including

oxidoreductases [65]. Such targets may help prevent drug-induced cell damage that results from the generation of toxic molecules in response to azole exposure. This also suggests that multiple pathways are critical in order for the cell to survive the stress associated with azole exposure.

Like in *C. albicans*, efflux pump expression in *C. glabrata* is induced by xenobiotics, including azoles [67]. Efflux pump-mediated drug resistance in clinical *C. glabrata* isolates is caused by overexpression of the ABC transporters Cdr1p, Cdr2p, and Snq2p, and the same was observed in laboratory-generated fluconazole-resistant strains.

C. glabrata is phylogenetically closer to *S. cerevisiae* than *C. albicans*, which has facilitated the dissection of multidrug resistance mechanisms in this species. Homologs of the *S. cerevisiae* ABC transporters genes *PDR5* and *SNQ2*, designated as *CgCDR1* and *CgCDR2*, and *CgSNQ2*, respectively, have been identified in *C. glabrata*. In fact, the deletion of *CgCDR1* in an azole-resistant *C. glabrata* strain resulted in an increase of intracellular fluconazole accumulation and hypersusceptibility to different azoles, and the additional deletion of *CgCDR2* further increased the susceptibility of the double mutants [68]. Deletion of *CgSNQ2* in another azole-resistant *C. glabrata* strain also resulted in increased susceptibility to different azoles [69], demonstrating that all three ABC transporters mediate azole drug resistance in *C. glabrata*.

Pdr1p is known to be one of the major pleiotropic drug resistance regulators in yeast, both in *S. cerevisiae* and in *Candida glabrata*, by controlling the expression of genes responsible for multidrug resistance phenotypes [70]. The *C. glabrata* genome sequence contains a single homolog of the *S. cerevisiae* zinc cluster transcription factors *PDR1* and *PDR3*, which regulate the expression of various efflux pumps in this organism. Pdr1p has been found to form a heterodimer with Stb5p in *S. cerevisiae*. Transcriptional analysis signposted a shared regulon among the homologs of these two genes, *PDR1* and *STB5*, in *C. glabrata*, and many of the genes upregulated by the overexpression of *PDR1* were also upregulated by the deletion of *STB5*. Thus, *PDR1* overexpression and *STB5* deletion appear to be correlated. The overexpression of *CgSTB5* in *C. glabrata* represses azole resistance, while the deletion of *CgSTB5* produces a shy intensification in resistance. Expression analysis assays established that Stb5p shares many transcriptional targets with Pdr1p but, unlike the second, it is a negative regulator of pleiotropic drug resistance (including the ABC transporter genes *CDR1*, *PDH1*, and *YOR1*) [71].

Inactivation of *CgPDR1* resulted in reduced *CgCDR1*, *CgCDR2* and *CgSNQ2* expression and increased susceptibility to azoles and other drugs, whereas *CgPDR1* overexpression causes a strong upregulation of the efflux pumps and increased drug resistance (Table 1.4.) [69]. *CgCDR1* and *CgCDR2* promoter regions share a putative binding site for a Pdr1p/Pdr3p-like transcription factor, and both genes are induced by azole treatment and are concomitantly upregulated in many clinical and *in vitro* generated azole-resistant *C. glabrata* strains [67]. Some of these strains also overexpressed *CgSNQ2*, which contains as well a Pdr1p/Pdr3p binding site in its promoter region, whereas others overexpressed only one or two of the efflux pumps in different combinations [69], suggesting the involvement of common as well as specific mechanisms in the upregulation of the different efflux pumps.

Table 1. 4. | Genes encoding drug efflux pumps and their regulators in pathogenic fungi. [a]Gain-of-function mutations in the regulator that cause constitutive overexpression of the corresponding efflux pump in clinical isolates, adapted from Morschhäuser *et al.* (2010) [57].

Species	Efflux pump	Type	Regulator	GOF mutations [a]
C. albicans	*CDR1*	ABC	*TAC1*	Yes
			NDT80	-
	CDR2	ABC	*TAC1*	Yes
	MDR1	MFS	*MRR1*	Yes
C. glabrata	*CDR1*	ABC	*PDR1*	Yes
	CDR2	ABC	*PDR1*	Yes
	SNQ2	ABC	*PDR1*	Yes
	FLR1	MFS	*YAP1*	-

Under stress, *CgPDR1* can undergo gain-of-function (GOF) mutations resulting in increased expression of efflux pumps (Figure 1. 6.). Different single point mutations cause activation of different regulons, and several dozens of mutations in *CgPDR1* have been identified in fluconazole-resistant isolates. These GOF mutations can take place in several domains of the gene, including the putative activation domain, the xenobiotic binding domain and the putative inhibition domain [44]. It was demonstrated that GOF mutations in *CgPDR1*, from clinical and *in vitro* generated azole-resistant *C. glabrata* strains, when introduced into a drug-susceptible strain, cause upregulation of *CgCDR1*, *CgCDR2*, and *CgSNQ2* and resistance to azoles [67, 69]. However, it was also shown that, in some azole-resistant clinical isolates that overexpressed *CgCDR1* or both *CgCDR1* and *CgCDR2*, *CgPDR1* sequences were identical to those of matched susceptible isolates from the same patients, indicating that these efflux pumps can also be upregulated by other mechanisms in *C. glabrata* [67]. Interestingly, in other studies, it was demonstrated that, depending on the *CgPDR1* GOF mutation, different efflux pumps can be upregulated (only *CgSNQ2* but not *CgCDR1* and *CgCDR2* [69]; or *CgCDR1* overexpression without a concomitant upregulation of *CgCDR2* and/or *CgSNQ2* [72]) suggesting that mutations in *CgPDR1* may have distinct promoter-specific effects.

Although typical regulatory targets of *CgPDR1* include the ATP efflux pumps encoding genes *CgCDR1* and *CgCDR2*, it was also found to activate the expression of efflux pumps from the MFS, including *CgQDR2* [73] and *CgTPO3* [74], thus reaffirming its role as a major regulator of drug resistance in *C. glabrata.* Pais *et al.* (2016) [75] interestingly demonstrated that the MFS MDR encoding genes *CgTPO1_1* and *CgTPO1_2* confer resistance to azole antifungal drugs, including the imidazoles clotrimazole, miconazole, tioconazole, and ketoconazole, used in the treatment of superficial skin and mucosal infections, but also the triazoles itraconazole and fluconazole, used against systemic infections. Significantly, the expression of *CgQDR2*, *CgTPO3* and *CgTPO1_1* were found to be consistently upregulated in clotrimazole resistant clinical isolates, when compared to susceptible ones, suggesting

that the activity of the encoded proteins is relevant in the clinical acquisition of azole drug resistance [76].

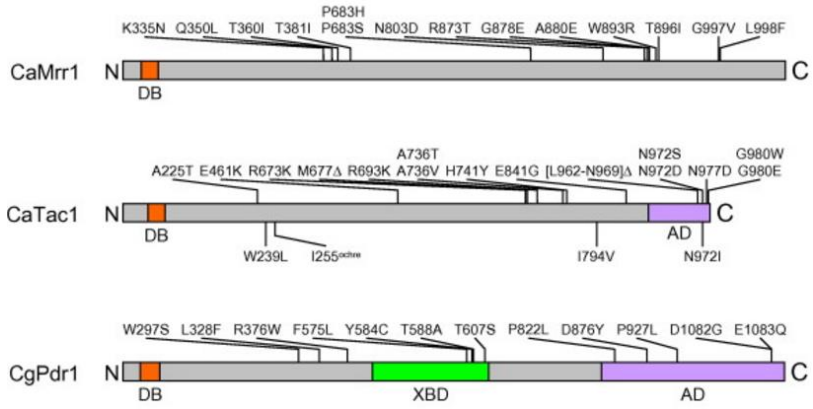

Figure 1. 6. | Location of gain-of-function mutations in *MRR1* and *TAC1* of *C. albicans* and *PDR1* of *C. glabrata.* Adapted from Morschhäuser *et al.* (2010) [57].

Yap1p (yeast activator protein-1) is known as a central regulator of the oxidative stress response in *S. cerevisiae,* but is also required for response to other chemical stresses via the transcriptional regulation of its target genes, like *FLR1* (fluconazole resistance-1). This gene encodes a MFS membrane transporter and is known as a target gene of Yap1p, whose overexpression confers multidrug resistance in *S. cerevisiae*. *CgYAP1* is a structural and functional ortholog of *S. cerevisiae YAP1* which was previously shown to be able to complement both *Δyap1* and *Δcgyap1* phenotype and, when overexpressed in *S. cerevisiae*, showed ScYap1p properties in drug resistance [77].

S. cerevisiae FLR1 gene has one homolog in *C. albicans*, *CaMDR1*, and two homolog ORFs in *C. glabrata* genome sequence, *CgFLR1* (ORF *CAGL0H06017g*) and *CgFLR2* (ORF *CAGL0H06039g*) [78], [79]. On one hand, *CaMDR1* has been one of the few DHA transporters linked so far to azole drug resistance [73], being an important determinant of clinical acquisition of resistance against these antifungals. On the other hand, Chen *et al.* (2007) [77] demonstrated that the deletion of *CgFLR1* in *C. glabrata* only resulted in increased sensitivity to benomyl, diamide, and menadione, but not 4-NQO, cycloheximide, or fluconazole. Interestingly, it was recently demonstrated that the regulation of the *CgFLR1* and *CgFLR2* genes is controlled at the transcription level by *CgPDR1* in the presence of the azole drug clotrimazole, but not in the presence of fluconazole [80]. This finding suggests that this effect may be specific to imidazole antifungals, such as clotrimazole, but not to triazole antifungals such as fluconazole. Additionally, given the importance of *CgPDR1* in the clinical acquisition of azole drug resistance, *CgFLR1* and *CgFLR2* may be relevant in the clinical context.

1.4.1.1.3 Bypass pathways

In addition to these mechanisms, including target alteration and upregulation of drug transporters, *Candida spp.* have evolved stress response pathways that enable the cell to handle diverse stresses present in its environmental niche: bypass pathways.

One well-characterized mechanism that moderates drug toxicity and confers resistance that is contingent upon stress responses involves a mutation in the Δ-5,6-desaturase encoded by *ERG3*. This mutation blocks the production of the toxic sterol 14-α-methyl-3,6-diol, which would otherwise accumulate in the membrane when Erg11p is inhibited. Instead, an alternate sterol, 14α-methyl fecosterol, becomes incorporated into the membrane, allowing the fungal cell to continue to grow and divide in the presence of azoles [44].

Another mechanism that has been proposed to improve azole resistance is the aerobic uptake of exogenous sterol. In fact, some isolates of *C. glabrata* are able to uptake sterol in order to overcome the blockage of ergosterol biosynthesis [81] and a putative sterol transporter gene for *C. glabrata*, *AUS1*, has been identified [82]. It was reported that a clinical isolate of *C. glabrata* (CG156), that persisted under treatment with high doses of fluconazole, voriconazole, and amphotericin B, was an ergosterol-deficient *ERG11* (sterol 14α-demethylase) mutant [81]. The mutant harbored a single-amino-acid substitution (G315D) which abolished the function of Erg11p. However, this mutant presented the capacity to sequester and metabolize lathosterol, cholestanol and demosterol, which are precursors of cholesterol. These alterations lead to changes in membrane composition, which apparently underlie its ability to surpass the perturbation in the sterol composition exerted by azole antifungal agents.

Mitochondrial dysfunction has been linked as well to increased resistance to azoles and other antifungal agents. It has been reported that *C. glabrata* isolates exhibiting a *petite* phenotype, that corresponds to the absence of growth on non-fermentable carbon sources, deficient growth in media supplemented with glucose, reduced oxygen consumption and partial or total mtDNA deletion, displayed increased resistance to fluconazole and clotrimazole [83]. It was proposed that this respiratory deficiency, observed in the *petite* mutants, could promote the exhibited azole resistance, since the biosynthesis of P-450-dependent 14α-sterol demethylase is stimulated by anaerobic conditions [84]. Indeed, a higher biosynthesis of ergosterol leads to a gain of resistance toward azole antifungals. Moreover, the development of the *petite* mutants upregulates the CDR ABC transporter genes.

In *C. albicans*, mutations in *ERG11* are reported to be one of the main mechanisms underlying this pathogen resistance to azoles. However, Sanguinetti *et al.* (2005) [85] demonstrated that two fluconazole-resistant *C. glabrata* isolates had no *CgERG11* mutations or upregulation, suggesting that *CgERG11* is not involved in azole resistance. Additionally, they showed that when the isolates were grown in the presence of fluconazole, the expression profile of *CgERG11* was not changed, whereas marked increases in the levels of gene expression of *CgCDR1* and *CgCDR2* were observed.

1.4.2. Echinocandins

The most recently approved class of antifungal agents is that of the echinocandins, which are semisynthetic lipopeptides, with a chemical structure containing cyclic hexapeptides N linked to a fatty acyl side chain. The primary and specific antifungal drug target is the cell wall, whose structure and composition are tightly regulated to reflect its multiple functions in pathogenic fungi. Echinocandins disrupt cell wall biogenesis and are rapidly fungicidal against most *Candida spp*. This class of fungicidal drugs comprises micafungin, anidulafungin and caspofungin, the most widely used echinocandin, and minimum inhibitory concentrations of all three are much lower than for amphotericin B and fluconazole against all *Candida spp*. This class of antifungal agents is considered to be the first-line treatment of candidiasis due to *C. glabrata*, but this NAC species has already been described as developing reduced susceptibility to caspofungin during prolonged therapy [1].

Echinocandins are large lipopeptide molecules that act as non-competitive inhibitors of (1,3)-β-D-glucan synthase, the enzyme which catalyses the production of glucan, the major component in *Candida* cell walls [86]. It is responsible for transferring sugar moieties from activated donor molecules to specific acceptor molecules forming glycosidic bonds [87]. The disruption of (1,3)-β-D-glucans causes a loss of cell wall integrity and severe cell wall stress on the fungal cell. As a result of its unique mechanism of action, cross-resistance between echinocandins and other classes of drugs is rare [88]. However, different mechanisms of resistance to echinocandins have been described, encompassing multiple stress response pathways, including alteration of the drug target and bypass pathways.

1.4.2.1 Echinocandins resistance mechanisms in *C. albicans* and *C. glabrata*

1.4.2.1.1. Alteration of the drug target

Similar to the azoles, a mechanism of resistance that bypasses the effect of the echinocandin on the cell is an alteration of the drug target (Figure 1. 7.). Echinocandins act by targeting the catalytic subunits of (1,3)-β-D-glucan synthase, which are encoded by 3 genes, *FKS1*, *FKS2*, and *FKS3* [89] in *C. albicans*, *C. tropicalis* and *C. krusei,* and 2 genes in *C. glabrata*, *FKS1* and *FKS2*. Therefore, some mutations in these targets increase the pathogen resistance to echinocandins.

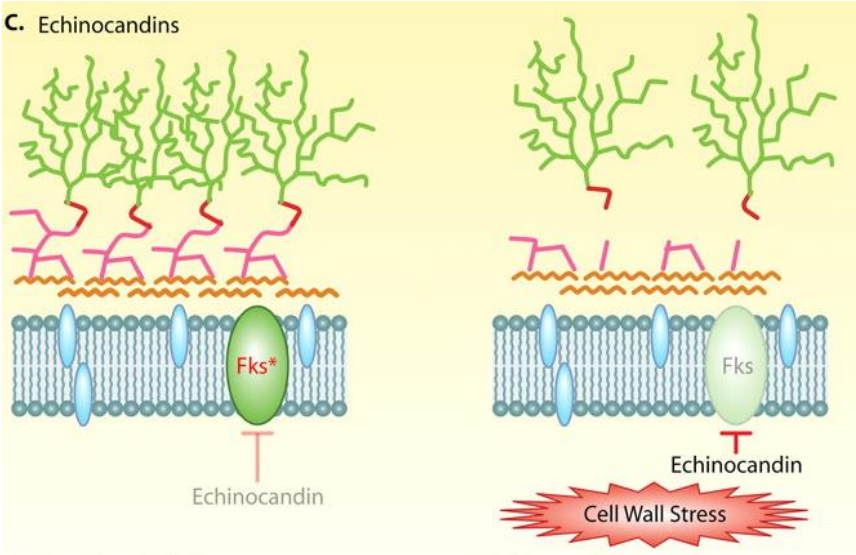

Figure 1. 7. | *Candida* resistance to echinocandins through mutations (*) in hot-spot regions in *FKS1* and induction of cellular stress responses. Adapted from Shapiro *et al.* (2010) [47].

Two hot-spot regions in the *C. albicans FKS1* gene were reported: the first encompasses amino acids 641 to 648 and results in the mutation of Ser645 to Pro645, Phe645 or Tyr645, being the most prevalent mutation in *C. albicans* isolates and correlates with significantly higher levels of echinocandin resistance [90]; the second corresponds to amino acids 1345 to 1365 and results in a key mutation named R1357S, which increases resistance to echinocandins [91]. In *C. albicans* isolates collected from a single patient, the progressive decline of a clinical response to micafungin therapy was associated with the acquisition of mutations in *FKS1* [92].

Accordingly, it was reported that a series of *C. glabrata* bloodstream isolates, that showed elevated echinocandin MIC, contained mutations in the drug targets Fks1p and Fks2p in previously identified hot-spot regions, implicating frequent drug target alterations in clinical echinocandin resistance [93]. For instance, micafungin MICs of *C. glabrata FKS* hot-spot mutant isolates were perceived to be less elevated than those obtained for the other echinocandins, showing that the efficacy of micafungin could be differentially dependent on specific *FKS* genes mutations [94]. Interestingly, in another study, echinocandin MICs and *FKS1* and *FKS2* mutations among *C. glabrata* isolates were correlated with echinocandin therapeutic responses. *FKS* mutations were detected and the median caspofungin and anidulafungin MICs were higher for patients who failed therapy [95]. In another study [89] from patients with *C. glabrata* bloodstream infections at Duke University Hospital in Durham, NC, the treatment outcome (using anidulafungin, caspofungin, and micafungin) was correlated with the MIC results and the presence of *FKS1* and *FKS2* gene mutations. The results showed that the resistance to echinocandins increased from 4.9 to 12.3 % between 2001 and 2010. Moreover, among the 78 fluconazole-resistant isolates, 14.1 % were resistant to one or more echinocandins. Almost 8 % of the isolates had an *FKS* mutation, which appeared due to a prior echinocandin therapy, and virtually all of them demonstrated intermediate or resistant MICs to an echinocandin (failure or recurrence of infection).

1.4.2.1.2. Bypass pathways

Calcineurin, a calcium and calmodulin dependent serine/threonine protein phosphatase, is a key regulator of cellular stress response and was recently reported to play a role in both *C. albicans* and *C. glabrata* resistance to echinocandins. Singh *et al.* (2009) [96] demonstrated that the pharmacological inhibition of calcineurin, with cyclosporine, blocked the echinocandin-mediated upregulation of calcineurin-dependent stress responses. The inhibition of calcineurin also had a synergistic effect with echinocandins against some but not all clinical isolates of *C. albicans* that evolved echinocandin resistance in the host by mutations in *FKS1.*

Calcineurin stability and function are regulated by Hsp90. Thus, the targeting of fungal Hsp90 provides a powerful strategy for treating fungal disease by increasing the potency of existing antifungal agents. Indeed, the pharmacological or genetic compromise of Hsp90 was demonstrated to abrogates echinocandin tolerance in *C. albicans* and results in a fungicidal combination under conditions where echinocandins alone are fungistatic [96].

The *C. albicans* PKC (protein kinase C) pathway has been implicated in upregulation of the expression of chitin synthase (*CHS*) genes in response to (1,3)-β-D-glucan synthase inhibition by the echinocandins [47]. In *C. albicans* there are four members of the chitin synthase gene family: *CHS1*, *CHS2*, *CHS3*, and *CHS8.* It was demonstrated that in some *C. albicans* isolates, in the presence of caspofungin, (1,3)-β-D-glucan levels decreased by 81% in contrast with the chitin levels, which increased by 89% [97]. These findings suggest that the compensation of another polymer in the cell wall may provide a mechanism of echinocandin resistance. An additional MAPK cascade, the HOG pathway, is known to be implicated in *C. albican*s cell wall architecture regulation [98]. PKC, HOG, and calcineurin signalling co-ordinately controls chitin synthesis in *C. albicans* in response to a variety of cell wall and cell membrane stresses. In fact, Munro *et al.* (2007) [99] demonstrated that under normal conditions, *HOG1* is required for basal levels of *CHS1* transcription in *C. albicans.* However, under stress conditions both *HOG1* and *CRZ1* are required. Furthermore, the expressions of *CHS2* and *CHS8* are dependent on *CRZ1*, *HOG1*, and *MKC1* under normal and stress conditions. The upregulation of the *CHS* genes in response to echinocandins is then dependent on the PKC, HOG, and calcineurin pathways, and the pre-treatment of cells with a cell wall stressor increases echinocandin resistance through the activation of these pathways.

In *C. glabrata*, both calcineurin and PKC signalling have been implicated in basal tolerance to echinocandins [100]. However, the role of Hsp90 remains unknown as does the impact of any of these referred regulators on echinocandin resistance.

Unlike for azoles, the upregulation of multidrug transporters plays a rather minor role in echinocandin resistance. Previous studies reported strong activity of echinocandins in *C. albicans* clinical isolates that show increased levels of azole resistance, suggesting that they are not substrates for the Cdr1p, Cdr2p, or Mdr1p drug transporters [101].

The biofilm cellular state confers dramatic increases in resistance to azoles; however, this does not seem to be the case with echinocandins [47].

1.5. The role of biofilms in *Candida*'s resistance to antifungals

The ability of fungal pathogens to cause disease relies upon an array of strategies to colonize surfaces and invade host tissues. Biofilm formation is one of the main pathogenesis traits presented by human pathogens. Once inside the host, the formation of biofilms enables the pathogens to overcome environmental stresses, such as drug exposure and immune system attack. In fact, comparing planktonic cells to biofilms, the latter are much more resistant to antimicrobials. In fact, it has been proved that the cells that detach from the biofilm have higher mortality than equivalent planktonic yeasts [102]. So far, however, there appears not to be one specific resistance factor responsible for the increased resistance to antifungal agents exhibited by biofilm cells. Instead, biofilm resistance is a complex multifactorial phenomenon, which remains to be fully elucidated and understood. Different mechanisms may be responsible for the intrinsic resistance of *Candida* biofilms and specifically *C. glabrata*. These include: (i) high density of cells within the biofilm; (ii) effects of the biofilm matrix; (iii) decreased growth rate and nutrient limitation; (iv) expression of resistance genes, particularly those encoding efflux pumps; and (v) presence of "persistent" cells. It is known that planktonic cells generally rely on irreversible genetic changes to maintain a resistant phenotype, whereas biofilms can persist due to their physical presence and the density of the population, which provides an almost inducible resistant phenotype irrespective of defined genetic alterations [103].

The generation of new antifungals against *Candida spp.* biofilms has become a major priority, since biofilms are likely the predominant mode of device-related microbial infection and exhibit resistance to antifungal drugs leading to treatment failures [104]. Several azole-derivative antifungals, including imidazole and triazole derivatives, affect hyphal development by limiting branch formation in hyphae and, at high concentrations, arrest hyphal development completely [105]. Despite not being able to form filaments, *C. glabrata* is capable of colonizing host tissues as well as abiotic surfaces, where it develops as a multilayered biofilm structure [106]. When compared to other *Candida* species, *C. glabrata* appears to be one of the more robust, being able to survive on inanimate surfaces for more than 5 months, while the viability of *C. albicans* is limited to 4 months and *C. parapsilosis* cells die after 2 weeks [107]. However, comparing with the other *Candida* species, *C. glabrata* displays the lowest biofilm metabolic activity, thus having less total biomass. Remarkably, its biofilm matrices have relatively higher quantities of protein and carbohydrate compared to other NACs [108].

1.5.1. Trancriptional control of biofilm formation in *C. glabrata* and *C. albicans*

Concerning biofilm formation, *BCR1, TEC1, EFG1, NDT80, ROB1,* and *BRG1* are reported to be the major players in the transcriptional network controlling biofilm development in *C. albicans* (Figure 1. 8.). In fact, Nobile *et al.* (2012) [109] reported that the six regulators, originally identified in their genetic screen, control each other's expression: all the six regulators bind to the upstream promoter regions of *BCR1*, *TEC1*, *EFG1,* and *BRG1.* Moreover, the same group performed a full-genome chromatin immunoprecipitation microarray (ChIP-chip) to map the position across the genome to which each of the six transcription regulators is bound during biofilm formation and found 1,061 target genes directly

regulated by at least one of the six biofilm transcription factors. They also demonstrated that each regulator activates its own synthesis and positively regulates each of the other regulators (Figure 1. 8.).

Through gene expression analysis, 234 genes were found to be downregulated and 173 genes upregulated in the *bcr1Δ/Δ* mutant relative to the isogenic parent. Of the genes directly bound by *BCR1*, half were downregulated and half were upregulated in the *bcr1Δ/Δ* mutant, indicating that this transcription factor can act as both an activator and repressor of its direct target genes. Similar analysis indicated that *EFG1*, *NDT80*, *ROB1*, and *BRG1* are all both activators and repressors of their biofilm-relevant direct target genes and that *TEC1* is primarily an activator of its biofilm-relevant direct target genes [109]. 19 target genes were found to be differentially regulated in all six biofilm regulator mutants. Eight of these target genes (*ORF19.3337*, *ALS1*, *TPO4*, *ORF19.4000*, *EHT1*, *HYR1*, *HWP1*, and *CAN2*) were expressed at lower levels in all six of the biofilm regulator mutants compared to the reference strain, and seven of these genes were also expressed at higher levels in biofilm compared to planktonic wild-type cells. Additionally, all of these eight target genes were bound in their upstream promoter regions by at least one of the six biofilm regulators; most were bound by multiple regulators [109].

However, while extensive work has been performed on the *C. albicans* genes involved in adhesion/colonization and biofilm formation, little is known about equivalent controlling genes in *C. glabrata*. Similarly to the flocculin/lectins encoded by *FLO* genes in *S. cerevisiae*, *C. glabrata* Epa proteins are predicted to be glycosylphosphatidylinositol (GPI)-anchored cell wall proteins that bind host cell carbohydrates. This link between *FLO* and *EPA* genes suggest that *EPA* regulation may control the adherence of *Candida* species during the host interactions, conferring distinct adhesion profiles towards human proteins and cells. This regulation is variable among species and even between strains of the same species [110]. For instance, *CgEPA3* has been shown to be upregulated in *C. glabrata* biofilm cells [111]; *CgEPA1*, *CgEPA6* and *CgEPA7* have been shown to be involved in kidney colonization of *C. glabrata* [112].

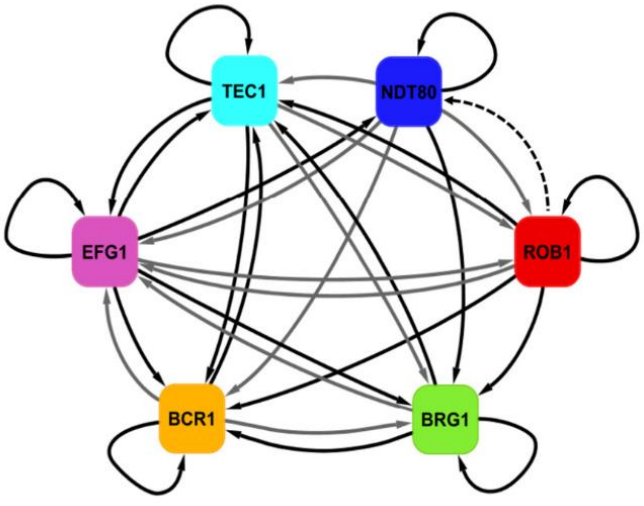

Figure 1. 8. | *C. albicans* biofilm network model based on ChIP-chip and expression data. Solid arrows indicate direct binding interactions determined by ChIP-chip. Solid black arrows indicate experimentally validated regulatory interactions in addition to direct binding interactions, and solid grey arrows indicate direct binding interactions only. The dashed black arrow indicates an indirect regulatory interaction only. Adapted from Nobile *et al.* (2012) [105].

The expression of all of the characterized *EPA* genes, in *C. glabrata*, is regulated by transcriptional silencing at telomers via the SIR complex [106]. Silent Information Regulator (SIR) proteins are involved in regulating gene expression and some SIR family members are conserved from yeast to humans [113]. This regulation process is initiated by the association of Rap1 and Hdf1 proteins with the telomeres. These proteins recruit a SIR complex proteins: Sir2, Sir3 and Sir4. Sir2, a NAD+-dependent histone deacetylase that provides high affinity binding sites to Sir3 and Sir4 and deacetylates histones H3 and H4 of a targeted nucleosome, is responsible for the catalytic activity of the SIR complex. The capacity of this complex to bind to hypoacetylated histones allows its spread along the telomere until it reaches the sub-telomeric region as adjacent nucleosomes are sequentially deacetylated by Sir2 and are bound by all complex [19].

Despite SIR complex is established as the main *EPA* genes regulator, Swi/Snf (Switch/Sucrose Non-Fermentable) complex, that is a group of proteins that associate to remodel the way DNA is packaged, was demonstrated to regulate *CgEPA6* in a specific manner, since it did not regulate expression of *CgEPA1* in the same way as *CgEPA6*. The Swi/Snf complex modulates *CgEPA6* expression in a Sir4-dependent manner [114]. In fact, differential regulation of *EPA* genes by the different proteins of the subtelomeric silencing machinery has already been reported [106]. Similarly, in *C. albicans* the Swi/Snf complex is required for hyphal development and pathogenicity [115], but the direct target(s) of this complex are still unknown.

On one hand, Yak1p kinase regulates indirectly the expression of *CgEPA6*, in the dependency of the presence of the intact subtelomeric silencing machinery (Yak1p/Sir4p signaling pathway). On the other hand, Cst6 transcription factor, similar to *S. cerevisiae* Cst6, a basic leucine zipper (bZIP) transcription factor of the ATF/CREB family involved in chromosome stability and telomere maintenance, was reported to be a negative regulator of the adhesin-encoding gene *CgEPA6*. Moreover, a phenotypic analysis of the *cst6Δyak1-1* double mutant suggested that Cst6 regulates *CgEPA6* expression and consequently biofilm formation independently of the Yak1p/Sir4p signalling pathway [114].

Altogether, the regulation of adhesin genes in *C. glabrata* appears very complex and different external signals have been demonstrated to alter *EPA* gene expression (Figure 1. 9.). For instance, *CgEPA6* is expressed during murine urinary tract infection, but remains silent in a systemic infection. Domergue *et al.* (2009) [116] demonstrated that its expression in the urinary tract is the result of nicotinic acid limitation in this host niche. Those conditions would result in a reduction of NAD+, which is necessary for the Sir2p deacetylase activity. Moreover, Mundy & Cormack (2009) [117] demonstrated that *CgEPA6* and *CgEPA1*, but not *CgEPA7*, are activated in the presence of the two widely used preservatives paraben and sorbic acid.

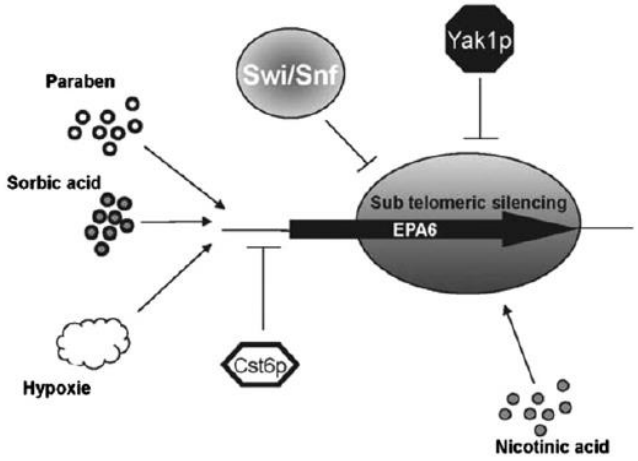

Figure 1. 9. | Model for *CgEPA6* regulation in *C. glabrata*. Adapted from Riera *et al.* (2012) [114].

This complex regulation of adhesin genes in *C. glabrata* is reminiscent of the highly complex regulation of *S. cerevisiae FLO* genes. Indeed, *FLO11* is one of the genes regulated by the Swi/Snf complex. Similarly, in *S. cerevisiae*, regulation of *FLO11* expression appears to be dependent on several factors acting directly or indirectly at the level of transcription [116]. Hence, understanding the regulation of expression of *EPA* genes will represent a major challenge in the future, as their adhesin gene products represent key elements in the regulation of *C. glabrata* interactions with the host.

1.6. Role and regulation of Rpn4 transcription factor in *S. cerevisiae* and *C. glabrata*

In *S. cerevisiae,* the stress-response network is mainly mediated by the transcription factor Rpn4p [118]. This is a transcription factor known as a stimulator of proteasomal gene expression and is transcriptionally regulated in response to various stresses.

The proteasome homeostasis in *S. cerevisiae* is regulated by a negative feedback loop in which the transcription factor Rpn4p induces the proteasome genes and is rapidly ($t_{1/2} \leq 2$ min) degraded by the assembled proteasome. However, stabilization of Rpn4p, achieved through the inhibition of proteasome, results in an increase of proteasomal genes expression [119]. Together, these observations led to a model in which the proteasome homeostasis is regulated by a negative feedback circuit. On one hand, *RPN4* upregulates the proteasome genes; on the other hand, Rpn4p is rapidly degraded by the assembled/active proteasome. This system enables an efficient control of the proteasome abundance in *S. cerevisiae*.

In addition to the proteasome genes, Rpn4p regulates numerous other genes involved in a wide range of cellular pathways. The promoter region of *RPN4* carries the binding sites for heat-shock transcription factor 1 and multidrug resistance-related transcription factors Pdr1p, Pdr3p and Yrr1p. Additionally, besides being regulated by these multidrug resistance transcription factors, *RPN4* is also regulated by the Yap1p transcription factor, that plays an important role in the oxidative stress response and multidrug resistance [120]. Stress conditions promote the activation of these transcription factors

that in turn induce *RPN4* expression. Wang *et al*. (2008) [118] demonstrated that the disruption of Rpn4-induced proteasome expression severely reduces cell viability under stressed conditions. The same authors, in 2010 [121], showed that inhibition of Rpn4p degradation dramatically sensitizes the cells to several genotoxic and proteotoxic stressors. This damaging effect is abrogated by a point mutation that inactivates the transcription activity of *RPN4,* suggesting that overexpression of Rpn4p target genes impairs the cell's ability to tolerate stress. Additionally, they demonstrated that stabilization of Rpn4p exhibits synthetic growth defects with proteasome impairment.

Although Rpn4p is involved in the regulation of several pathways, the Rpn4-proteasome negative feedback loop likely plays a central role since, in addition to controlling proteasome homeostasis, it also regulates the expression of other Rpn4p target genes through proteasomal degradation of Rpn4p.

RPN4 deletion only slightly reduces the cell growth rate in normal conditions and dramatically impairs the mutant cell survival in stress. Rpn4p confers resistance to a variety of protein or DNA-damaging chemical and physical factors, including heat shock, UV irradiation, oxidants, DNA-methylating agents, etc. [122].

Although little is known about the *C. glabrata RPN4* homolog, *CgRPN4*, it has been described as a putative transcription factor for proteasome genes and was found to be upregulated in azole-resistant strains. Vermistky *et al*. (2006) [123] demonstrated that *CgRPN4* was two-fold upregulated in *C. glabrata* fluconazole-resistant mutant with a putative gain-of-function mutation in *CgPDR1*. Additionally, Tsai *et al*. (2010) [124] analysed gene expression in *C. glabrata* oropharyngeal isolates from seven hematopoietic stem cell transplant recipients whose isolates developed azole resistance while the recipients received fluconazole prophylaxis, and they found that the ORF encoding the transcription factor *CgRPN4* (*CAGL0K01727g*) was upregulated in most resistant isolates compared to their paired susceptible isolates.

Moreover, Salin *et al.* (2008) [125] demonstrated that, in *S. cerevisiae*, toxic doses of selenite activate various stress response pathways, including the proteasome, oxidative stress, iron homeostasis and general stress pathways. In these growth conditions, the expression of *ScPDR1* and *ScRPN4* was coordinated through a positive transcriptional loop. This loop contributed to the optimal Yap1p-dependent oxidative stress induction of several genes encoding membrane proteins, including *FLR1*, *ATR1* and *FRM2*. This function was found to be conserved in *C. glabrata*. *C.* Microarrays were used to investigate the expression patterns of *CgYAP1*, *CgRPN4* and *CgPDR1* in response to the oxidative stress caused by the antifungal drug benomyl, leading to the observation of an induction of the *C. glabrata* homologs of *ScYAP1*, *ScRPN4* and *ScPDR1* in these same conditions. Additionally, two Pdr responsive elements (PDRE) and one Yap responsive element (YRE) binding motifs were found in the *CgRPN4* promoter, whereas one proteasome associated control element (PACE) was found in the *CgPDR1* and *CgYAP1* promoters [125]. These data strongly suggest that the cross-regulation between *PDR1* and *RPN4*, on one hand, and of *YAP1* and *RPN4*, on the other, is conserved from *S. cerevisiae* to *C. glabrata*.

Concerning *C. glabrata* biofilm formation, there are no evidences of any role of *CgRPN4* in this phenomenon. However, it was previously demonstrated that the impairment of proteasomal activity (using tea polyphenols) contributes to cellular metabolic and structural disruptions that expedite the inhibition of biofilm formation and maintenance by *C. albicans* [126].

2. Materials and Methods

2.1. Strains and plasmids

Saccharomyces cerevisiae parental strain BY4741 (*MATa, ura3Δ0, leu2Δ0, his3Δ1, met15Δ0*) and the derived single deletion mutant BY4741_*Δrpn4* were obtained from the Euroscarf collection. *C. glabrata* parental strain KUE100 and derived single deletion mutants KUE100_*Δcgrpn4,* KUE100_*Δcgstb5,* KUE100_*Δcgpdr1,* KUE100_*Δcgyrm1_1,* KUE100_*Δcgyrm1_2,* KUE100_*Δcghap1,* KUE100_*Δcgmrr1,* KUE100_*Δcghal9,* KUE100_*Δcgtac1,* KUE100_*Δcgskn7,* KUE100_*Δcgyap1,* KUE100_*Δcgcad1,* KUE100_*Δcgtog1,* KUE100_*Δcgtec1_1,* KUE100_*Δcgtec1_2,* KUE100_*Δcgbcr1* and *KUE*100_*Δcgndt80* (Table S1. and S2.) were kindly provided by Hiroji Chibana, from the Medical Mycology Research Center (MMRC), Chiba University, Chiba, Japan. *C. glabrata* strain L5U1 (*cgura3Δ0*, *cgleu2Δ0*) was kindly provided by John Bennett from the National Institute of Allergy and Infectious Diseases, NIH, Bethesda, USA. Also, the CBS138 *C. glabrata* strain, whose genome sequence was released in 2004, was used in this study for gene amplification purposes.

The plasmids pGREG576 and pGREG515 were obtained from the Drag & Drop collection (Figure S1.) [127].

2.2. Screening for pathogenesis-related phenotypes among *C. glabrata* transcription factors deletion mutants

2.2.1. Antifungal susceptibility assays

The susceptibility of the parental *C. glabrata* strain KUE100 and the derived single deletion mutants toward toxic concentrations of selected drugs was compared through spot assays. The cells were batch-cultured at 30°C, with orbital agitation (250 rpm), in minimal medium without supplementation (MMB), containing (per liter): 1.7 g of yeast nitrogen base without amino acids or NH_4^+ (Difco), 20 g of glucose (Merck) and 2.7 g of $(NH_4)_2SO_4$ (Merck). The cell suspensions used to inoculate the agar plates were mid-exponential cells grown until a standard culture final $OD_{600\ nm}$ = 0.4 ± 0.04 was reached and then diluted in sterile water to obtain suspensions with final $OD_{600\ nm}$ = 0.05 ± 0.005. These cell suspensions and subsequent dilutions (1:5; 1:25) were applied as 4 µL spots onto the surface of solid MMB medium, supplemented with adequate chemical stress concentrations. Agarized solid media contained, besides the previously indicated ingredients, 20 g/L agar (Iberagar).

The tested drugs included the following compounds, used in the specified concentration ranges: the azole antifungal drugs ketoconazole (30 to 40 mg/L), fluconazole (100 to 150 mg/L), miconazole (0.4 to 0.5 mg/L), tioconazole (0.5 to 1.2 mg/L), itraconazole (15 to 25 mg/L), and clotrimazole (10 to 12.5 mg/L), the polyene antifungal drug amphotericin B (0.25 to 0.35 mg/L), the fluoropyrimidine 5-flucytosine (0.005 to 0.03 mg/L), the pesticide mancozeb (3 to 4,5 mg/L) and the polyamines putrescine (100 to 150 mg/L), spermine (4 to 7 mM) and spermidine (8 to 10 mM) (all from Sigma).

Additionally, minimal inhibitory concentration assays were performed to compare the susceptibility of the wild-type KUE100 *C. glabrata* strain and the derived single deletion mutants toward standardized concentrations of ketoconazole, fluconazole (azoles), amphotericinB (polyene), flucytosine (pyrimidine) and caspofungin (echinocandin). The MIC (minimum inhibitory concentration) was defined as the lowest drug concentration inhibiting growth at least 50% relative to the drug-free control, called MIC 50% (MIC_{50}). The cells were grown at 30°C, with orbital agitation (250 rpm), in liquid rich medium YPD and the assays were performed as described by Rodríguez-Tudela *et al* (2003) [128], using a standard cellular suspension with final $OD_{600\ nm}$ = 0.05 ± 0.005. The microtiter plates were incubated without agitation at 37°C for 24 hours and then were read in a microplate reader (SPECTROstar Nano from BMG LabTech) using a wavelength of 530 nm. The value of the blank (background column 12) was subtracted from readings for the rest of the wells. Before the readings, the wells in the microtiter plates were resuspended with a multichannel pipette to ensure a uniform turbidity and resuspend any yeast cells that may have sedimented.

2.2.2. Biofilm quantification assays

The crystal-violet method [129] was used to study the capacity of biofilm formation in the *C. glabrata* strains. Cells were batch-cultured at 30ºC, with orbital agitation (250 rpm) in double-strength Sabouraud Dextrose Broth (SDB) medium, at pH 5.6, containing (per liter): 80 g glucose (Merck) and 20 g meat peptone (Merck). The pH of 5.6 was achieved using a HCl 1M solution. The double-strength RPMI 1640 media used to grow the cells in the microtiter plates is composed (per 300 mL) by: 6.24 g RPMI 1640 (Sigma), 20.72 g MOPs (Sigma) and 10.8 g glucose (Merck). The pH was adjusted to 4 using a HCl 1M solution.

Cells were collected by centrifugation at mid-exponential phase and a cellular suspension with final $OD_{600\ nm}$ = 0.1 ± 0.01was prepared. Cells were then inoculated in 96-well polystyrene titter plates (Greiner), which were previously filled with the appropriated growth medium. The first four lines (1-4) were filled with 100 µL of double-strength RPMI medium, at pH 4, and the last four (5-8) with 100 µL of double-strength SDB medium at pH 5.6, in order to have an initial OD_{600nm} = 0.05 ± 0.005. Each well of columns 2-6 and 8-12 of the microtiter plates was inoculated with 100 µL of cellular suspension. Columns 1 and 7 of the microtiter plates were filled with 100 µL of sterile distilled water, from the lot used to prepare the inoculum, as a sterility control for media and sterile distilled water. The microtiter plates were sealed with a membrane (Greiner Bio-One) and incubated at 30°C, with mild orbital agitation (70 rpm) for 16h. Then, the growth medium on the biofilm-coated wells of microtiters plates was removed and the biofilm formed was washed three times with 200 µl of sterile distilled water to remove cells that were not attached to the formed biofilm. After this washing step, 200 µL of 1% crystal-violet (Merck) alcoholic solution was added to each well in order to stain the formed biofilm (15 min of incubation). Then, microtiter plates were washed three times with 250 µL of sterile distilled water. At this point, biofilms were visible as purple rings formed on the bottom of each well. Finally, 200 µL of 96% (v/v) ethanol was added to each well, to elute the stained biofilm. The destaining solution was measured with a microplate reader (SPECTROstar Nano, BMG LabTech) at 590 nm. The control absorbance values were subtracted from the values of the test wells in order to minimize background interference.

2.3. *S. cerevisiae* and *C. glabrata* transformation

For transformation purposes, cells were batch-cultured at 30°C, with orbital agitation (250 rpm) in liquid rich medium Yeast extract–Peptone-Dextrose (YPD), with the following composition (per liter): 20 g of glucose (Merck), 20 g of bacterial peptone (Dickson) and 10 g of yeast extract (HIMEDIA).

All transformation reactions were performed using the Alkali-Cation Yeast Transformation Kit (MP Biomedicals), according to the manufacturer's instructions. Mid-exponential *S. cerevisiae* BY4741 and *C. glabrata* L5U1 cells were batch-cultured at 30ºC with orbital shaking (250 rpm) in YPD liquid medium until a standard OD600nm 0.4 ± 0.04 was reached. The cells were harvested by centrifugation at 7 000 rpm for 5 min at 4ºC and the resulting pellets were resuspended in 2.7 mL of TE buffer, pH 7.5. After a second centrifugation step, the cells were harvested and rinsed with 1.5 mL of 0.15 M Lithium Acetate solution and shaken gently (100 rpm) at 30ºC for 25 minutes. Cells were harvested by centrifugation (7 000 rpm, 5 min, 4ºC) and resuspended in 300 µL TE buffer, pH 7.5. Cells were then transferred to 1.5 mL tubes, combining: 100 µL yeast cells, 5 µL Carrier DNA, 5 µL Histamine Solution and 100-200 ng plasmid DNA. Cells were gently mixed and incubated at room temperature for 15 min. A mixture of 0.8 mL PEG and 0.2 mL TE/Cation MIXX solution was added to each transformation reaction, followed by 10 min incubation at 30ºC and heat shock at 42ºC for 10 minutes. Cells were then pelleted in a microcentrifuge and resuspended in 100 µL YPD liquid medium before plating in appropriate medium agar plates.

2.4. Cloning of the *C. glabrata CgRPN4* gene (ORF *CAGL0K01727g*), under the control of the *MTI* promoter

The pGREG576 plasmid from the Drag & Drop collection (Figure S1.) [127] was used to clone and express the *CgRPN4* ORF *CAGL0K01727g* in *S. cerevisiae*, as described before for other heterologous genes [130]. pGREG576 was acquired from Euroscarf and contains a galactose inducible promoter (*GAL1*), the yeast selectable marker *URA3* and the *GFP* gene, encoding a Green Fluorescent Protein (GFP^{S65T}), which allows monitoring of the expression and subcellular localization of the cloned fusion protein. The plasmid was restricted with the restriction enzyme *SalI* (Takara) in the cloning site harboring the *HIS3* gene. Additionally, it was treated with *CiAP* (Invitrogen) during 45 minutes at 37ºC to prevent recircularization (Figure 2.1.). The *CAGL0K01727g* DNA was generated by PCR, using genomic DNA extracted from the sequenced CBS138 *C. glabrata* strain, and the specific primers presented in Table 2.1..

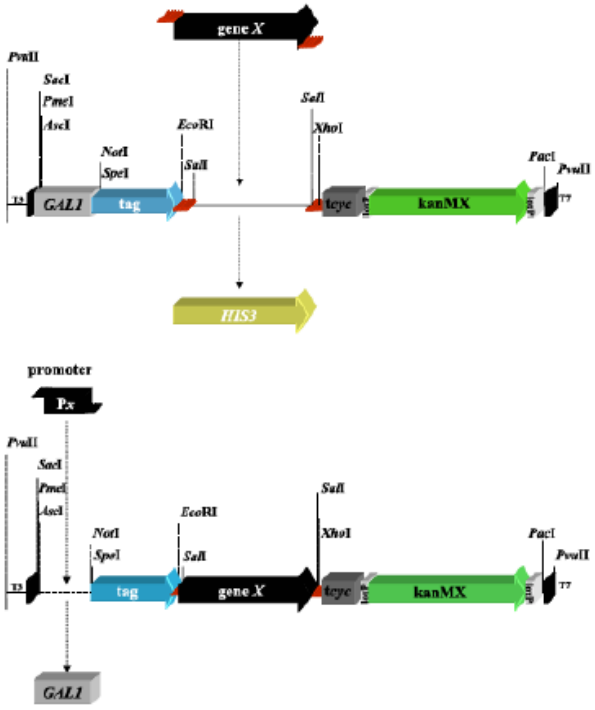

Figure 2. 1. | Schematic representation of the cloning procedure using pGREG576. The gene cloning site harbors a *HIS3* tag flanked by *SalI* restriction sites. The promo*ter cloning site harbors the GAL1* promoter, flanked by *SacI* and *NotI* restriction sites [127].

The designed primers contain, besides a region with homology to the first and the last 22 nucleotides of the *CAGL0K01727g* coding region (italic), nucleotide sequences with homology to the cloning site flanking regions of the pGREG576 vector (underlined). The amplified DNA fragment was co-transformed into the parental *S. cerevisiae* BY4741 with the pGREG576 vector (as described in Section 2.3.), previously cut with the restriction enzyme *SalI* (Takara), generating pGREG576_*CgRPN4* plasmid. Co-transformed *S. cerevisiae* cells were plated in minimal medium supplemented with 20 mg/L histidine, 20 mg/L methionine and 60 mg/L leucine (MMB-U), containing (per liter): 1.7 g of yeast nitrogen base without amino acids or NH_4^+ (Difco), 5 g of glucose (Merck), 1 g of galactose (Sigma), 2.7 g of $(NH_4)_2SO_4$ (Merck) and 20 g/L agar (Iberagar). The plates were incubated at 30°C to select the transformants.

Table 2. 1. | Design of primers. Primer sequences used to obtain *CgRPN4 (CAGL0K01727g)* DNA for pGREG576 cloning procedure. The sequences present a region with homology to the cloning site flanking regions of the vector (underlined) and homology regions to the gene to be amplified (italic).

Gene	Primer	Sequence
CgRPN4 (*CAGL0K01727g*)	Forward	5'-GAATTCGATATCAAGCTTATCGATACCGTCGACA*ATGACGTCTATAGATTTGGGAC*-3'
	Reverse	5'-GCGTGACATAACTAATTACATGACTCGAGGTCGAC*TTATGCAGTGACAAATCCGATG*-3'

In order to confirm that the transformant grown colonies had the vector with the cloned gene, and not only the empty vector, a colonyPCR was performed with independent primers of the cloned gene (D&D primers – Fw: CATGGCATGGATGAACTATAC; Rv: CGGTTAGAGCGGATGTGGG).

Since the *GAL1* promoter only allows a slight expression of downstream genes in *C. glabrata*, to both observe the overexpression effect and to visualize, by fluorescence microscopy, the subcellular localization of the CgRpn4 protein in *C. glabrata*, new constructs were obtained. The *GAL1* promoter present in the pGREG576_*CgRPN4* plasmid was replaced by the copper-induced *MTI C. glabrata* promoter, originating the pGREG576_*MTI_CgRPN4* plasmid. *MTI* promoter DNA was generated by PCR, using genomic DNA extracted from the sequenced CBS138 *C. glabrata* strain, and the specific primers present in Table 2.2.. The designed primers contain, besides a region with homology to the first 26 and the last 27 nucleotides of the first 1000 bp of the *MTI* promoter region (italic), nucleotide sequences with homology to the cloning site flanking regions of the pGREG576 vector (underlined). The amplified fragment was co-transformed into the parental strain BY4741 with the pGREG576_*CgRPN4* plasmid (as described in Section 2.3.), previously cut with *SacI* and *NotI* (Takara) restriction enzymes to remove the *GAL1* promoter, generating the pGREG576_*MTI_CgRPN4* plasmid.

Table 2. 2. | Design of primers. Primer sequences used to obtain *MTI* promoter DNA for pGREG576 cloning procedure and for colonyPCR. The sequences present a region with homology to the cloning site flanking regions of the vector (underlined) and homology regions to the target (italic).

Gene	Primer	Sequence
MTI promoter	Forward	5'-<u>TTAACCCTCACTAAAGGGAACAAAAGCTGGAGCTC</u>*TGTACGACACGCATCA TGTGGCAATC* - 3'
	Reverse	5'-<u>GAAAAGTTCTTCTCCTTTACTCATACTAGTGCGGC</u>*TGTGTTTGTTTTTGTAT GTGTTTGTTG* - 3'

The PCR amplification reactions of *CgRPN4* and *MTI* promoter were performed using a C1000 Thermal Cycler (Bio-Rad) and the following program present in Table 2.3.. The reaction mixture used for genes and promoter DNA attainment was prepared as displayed in Table 2.4..

Table 2. 3. | PCR program. PCR program used for amplification of *CgRPN4* and *MTI* promoter genes for pGREG576 cloning procedure.

Step	Time	Temperature (℃)	Cycles
Initial denaturation	30 secs	98	1
Denaturation	10 secs	98	
Annealing	20 secs	56	30
Extension	2 min	72	
Final extension	7 min	72	1

Table 2. 4. | PCR mix. Reaction mixture composition for PCR amplification of *CgRPN4* and *MTI* promoter genes for pGREG576 cloning procedure.

Component	Volume per reaction (µL)
10x HF buffer	10
Primer forward (50pmol)	1
Primer reverse (50pmol)	1
dNTPs (10mM)	1
$MgCl_2$ (50 mM)	2
DMSO	1.5
DNA template	2
ddH_2O	31
Taq Phusion (2 $U.\mu L^{-1}$)	0.5
TOTAL	50

The recombinant plasmids pGREG576_*CgRPN4* and pGREG576_*MTI_CgRPN4* were obtained through homologous recombination in *S. cerevisiae* using the Alkali-Cation Yeast Transformation Kit (MP Biomedicals) according to the manufacturer's instructions, and verified by DNA sequencing.

2.5. CgRpn4p subcellular localization assessment

The subcellular localization of the CgRpn4 protein was determined based on the observation of L5U1 *C. glabrata* cells transformed with the pGREG576_*MTI_CgRPN4* plasmid. These cells express the CgRpn4_GFP fusion protein, whose localization may be determined using fluorescence microscopy.

C. glabrata cell suspensions were prepared in minimal medium supplemented with 60 mg/L leucine (MMG-U), until a standard culture OD_{600nm} = 0.4 ± 0.04 was reached, and transferred to the same medium MMG-U supplemented with 50 µM $CuSO_4$ (Sigma), to induce protein overexpression.

After 6h of incubation, 150 mg/L fluconazole or 40 mg/L ketoconazole were added to the culture and cells were harvested after 1h of exposure. As control samples, culture grown in the absence of antifungal drugs were also inspected. 2 mL of cell suspension were centrifuged at 13 500 rpm for 2 minutes, and the pelleted cells were resuspended in 5 µL distilled water. The distribution of CgRpn4_GFP fusion protein in *C. glabrata* living cells was detected by fluorescence microscopy in a Zeiss Axioplan microscope (Carl Zeiss MicroImaging), using excitation and emission wavelength of 395 and 509 nm, respectively. Fluorescence images were captured using a cooled CCD camera (Cool SNAPFX, Roper Scientific Photometrics).

2.6. Antifungal susceptibility assays in *S. cerevisiae* and *C. glabrata* cells overexpressing *CgRPN4*

The ability of *CgRPN4* gene expression to increase *S. cerevisiae* and *C. glabrata* cells resistance toward azole drugs was assessed, through spot assays, in the *URA3*- strains BY4741 *S. cerevisiae* and L5U1 *C. glabrata*, using pGREG576_*CgRPN4* and pGREG576_*MTI_CgRPN4* centromeric plasmids, respectively. Additionally, the capability of *CgRPN4* gene expression to complement the absence of its *S. cerevisiae* homolog (*ScRPN4*) in BY4741_*Δrpn4* strain was also assessed through spot assays, using pGREG576_*CgRPN4.*

S. cerevisiae cells were first batch-cultured in MMB-U 0.5% glucose and 0.1% galactose medium, at 30°C, with orbital agitation (250 rpm) until a standard culture OD_{600nm} = 0.4 ± 0.04 was reached. Then, the cells from this first culture were used to initiate a new batch-culture, with an initial OD_{600nm} = 0.1 ± 0.01, in MMB-U 0.1% glucose and 1% galactose medium at 30°C, with orbital agitation (250 rpm).

C. glabrata cell suspensions were prepared in MMG-U, at 30°C, with orbital agitation (250 rpm), until a standard culture OD_{600nm} = 0.4 ± 0.04 was reached. Then, the cells were transferred, with an initial OD_{600nm} = 0.1 ± 0.01, to the same medium MMG-U supplemented with 50 µM $CuSO_4$ (Sigma), to induce protein overexpression.

Cell suspensions used to inoculate the agar plates were mid-exponential cells grown until culture OD_{600nm} = 0.4 ± 0.04 was reached and then diluted in sterile water to obtain suspensions with OD_{600nm} = 0.05 ± 0.005. These *S. cerevisiae* and *C. glabrata* cell suspensions and subsequent dilutions (1:5; 1:25) were applied as 4 µL spots onto the surface of solid MMB-U 0.1% glucose and 1% galactose or MMG-U with 50 µM $CuSO_4$, respectively. The plates were supplemented with adequate stress concentrations of the azole antifungal drugs ketoconazole (30 to 40 mg/L for *C. glabrata*, and 15 to 20 mg/L for *S. cerevisiae*) and fluconazole (100 to 150 mg/L for *C. glabrata*, and 60 to 80 mg/L for *S. cerevisiae*).

2.7. RNA-sequencing analysis

Next-Generation-Sequencing of cDNAs derived from RNA samples (RNA-Seq) does not only help to study gene expression but also to elucidate gene structures. For this technique, mRNA (and other RNAs) are first converted to cDNA. The cDNA is then used as the input for a next-generation sequencing library preparation. This approach provides digital data in the form of aligned read-counts, resulting in a very wide dynamic range, improving the sensitivity of detection for rare transcripts. These reads are aligned to the genome or transcriptome and are counted to determine differential gene expression. The transcriptional landscape i.e. the location of the reads within the genome can hint toward the locations of exons and introns (spliced reads) during gene prediction. Moreover, reads can be used to assemble full lengths transcripts under different conditions [131]. When compared to microarrays, RNA-seq is more sensitive, more robust and can be more cost effective.

C. glabrata cells for RNA-seq analysis were grown in MMB, at 30°C, with orbital agitation (250 rpm), until mid-log phase. Subsequently, 250 mg/L fluconazole were added to the culture and cells were harvested after 1h. For control samples, no fluconazole was added to the culture. Total RNA was isolated using an Ambion Ribopure-Yeast RNA kit, according to manufacturer's instructions.

Strand specific RNA-seq library preparation and sequencing was carried out as a paid service by the NGS core from Oklahoma Medical Research Foundation, Oklahoma City, Oklahoma, USA. Paired-end reads (Illumina HiSeq 3000 PE150, 2x150 bp, 2 GB clean data) were obtained from wild type *C. glabrata* KUE100 and correspondent deletion mutant strain KUE100_*Δcgrpn4* (ORF *CAGL0K01727g*). Two replicates of each sample were obtained from three independent RNA isolations, subsequently pooled together. Sample reads were trimmed using Skewer [132] and aligned to the *C. glabrata* CBS138 reference genome, obtained from the Candida Genome Database (CGD) (http://www.candidagenome.org/), using TopHat [133]. HTSeq [134] was used to count mapped reads per gene. Differentially expressed genes were identified using DESeq2 [135] with an adjusted p-value threshold of 0.01 and a $\log_2$ fold change threshold of -1.0 and 1.0. Default parameters in DESeq2 were used. *Candida albicans* and *Saccharomyces cerevisiae* homologs were obtained from the Candida Genome Database and *Saccharomyces* Genome Database (SGD) (https://www.yeastgenome.org/), respectively. The GO term finder from *Candida* Genome Database (CGD) (http://www.candidagenome.org/) [136] was used to carry out Gene Ontology (GO) analyses.

3. Results

3.1. Screening for pathogenesis-related phenotypes among *C. glabrata* transcription factor deletion mutants

3.1.1. Antifungal susceptibility assays

The difference in the susceptibility of *C. glabrata* KUE100 wild-type strain and seventeen derived single deletion mutants toward inhibitory concentrations of several chemical stress inducers was accessed through spot assays and, in the case of selected antifungal drugs, confirmed by MIC assays.

Concerning the *C. glabrata* ORFs predicted to play a role in multidrug resistance (Table S1.), some were found to, indeed, confer antifungal drug resistance. For instance, the deletion of *CgPDR1*, *CgRPN4* or *CAGL0L04576g* (*CgYRM1_1*) was found to increase the susceptibility of *C. glabrata* cells toward all azole antifungal drugs tested, whereas the deletion of *CgSTB5* or *CAGL0L04400g* (*CgYRM1_2*) was found not to affect *C. glabrata* susceptibility to any of the tested antifungal drugs (Figure 3.1.).

In fact, *CgPDR1* demonstrated to be crucial for *C. glabrata* resistance to several azole antifungal drugs, since the corresponding deletion mutant KUE100_*Δcgpdr1* was unable to growth in the presence of used concentrations of clotrimazole, miconazole, ketoconazole (imidazoles), fluconazole and itraconazole (triazoles) (Figure 3.1.). The key role of *CgPDR1* in *C. glabrata* azole resistance was further confirmed by MIC determination, through which the KUE100_ *Δcgpdr1* mutant was found to exhibit an 8-fold difference in terms of MIC levels for fluconazole and ketoconazole, relatively to the wild-type strain (Table 3.1.).

Studies in the related yeast *S. cerevisiae* have shown that Pdr1p forms a heterodimer with the transcription factor, Stb5p [137]. In *C. glabrata*, it was demonstrated that many of the genes upregulated by overexpression of *CgPDR1* were upregulated by deletion of *CgSTB5* [123]. Additionally, the overexpression of *CgSTB5* was shown to repress azole resistance, whereas it's deletion caused a modest increase in resistance [137]. As shown by spot assays (Figure 3.1.), although the KUE100_*Δcgstb5* mutant presented reduced growth in the control conditions when compared with the wild-type strain, there was no increase in susceptibly of this mutant in the presence of several azole antifungal drugs or even toward amphotericin B or flucytosine (Figure S2.). In fact, there seems to be a slight increase of this mutant resistance toward some of the azoles tested, such as tioconazole and miconazole, but these differences were not further analysed here. MIC assays showed no differences in terms of MIC levels for fluconazole, ketoconazole, amphotericin B or flucytosine between KUE100_ *Δcgstb5* mutant and the wild-type strain (Table 3.1.).

The deletion of *CgRPN4* was found to increase the susceptibility of *C. glabrata* toward all azole drugs tested (Figure 3.1.). This was confirmed by MIC assays, for fluconazole and ketoconazole, with a 4-fold difference in terms of MIC levels between the wild-type and the *Δcgrpn4* mutant strain (Table

3.1.). These results suggest a clear role of *CgRPN4* encoded protein as multidrug resistance determinant protein in *C. glabrata*.

The deletion of *CAGL0L04576g* (*CgYRM1_1*) seemed to increase the mutant susceptibility toward some azoles, mainly to ketoconazole (Figure 3.1.). However, the fluconazole and ketoconazole MIC levels exhibited by the ***Δcgyrm1_1*** deletion mutant was found to be similar to those displayed by the wild-type strain (Table 3.1.).

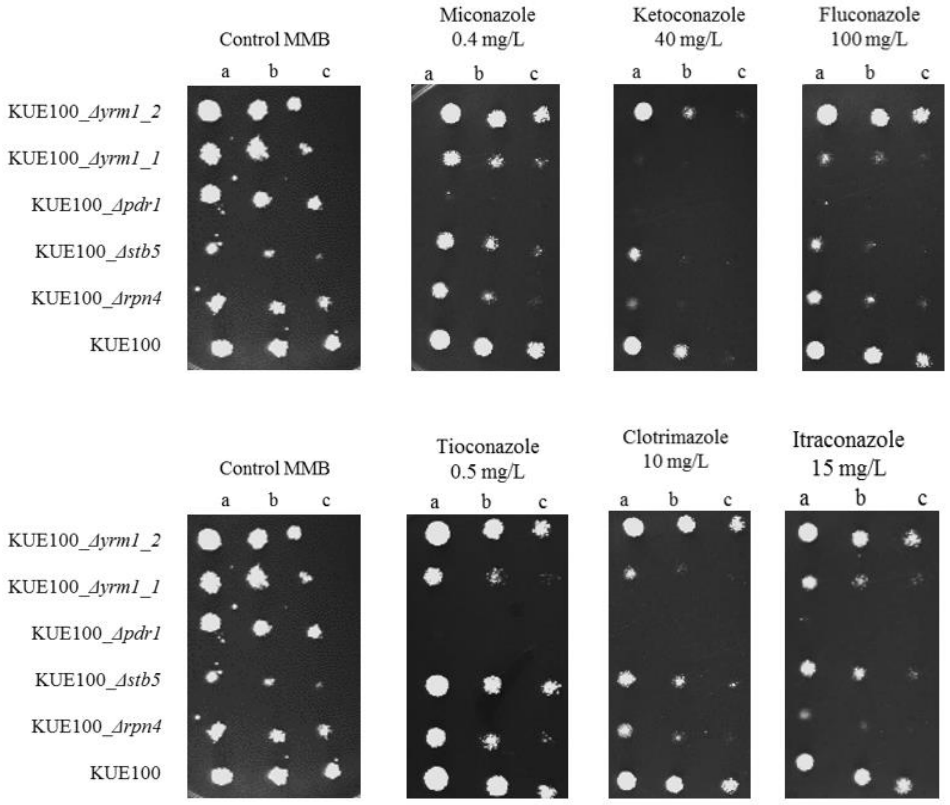

Figure 3. 1. | Comparison of the susceptibility toward inhibitory concentrations of several chemical stress inducers, at the indicated concentrations, of the *C. glabrata* wild-type KUE100, KUE100_*Δcgrpn4*, KUE100_*Δcgstb5*, KUE100_*Δcgpdr1*, KUE100_*Δcgyrm1_1*, KUE100_*Δyrm1_2* strains, in MMB plates through spot assays. The inocula were prepared as described in Section 2.2.1. Cell suspensions used to prepare the spots were 1:5 (b) and 1:25 (c) dilutions of the cell suspension used in (a). The displayed images are representative of at least three independent experiments.

Within the *C. glabrata* ORFs whose closest *S. cerevisiae* homologs play a role in oxidative stress response (Table S1.), none was found to play a role in *C. glabrata* resistance toward azole drugs, since all the mutants grew as the wild-type strain in the presence of several azole inhibitory concentrations (Figure S4.). Yet, the deletion of *CgYAP1* was found to slightly increase the susceptibility of *C. glabrata* to flucytosine (Figure 3.2.), although no difference between fluconazole and ketoconazole MIC levels was found between the ***Δcgyap1*** deletion mutant and its parental strain (Table 3.1.).

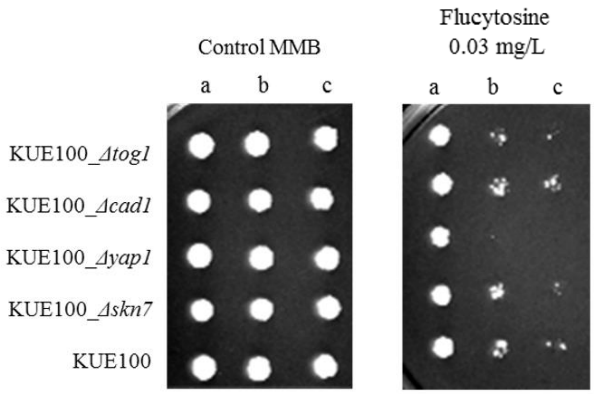

Figure 3. 2. | Comparison of the susceptibility to inhibitory concentrations of several chemical stress inducers, at the indicated concentrations, of the *C. glabrata* wild-type KUE100, KUE100_***Δcgskn7***, KUE100_***Δcgyap1***, KUE100_***Δcgcad1***, KUE100_***Δcgtog1*** strains, in MMB plates by spot assays. The inocula were prepared as described in Section 2.2.1. Cell suspensions used to prepare the spots were 1:5 (b) and 1:25 (c) dilutions of the cell suspension used in (a). The displayed images are representative of at least three independent experiments.

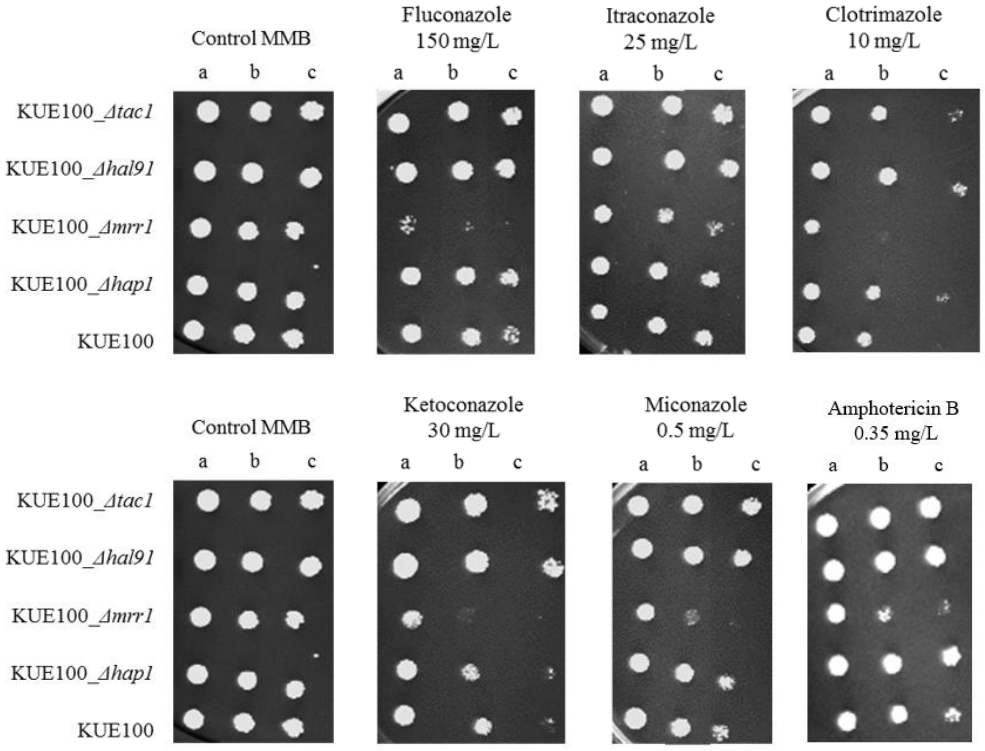

Figure 3. 3. | Comparison of the susceptibility to inhibitory concentrations of several chemical stress inducers, at the indicated concentrations, of the *C. glabrata* wild-type KUE100, KUE100_***Δcghap1***, KUE100_***Δcgmrr1***, KUE100_***Δcghal9***, KUE100_***Δcgtac1*** strains, in MMB plates by spot assays. The inocula were prepared as described in Section 2.2.1. Cell suspensions used to prepare the spots were 1:5 (b) and 1:25 (c) dilutions of the cell suspension used in (a). The displayed images are representative of at least three independent experiments.

The deletion of *CAGL0B03421g* (*CgMRR1*), the closest homolog to *C. albicans MRR1* (Table S2.), encoding an azole resistant determinant in this species, was found to increase the susceptibility of *C. glabrata* to all azole antifungal drugs tested (Figure 3.3.). Additionally, KUE100_*Δcgmrr1* mutant presented slightly increased susceptibility toward other antifungal drug families, namely to the polyene amphotericin B. As it is clear in Figure 3.3., the wild-type strain KUE100 grew in the tested drug concentrations, while the KUE100_*Δcgmrr1* mutant displayed growth limitation when exposed to all azoles tested and also to amphotericin B. On one hand, MIC assays confirmed the increased susceptibility of KUE100_*Δcgmrr1* mutant toward fluconazole and ketoconazole, with a 2-fold difference in terms of MIC levels, when compared to the wild-type. On the other hand, no differences in amphotericin B susceptibility were found between the mutant and the wild-type strains (Table 3.1.).

Within the *C. glabrata* ORFs whose closest *C. albicans* homologs play a role in biofilm formation (Table S2.), none was found to confer resistance to the tested antifungal drugs. Indeed, spot assays showed no differences in susceptibility of *C. glabrata* mutants and the wild-type strain toward all antifungals tested (Figure S6.). Moreover, MIC assays confirmed the absence of drug resistance-related phenotype of the mutant strains relatively to the wild-type (Table 3.1.).

Table 3. 1. | Minimal inhibitory concentration (MIC) assays. Minimum inhibitory concentration of fluconazole, ketoconazole, flucytosine, amphotericin B or caspofungin inhibiting growth at least 50% relative to the drug-free control (MIC_{50}) of *C. glabrata* single deletion mutants comparing to the wild-type. The displayed values are representative of three independent experiments.

Drug / Strain	Fluconazole (mg/L)	Ketoconazole (mg/L)	Flucytosine (mg/L)	Amphotericin B (mg/L)	Caspofungin (mg/L)
KUE100	16	1	1	0.125	0.125
KUE100_*Δcgrpn4*	4	0.25	1	0.125	0.0625
KUE100_*Δcgstb5*	16	1	1	0.125	0.125
KUE100_*Δcgpdr1*	2	0.125	1	0.125	0.125
KUE100_*Δcgyrm1_1*	16	1	1	0.125	0.125
KUE100_*Δcgyrm1_2*	16	1	1	0.125	0.125
KUE100_*Δcgyap1*	16	1	1	0.125	0.125
KUE100_*Δcgtog1*	16	1	1	0.125	0.125
KUE100_*Δcgcad1*	16	1	1	0.125	0.125
KUE100_*Δcgskn7*	16	1	1	0.125	0.125
KUE100_*Δcghap1*	16	1	1	0.125	0.125
KUE100_*Δcgmrr1*	8	0.5	1	0.125	0.125
KUE100_*Δcghal9*	16	1	1	0.125	0.125
KUE100_*Δcgtac1*	16	1	1	0.125	0.125
KUE100_*Δcgtec1_1*	16	1	1	0.125	0.125
KUE100_*Δcgtec1_2*	16	1	1	0.125	0.125
KUE100_*Δcgbcr1*	16	1	1	0.125	0.125
KUE100_*Δcgndt80*	16	1	1	0.125	0.125

In order to determine if any of the *C. glabrata* ORFs under analysis are involved in this pathogen resistance toward echinocandins, MIC assays were performed to compare the single deletion mutant's susceptibility toward caspofungin relatively to the wild-type strain. Only KUE100_ *Δcgrpn4* mutant displayed increased susceptibility when exposed to inhibitory concentrations of caspofungin, presenting a 2-fold difference in terms of MIC levels comparing to the wild-type (Table 3.1.). These results reinforce the role of *CgRPN4* encoded protein as multidrug resistance determinant protein in *C. glabrata*, since this mutant also demonstrated greatly increased susceptibility toward all azole antifungals tested.

3.1.2. Biofilm quantification assays

In order to screen for novel regulators of biofilm development, biofilm formation was assessed in the *C. glabrata* parental strain KUE100 and in KUE100_*Δrpn4*, KUE100_*Δstb5*, KUE100_*Δyrm1_1*, KUE100_*Δyrm1_2,* KUE100_*Δtog1*, KUE100_*Δhap1*, KUE100_*Δmrr1*, KUE100_*Δtac1*, KUE100_*Δyap1*, KUE100_*Δskn7* and KUE100_*Δcad1* derived single deletion mutants on a polystyrene surface using the crystal violet staining method, as described before in Section 2.2.2. Other *C. glabrata* genes predicted to be involved in biofilm formation, namely *CgTEC1_1, CgTEC1_2, CgBCR1 and CgNDT80* (Table S2.), were not included in this analysis as they had been previously demonstrated to be involved in this pathogen biofilm formation, thus they were not tested herein [Rui Filipe Ramos Santos, "Role and regulation of multidrug transporters in *Candida glabrata* virulence and antifungal drug resistance", MSc thesis in Microbiology, Instituto Superior Técnico, 2015.].

Biofilm formation is dependent on environmental conditions, such as growth medium, which can significantly affect not only biofilm architecture, but also the expression profile of several genes involved during the different stages of biofilm development [138]. Additionally, pH plays an important role, as *Candida spp*. may colonize different niches according to the environmental pH [139]. Thus, biofilm formation was quantified in both RPMI 1640 pH 4 and SDB pH 5.6 medium (Figure 3.4.).

Most of the strains tested showed greater biofilm production when the cells were grown in RPMI 1640 pH 4 rather than in SDB pH 5.6. In fact, previous studies reported that *C. glabrata* cells formed significantly thicker biofilms in RPMI 1640 medium compared with others, and perceives low pH as less stressful than higher pH, contrasting with *C. albicans*, which reinforce the greater biofilm production in RPMI 1640 pH 4 rather than in SDB pH 5.6 [139]. Additionally, SDB medium is less nutrient-rich than RPMI 1640 medium which mimics the composition of human fluids [140].

According to the results obtained, KUE100_*Δcghap1,* KUE100_*Δcgmrr1,* KUE100_*Δcgyap1,* KUE100_*Δcgcad1* and KUE100_*Δcgskn7* mutants presented significant ($p<0.05$) decreased biofilm formation in both RPMI and SDB medium compared to wild-type (Figure 3.4.A and D). KUE100_*Δcgtog1,* KUE100_*Δcgyrm1_2 and* KUE100_*Δcgstb5* mutant strains presented significantly increased biofilm formation when cells were cultured in SBD comparing to the wild-type, but not in RPMI (Figure 3.4.). In contrast, *Δcgrpn4* and *Δcgtac1* mutants displayed greatly decreased biofilm production in SDB whereas, in RPMI, the values equal or even exceeds those for wild-type.

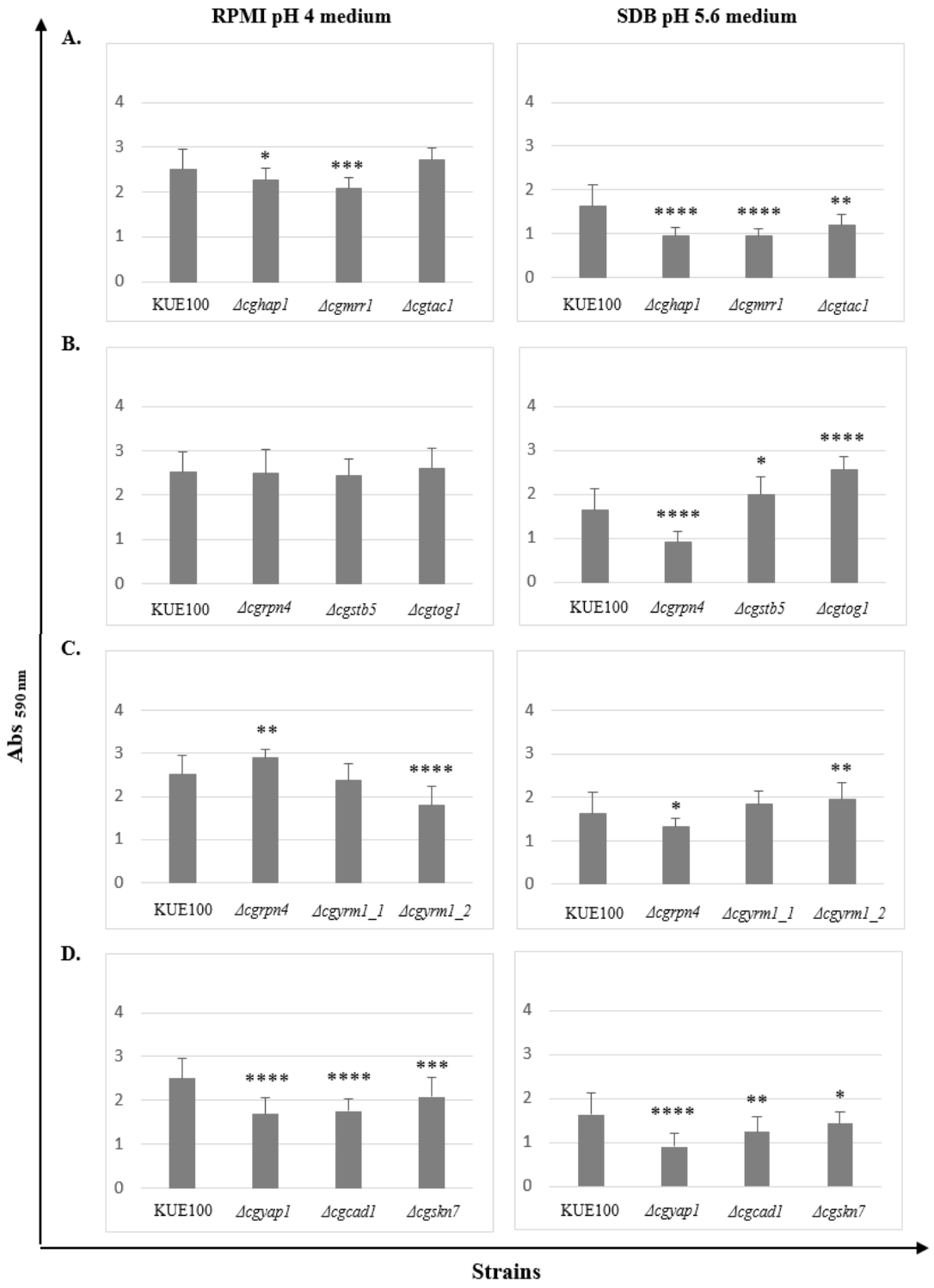

Figure 3. 2. | Biofilm formation followed by crystal violet staining and measurements of absorbance at 590 nm for the KUE100 wild-type strain and derived single deletion mutants KUE100_*Δcghap1*, KUE100_*Δcgmrr1*, KUE100_*Δcgtac1* **(A)**, KUE100_*Δcgrpn4*, KUE100_Δcgstb5, KUE100_Δcgtog1 **(B)**, KUE100_*Δcgrpn4*, KUE100_*Δcgyrm1_1*, KUE100_*Δcgyrm1_2* **(C)**, KUE100_*Δcgyap1*, KUE100_*Δcgcad1* and KUE100_*Δcgskn7* **(D)**. Cells were grown for 16h and the experiment was performed in SDB medium pH 5.6 and RPMI 1640 pH 4. In the bar chart, each bar corresponds to the level of biofilm formed in each sample. The average level of formed biofilm corresponds to at least 4 independent experiments. Standard deviations are represented by error bars. *p<0.05, **p<0.01, ***p<0.001 and ****p<0.0001.

3.2. Functional characterization of the CgRpn4 transcription factor

Given the attained results concerning azole susceptibility assays, the transcription factor CgRpn4 (encoded by ORF *CAGL0K01727g*) was selected for further studies. CgRpn4 is the *C. glabrata* homolog to the *S. cerevisiae RPN4* transcription factor, which is a stimulator of proteasomal gene expression transcriptionally regulated in response to various stresses. Although little is known about the *C. glabrata RPN4* homolog, it has been described as a putative transcription factor for proteasome genes and was found to be upregulated in azole-resistant strains. Therefore, its functional characterization was undertaken.

3.2.1. CgRpn4 expression confers resistance to azole antifungal drugs

It was shown that the deletion of *CgRPN4* dramatically increases the susceptibility toward the azole antifungal drugs clotrimazole, miconazole, ketoconazole, tioconazole (imidazoles); and fluconazole and itraconazole (triazoles) (Figure 3.1.). Therefore, the effect of *CgRPN4* overexpression in *C. glabrata* cells azole resistance was assessed through spot assays using inhibitory concentrations of fluconazole (100 to 150 mg/L) or ketoconazole (30 to 40 mg/L).

C. glabrata L5U1 (*cgura3Δ0*, *cgleu2Δ0*) cells were transformed with the cloning vector pGREG576 or the recombinant plasmid pGREG576_*MTI_CgRPN4* (constructed as described in Section 2.4.) as described in Section 2.3. To perform the susceptibility assays, those transformed cells were prepared as described in Section 2.6.

As it is clear in Figure 3.5., both *C. glabrata* cells harboring the cloning or the recombinant plasmid grew similarly in control conditions, with the L5U1 cells carrying the recombinant plasmid exhibiting a slightly slower growth when compared to those harboring the cloning vector. This might be due to the metabolic weight caused by the overexpression of the *CgRPN4*. However, when the cells were grown in the presence of inhibitory concentrations of the azole antifungals fluconazole and ketoconazole, only L5U1 cells overexpressing *CgRPN4* were able to grow. In fact, *C. glabrata* cells harboring the cloning vector were completely unable to growth in any of the antifungal-induced stress conditions tested. These results reinforce the key role of the transcription factor CgRpn4 as a key regulator of azole drug resistance in *C. glabrata*.

Additionally, the capability of *CgRPN4* gene expression to complement the absence of its *S. cerevisiae* homolog (*ScRPN4*) in BY4741_*Δrpn4* mutant cells was also assessed through spot assays using inhibitory concentrations of fluconazole (60 to 80 mg/L) or ketoconazole (15 to 20 mg/L). Drug concentrations used for *S. cerevisiae* antifungal susceptibility assays was lower than that used for *C. glabrata* since the last displays intrinsically higher resistance to azoles than *S. cerevisiae*.

The pGREG576_*CgRPN4* recombinant plasmid, used to express the *C. glabrata* homolog *CgRPN4* in *S. cerevisiae*, was prepared as described in Section 2.4.. *S. cerevisiae* BY4741 (*MATa, ura3Δ0, leu2Δ0, his3Δ1, met15Δ0*) and BY4741_*Δrpn4* cells were transformed with the cloning vector pGREG576 or the recombinant plasmid pGREG576_*CgRPN4* as described in Section 2.3. To perform the susceptibility assays, those transformed cells were prepared as described in Section 2.6.

As depicted in Figure 3.5., both wild-type and mutant strains harboring the cloning or recombinant plasmid grew similarly in control conditions, without antifungal drug exposure. On one hand, as expected, the growth of BY4741_*Δrpn4* cells carrying the cloning vector was strongly or even fully affected when the cells were grown in the presence of inhibitory concentrations of both fluconazole and ketoconazole, whereas the cells from the same strain harboring the recombinant plasmid were able to grow in those conditions. These results demonstrate that *CgRPN4* gene expression is able to complement the absence of its *S. cerevisiae* homolog (*ScRPN4*) in *S. cerevisiae* cells, suggesting that *ScRPN4* and *CgRPN4* are orthologous genes.

On the other hand, surprisingly, the overexpression of *CgRPN4* in BY4741 *S. cerevisiae* wild-type cells does not seem to bring any advantage concerning this organism drug resistance. BY4741 cells harboring the cloning vector demonstrated a slightly lower susceptibility toward inhibitory concentrations of both fluconazole and ketoconazole when compared to those overexpressing *CgRPN4*, through the recombinant plasmid.

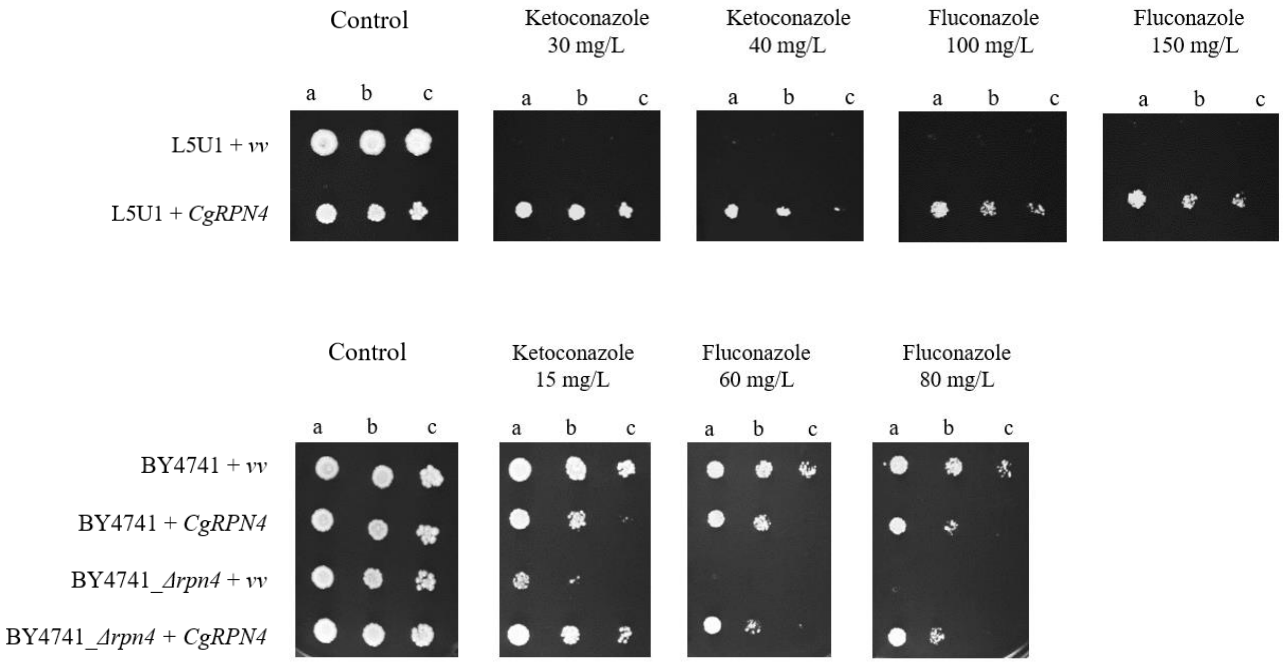

Figure 3. 3. | Comparison of the susceptibility to inhibitory concentrations of fluconazole or ketoconazole, at the indicated concentrations, of the *C. glabrata* L5U1 strain, harboring the pGREG576 cloning vector (*vv*) or the pGREG576_*MTI_CgRPN4* (*CgRPN4*) plasmid; of the *S. cerevisiae* BY4741strain, harboring the pGREG576 cloning vector (*vv*) or the pGREG576_*CgRPN4* (*CgRPN4*) plasmid; and of the *S. cerevisiae* BY4741_*Δrpn4*, harboring the pGREG576 cloning vector (*vv*) or the pGREG576_*CgRPN4* (*CgRPN4*) plasmid through spot assays. The inocula were prepared as described in Section 2.6. Cell suspensions used to prepare the spots were 1:5 (b) and 1:25 (c) dilutions of the cell suspension used in (a). The displayed images are representative of at least three independent experiments.

3.2.2. CgRpn4 expression and subcellular localization in *C. glabrata*

To address the issue of CgRpn4 transcription factor activation mechanisms, subcellular localization of CgRpn4p was assessed, using a GFP fusion, in *C. glabrata* cells. The localization of this transcription factor, in cells under control conditions, was compared to that in cells undergoing antifungal drug exposure.

To observe the subcellular localization of CgRpn4 transcription factor, *C. glabrata* cells harboring the pGREG576_*MTI_CgRpn4* plasmid were grown to mid-exponential phase in MMG-U and then transferred to the same medium containing 50 μM CuSO4, to promote expression in moderate controlled levels through the *MTI* promoter. The incubation time was defined as 6 hours to allow detectable protein expression levels, but not a high degree of overexpression which could lead to mis-localization. At a standard OD_{600nm} of 0.5 ± 0.05, cells were exposed to fluconazole or ketoconazole, for 1h, in order to see if the localization of CgRpn4 changes from control to azole-induced stress conditions.

C. glabrata cells expressing CgRpn4_GFP fusion protein were analysed by fluorescence microscopy and nuclear localization of the transcription factor was verified in both cells under control conditions (Figure 3.6.) and cells undergoing fluconazole or ketoconazole exposure (Figure 3.7.). To confirm that CgRpn4p nuclear localization verified in cells under control conditions was not a consequence of those cells being early stationary phase cells, its localization in exponential *C. glabrata* cells also was assessed. As displayed in both Figure 3.6 and Figure 3.7., CgRpn4p presents nuclear localization in all the tested conditions.

In order to sustain these observations, a quantitative analysis was undertaken to determine the ratio of cells with transcription factor nuclear localization relatively to the total cells presenting fluorescence in different preparations of each condition tested. A total of ± 400 *C. glabrata* fluorescent cells was analysed per condition. Concerning control conditions, as displayed in Figure 3.8., only 57.5% of exponential phase cells analysed presented CgRpn4 nuclear localization, in contrast with stationary phase cells in which more than 85% of the cells showed pronounced transcription factor nuclear localization. Under azole-induced stress conditions, the transcription factor remained in the cell's nucleus, with 90% of both fluconazole and ketoconazole-stressed cells presenting nuclear CgRpn4 accumulation. These results suggest that, although a large proportion of the population displays CgRpn4 accumulation in the nucleus, there is a certain degree of increased nuclear accumulation of CgRpn4 under stress, both that induced by antifungal drugs or by reaching stationary phase of growth.

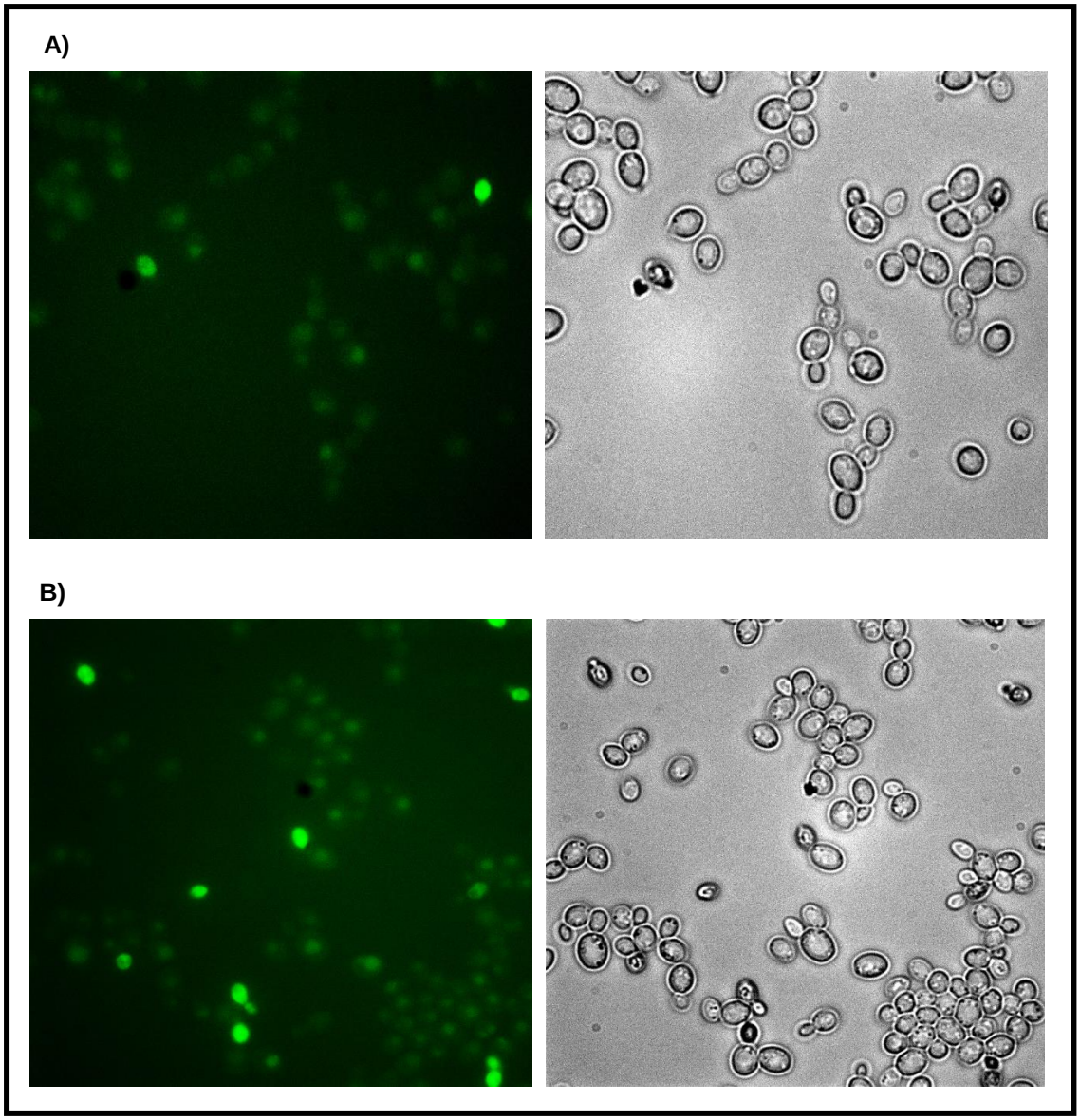

Figure 3. 4. | Fluorescence of exponential **(A)** and stationary **(B)** phase L5U1 *C. glabrata* cells, in control conditions, harboring the pGREG_*MTI_CgRPN4* vector, after copper-induced recombinant protein production.

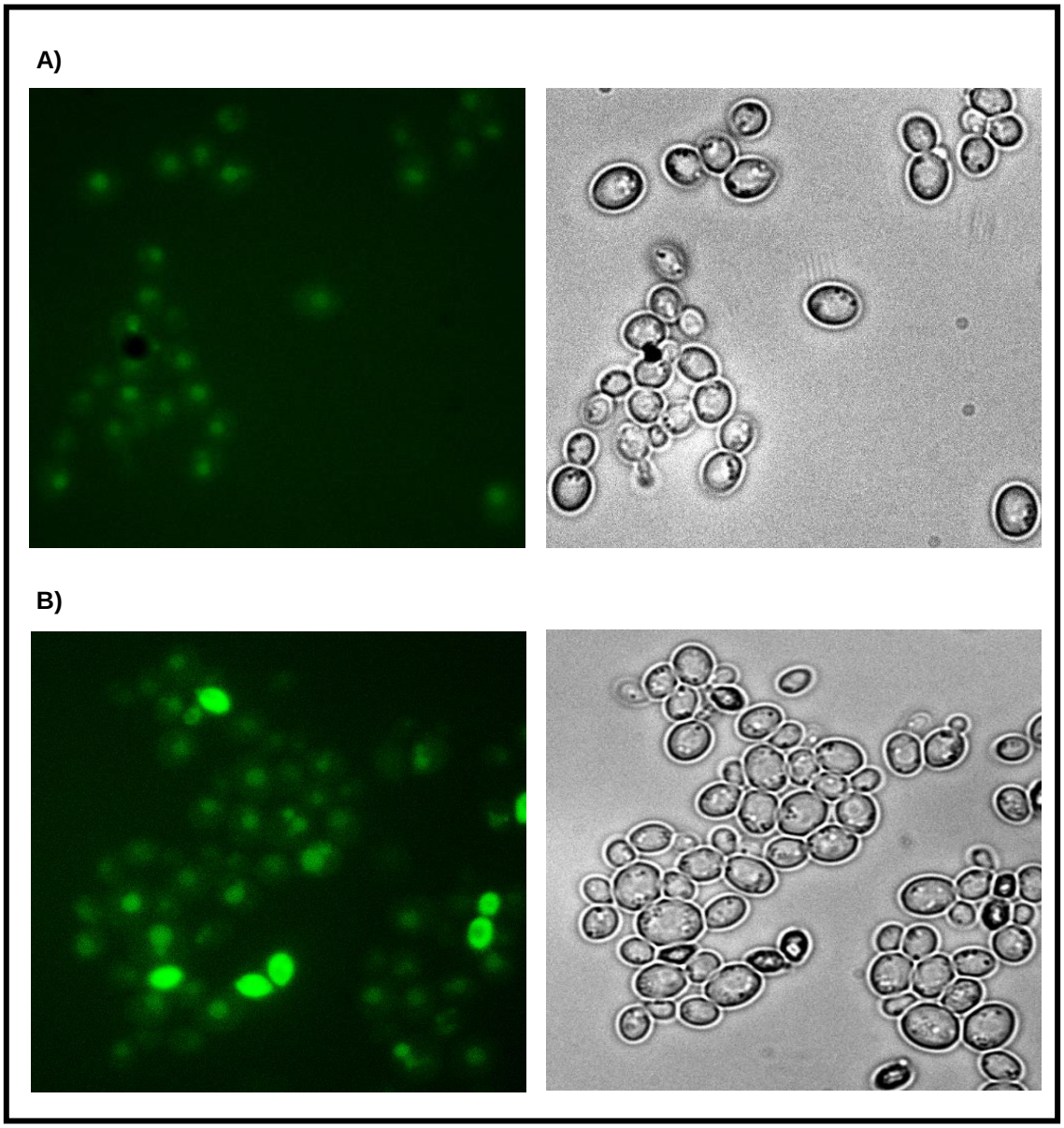

Figure 3. 5. | Fluorescence of exponential phase L5U1 *C. glabrata* cells harboring the pGREG_*MTI_CgRPN4* plasmid, after copper-induced recombinant protein production, under fluconazole-induced stress conditions **(A)** or ketoconazole-induced stress conditions **(B)**.

These findings represent a first step into the functional characterization of the *C. glabrata* putative transcription factor for proteasome genes CgRpn4, its nuclear localization, especially in cells underwent azole drug exposure, enhances its predicted role as stimulator of proteasomal gene expression transcriptionally regulated in response to environmental stresses.

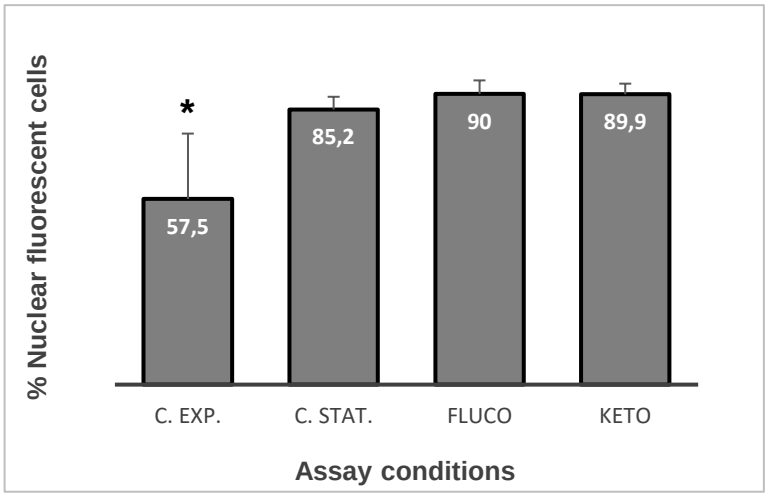

Figure 3. 6. | Fraction of *C. glabrata* cells presenting nuclear localized fluorescence. L5U1 cells harboring the pGREG*_MTI_CgRPN4* plasmid, after copper-induced recombinant protein production, were analysed by fluorescence microscopy under control conditions and under fluconazole-induced and ketoconazole-induced stress conditions (Section 2.5.). In the bar chart, each bar corresponds to the percentage of cells presenting nuclear localized fluorescence from a total of ± 400 control stationary phase, control exponential phase, fluconazole-stressed and ketoconazole-stressed cells. *p<0.05.

3.3. RNA-seq analysis

Herein, the effect of *CgRPN4* deletion in the transcriptome-wide response of *C. glabrata* cells to mild fluconazole-induced stress conditions was assessed through RNA-sequencing.

A comparison between the genes up or downregulated in the ***Δcgrpn4*** deletion mutant relatively to the wild-type strain, in the same conditions (control or mild fluconazole-induced inhibition), was performed. RNA-seq data was analysed for each condition, selecting the upregulated and downregulated genes. Those were identified using DESeq2 [135] with an adjusted p-value threshold of 0.01 and a $\log_2$ fold change threshold of -1.0 and 1.0. Differentially expressed genes in the *CgRPN4* mutant relatively to the wild-type are displayed in Table 3.2., for control conditions, and in Table 3.3. for fluconazole-induced stress conditions, along with their *S. cerevisiae* closest homologue described function, when it applies.

The experiment was carried out in order to see the mild fluconazole inhibition effect in global gene expression in wild-type and ***Δcgrpn4*** mutant *C. glabrata* cells. However, the drug concentration was not sufficiently inhibitory to induce a strong defense response in wild-type cells. This is proved by the absence of up or downregulated genes in the wild-type cells when stressed with fluconazole, comparing to control conditions. Nonetheless, the results obtained concerning the genes that are up or downregulated in the ***Δcgrpn4*** single deletion mutant, in both control and fluconazole-induced stress conditions, enabled the identification of a short list of genes whose expression was seen to depend on the CgRpn4 transcription factor. Altogether, CgRpn4 was found to activate the expression of 9 genes while repressing, possibly indirectly, 32 genes (Figure 3.9.). Among the CgRpn4 upregulated genes, three *C. glabrata* ORFs (*CAGL0M08552g*, *CAGL0D05214g* and *CAGL0D04840g*) have a close *S. cerevisiae* homolog known to be involved in azole resistance.

Table *3. 2.* | RNA-seq analysis. *C. glabrata* gene ID*, S. cerevisiae* homolog, differential expression in the *CgRPN4* mutant (*Δrpn4*) vs in the wild-type (log_2 fold change) and description for each gene under control conditions. Descriptions were obtained in SGD (https://www.yeastgenome.org/), for *S. cerevisiae* homologs, and in CGD (http://www.candidagenome.org/.), for some *C. glabrata* ORFs.

	***C. glabrata* gene ID**	***S. cerevisiae* closest homolog name**	**Differential expression in *Δrpn4* vs Wt under control conditions (log_2 Fold Change)**	**Description of the function of the *C. glabrata* protein or of its *S. cerevisiae* homolog**
Mitochondrial regulator	***CAGL0H04191g***	*ATP18*	2.67	Uncharacterized. *S. cerevisiae* homolog encodes a subunit of the mitochondrial F1F0 ATP synthase required for ATP synthesis; termed subunit I or subunit j.
Plasma membrane organization activity	***CAGL0L08008g***	*PMP1*	2.41	Uncharacterized. *S. cerevisiae* homolog encodes a regulatory subunit for the plasma membrane H(+)-ATPase Pma1p.
	CAGL0H02563g	*HOR7*	1.57	Uncharacterized. *S. cerevisiae* homolog encodes protein of unknown function which overexpression suppresses Ca^{2+} sensitivity of mutants lacking inositol phosphorylceramide mannosyltransferases Csg1p and Csh1p; transcription is induced under hyperosmotic stress.
	CAGL0M08552g	*PMP3*	1.53	Uncharacterized. *S. cerevisiae* homolog encodes a small plasma membrane protein; confers resistance to amphotericin B and is a potential target of this common antifungal drug; deletion causes hyperpolarization of the plasma membrane potential.
Protein Trafficking	***CAGL0C05461g***	*OST4*	1.36	Uncharacterized. *S. cerevisiae* homolog encodes a subunit of the oligosaccharyltransferase complex of the ER lumen; complex catalyzes protein asparagine-linked glycosylation.
Metal homeostasis	***MTI* (*CAGL0D01265g*)**	-	1.31	Copper-binding metallothionein, involved in sequestration of metal ions; inducible by copper and silver; gene used for molecular typing of *C. glabrata* strain isolates.
	CAGL0D05632g	*COX17*	1.28	Uncharacterized. *S. cerevisiae* homolog encodes a copper metallochaperone that transfers copper to Sco1p and Cox11p.

RNA Metabolism	***CAGL0B02137r***	**-**	1.45	Uncharacterized. U5 snRNA.
	CAGL0B03520r	**-**	1.39	Uncharacterized. Novel ncRNA.
	CAGL0K09823g	*YSF3*	1.25	Uncharacterized. *S. cerevisiae* homolog encodes a component of the SF3b subcomplex of the U2 snRNP; essential protein required for splicing and for assembly of SF3b.
	CAGL0K01961r	-	-1.18	Uncharacterized. ncRNA scR1 domain IV (SRP RNA).
	CAGL0D04840g	*MSS18*	-1.49	Uncharacterized. *S. cerevisiae* homolog encodes a nuclear encoded protein needed for splicing of mitochondrial intron.
	RDN25-1 (*CAGL0L13365r*)	-	-1.91	Uncharacterized. 25S rRNA.
Unknown function	***CAGL0I04328g***	*YJL133C-A*	1.65	Uncharacterized. *S. cerevisiae* homolog, also uncharacterized, encodes a putative protein of unknown function.
	CAGL0L06930g	*YDL085C-A*	1.21	Uncharacterized. S. cerevisiae homolog, also uncharacterized, encodes a putative protein of unknown function.
	CAGL0B05148g	-	1.09	Uncharacterized.
	CAGL0M05593g	-	1.01	Uncharacterized. ORF has domain(s) with predicted endoplasmic reticulum localization.
	CAGL0J07876g	*RTC4*	-1.09	Uncharacterized. *S. cerevisiae* homolog encodes a protein of unknown function.

Table 3. 3. | RNA-seq analysis. *C. glabrata* gene ID, *S. cerevisiae* homolog, differential expression in the *CgRPN4* mutant (*Δrpn4*) vs in the wild-type (log_2 fold change) and description for each gene under mild fluconazole-induced stress conditions. Descriptions were obtained in SGD (https://www.yeastgenome.org/), for *S. cerevisiae* homologs, and in CGD (http://www.candidagenome.org/.), for some *C. glabrata* ORFs.

	***C. glabrata* protein (ORF) name**	***S. cerevisiae* ortholog name**	**Differential expression in *Δrpn4* vs wt under fluconazole-induced stress conditions (log_2 Fold Change)**	**Description of the function of the *C. glabrata* protein or of its *S. cerevisiae* homolog**
Mitochondrial regulator	***CAGL0D00748g***	*COX9*	2.92	Uncharacterized. *S. cerevisiae* homolog encodes a subunit VIIa of cytochrome C oxidase (Complex IV); Complex IV is the terminal member of the mitochondrial inner membrane electron transport chain.
	CAGL0H04191g	*ATP18*	2.69	Uncharacterized. *S. cerevisiae* homolog encodes a subunit of the mitochondrial F1F0 ATP synthase required for ATP synthesis; termed subunit I or subunit j.
	CAGL0A03036g	*ATP17*	1.38	Uncharacterized. *S. cerevisiae* homolog encodes a subunit f of the F0 sector of mitochondrial F1F0 ATP synthase required for ATP synthesis.
	CAGL0H02491g	*COX7*	2.36	Uncharacterized. *S. cerevisiae* homolog encodes a subunit VII of cytochrome C oxidase (Complex IV); Complex IV is the terminal member of the mitochondrial inner membrane electron transport chain.
Plasma membrane organization activity	***CAGL0L08008g***	*PMP1*	4.14	Uncharacterized. *S. cerevisiae* homolog encodes a regulatory subunit for the plasma membrane H(+)-ATPase Pma1p.
	CAGL0H02563g	*HOR7*	2.13	Uncharacterized. *S. cerevisiae* homolog encodes protein of unknown function which overexpression suppresses Ca^{2+} sensitivity of mutants lacking inositol phosphorylceramide mannosyltransferases Csg1p and Csh1p; transcription is induced under hyperosmotic stress.

Plasma membrane organization activity	***CAGL0M08552g***	*PMP3*	2.07	Uncharacterized. *S. cerevisiae* homolog encodes a small plasma membrane protein; confers resistance to amphotericin B and is a potential target of this common antifungal drug; deletion causes hyperpolarization of the plasma membrane potential.
Protein trafficking	***CAGL0C05461g***	*OST4*	3.60	Uncharacterized. *S. cerevisiae* homolog encodes a subunit of the oligosaccharyltransferase complex of the ER lumen; complex catalyzes protein asparagine-linked glycosylation.
	CAGL0F02513g	*NCE101*	1.16	Uncharacterized. *S. cerevisiae* homolog encodes a protein of unknown function involved in secretion of proteins that lack classical secretory signal sequences.
	CAGL0J03245g	*YOS1*	1.05	Uncharacterized. *S. cerevisiae* homolog encodes an integral membrane protein required for ER to Golgi transport; localized to the Golgi, the ER, and COPII vesicles; interacts with Yip1p and Yif1p.
	CAGL0C02607g	*VPS33*	-1.62	Uncharacterized. *S. cerevisiae* homolog encodes a ATP-binding protein that is a subunit of the HOPS and CORVET complexes; essential for protein sorting, vesicle docking, and fusion at the vacuole; binds to SNARE domains.
Metal homeostasis	***MTI (CAGL0D01265g)***	-	2.26	Copper-binding metallothionein, involved in sequestration of metal ions; inducible by copper and silver; gene used for molecular typing of *C. glabrata* strain isolates.
	CAGL0D05632g	*COX17*	1.43	Uncharacterized. *S. cerevisiae* homolog encodes a copper metallochaperone that transfers copper to Sco1p and Cox11p.
RNA metabolism	***CAGL0K09823g***	*YSF3*	1.61	Uncharacterized. *S. cerevisiae* homolog encodes a component of the SF3b subcomplex of the U2 snRNP; essential protein required for splicing and for assembly of SF3b.

RNA Metabolism	***CAGL0I06721g***	*LSM5*	1.59	Uncharacterized. *S. cerevisiae* homolog encodes a (Like Sm) protein; part of heteroheptameric complexes (Lsm2p-7p and either Lsm1p or 8p): cytoplasmic Lsm1p complex involved in mRNA decay; nuclear Lsm8p complex part of U6 snRNP and possibly involved in processing tRNA, snoRNA, and rRNA.
	CAGL0B03520r	-	1.49	Uncharacterized. Novel ncRNA.
	TLC1 (CAGL0I04700r)	-	1.31	Telomerase RNA.
	CAGL0J07953r	-	1.28	Uncharacterized. Novel ncRNA.
	CAGL0A04532r	-	1.22	Uncharacterized. Novel ncRNA.
	CAGL0B02137r	-	1.21	Uncharacterized. U5 snRNA.
	CAGL0K00308r	-	1.06	Uncharacterized. Novel ncRNA.
	CAGL0K01961r	-	-1.22	Uncharacterized. ncRNA scR1 domain IV (SRP RNA).
	CAGL0D04840g	*MSS18*	-1.75	Uncharacterized. *S. cerevisiae* homolog encodes a nuclear encoded protein needed for splicing of mitochondrial intron.
	RDN25-1 (CAGL0L13365r)	-	-4.65	25S rRNA.
Amino acid metabolism	***CAGL0L02937g***	*HIS3*	-1.26	Uncharacterized. *S. cerevisiae* homolog encodes a putative imidazoleglycerol-phosphate dehydratase which catalyzes the sixth step in histidine biosynthesis.
Ribosomal Biogenesis and translation	***CAGL0D05214g***	*RPL29*	2.39	Uncharacterized. *S. cerevisiae* homolog encodes a ribosomal 60S subunit protein L29; not essential for translation, but required for proper joining of large and small ribosomal subunits and for normal translation rate.

Ribosomal Biogenesis and translation	***CAGL0L08110g***	-	1.93	Uncharacterized. ORF has domain(s) with predicted structural constituent of ribosome activity, role in translation and ribosome localization.
	CAGL0K06033g	*TMA7*	1.27	Uncharacterized. *S. cerevisiae* homolog encodes a protein of unknown function that associates with ribosomes; null mutant exhibits translation defects, altered polyribosome profiles, and resistance to the translation inhibitor anisomcyin; protein abundance increases in response to DNA replication stress.
	CAGL0G09713g	*RPS30B*	1.19	Uncharacterized. *S. cerevisiae* homolog encodes a protein component of the small (40S) ribosomal subunit; protein abundance increases in response to DNA replication stress.
Unknown function	***CAGL0I04328g***	*YJL133C-A*	1.87	Uncharacterized. *S. cerevisiae* homolog, also uncharacterized, encodes a putative protein of unknown function.
	CAGL0G09262g	-	1.59	Uncharacterized. Protein of unknown function.
	CAGL0L06930g	*YDL085C-A*	1.37	Uncharacterized. *S. cerevisiae* homolog, also uncharacterized, encodes a putative protein of unknown function.
	CAGL0B00594g	*YCL048W-A*	1.36	Uncharacterized. *S. cerevisiae* homolog, also uncharacterized, encodes a putative protein of unknown function.
	CAGL0M05593g	-	1.09	Uncharacterized. ORF has domain(s) with predicted endoplasmic reticulum localization.
	CAGL0B05148g	-	1.07	Uncharacterized. Protein of unknown function.
	CAGL0C02387g	*YER034W*	-1.24	Uncharacterized. *S. cerevisiae* homolog, also uncharacterized, encodes a protein of unknown function; non-essential gene; expression induced upon calcium shortage; protein abundance increases in response to DNA replication stress.

Unknown function	***CAGL0J07876g***	*RTC4*	-1.98	Uncharacterized. *S. cerevisiae* homolog encodes a protein of unknown function.
	CAGL0D00869g	-	-3.78	Uncharacterized. Protein of unknown function.

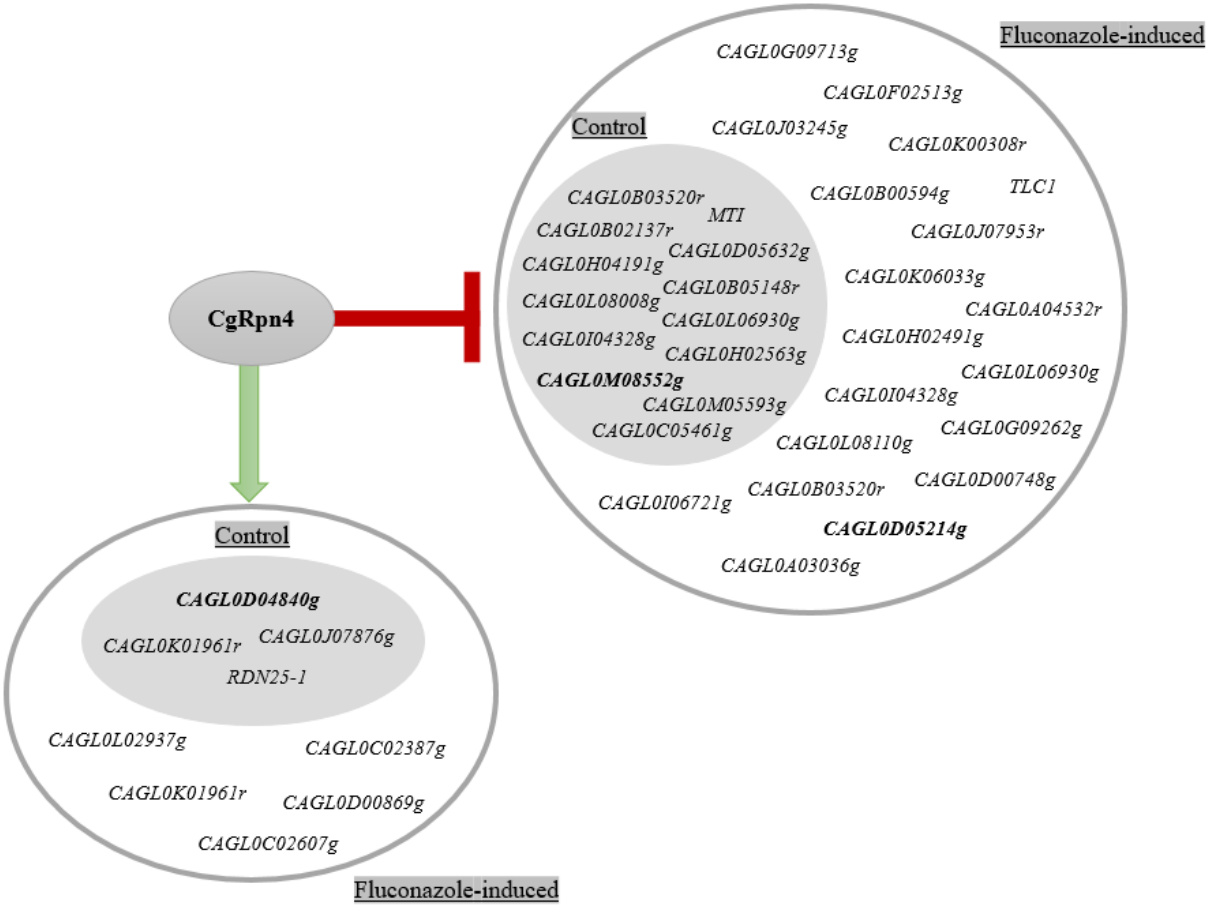

Figure 3. 7. | RNA- seq analysis. *C. glabrata* ORFs directly or indirectly up (green arrow) and downregulated (red lines) by the transcription factor CgRpn4. The ORFs downregulated by CgRpn4 are those demonstrated to be upregulated in *Δcgrpn4* mutant *C. glabrata* cells which transcriptome was analysed through RNA-seq in both control (grey circle) and fluconazole-induced stress conditions (white circle). The *C. glabrata* ORFs highlighted in bold are those which *S. cerevisiae* closest homologue is involved in this organism's resistance toward azoles.

The deletion of *MSS18*, *S. cerevisiae* closest homolog to *CAGL0D04840g*, was found to increase fluconazole resistance [141]. In the same way, the deletion of *RPL29*, *S. cerevisiae* closest homolog to *CAGL0D05214g*, was demonstrated to increase *S. cerevisiae* resistance toward miconazole [142]. In contrast, the deletion of *PMP3*, *S. cerevisiae* closest homolog to *CAGL0M08552g*, leads to an increased susceptibility to miconazole. Interestingly, the *C. glabrata RPL29* homolog was found to be down-regulated via *CgRpn4* in cells under fluconazole-induced stress conditions, an observation that could partially explain the *Δcgrpn4* azole susceptibility phenotype.

The ORFs found to be up and downregulated by CgRpn4, either in control conditions (Figure 3.10.) or mild fluconazole-induced stress conditions (Figure 3.11.), were grouped into predicted functional clusters based on the function of their *S. cerevisiae* closest homologs, or in some cases based on the description of the *C. glabrata* ORFs.

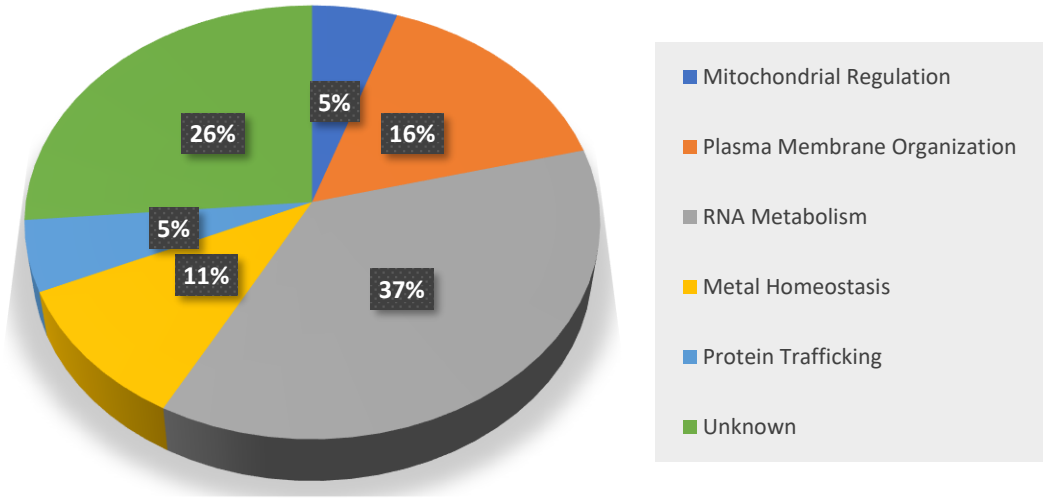

Figure 3. 8. | Major functional groups found to have significant expression changes in the *C. glabrata CgRNP4* deletion mutant relatively to the wild-type strain under control conditions.

In both control and fluconazole-induced stress conditions, the majority of genes found to have significant expression changes in the *C. glabrata RPN4* deletion mutant relatively to the wild-type are involved in RNA metabolism, constituting 37% of the ORFs up or downregulated in the mutant under control conditions and 29% of the ORFs up or downregulated in the mutant under fluconazole-induced stress conditions. Ribosomal biogenesis and translation associated ORFs were only found to have significant expression changes in mutant cells under fluconazole exposure (10%), as well as ORFs involved in amionacid metabolism (3%).

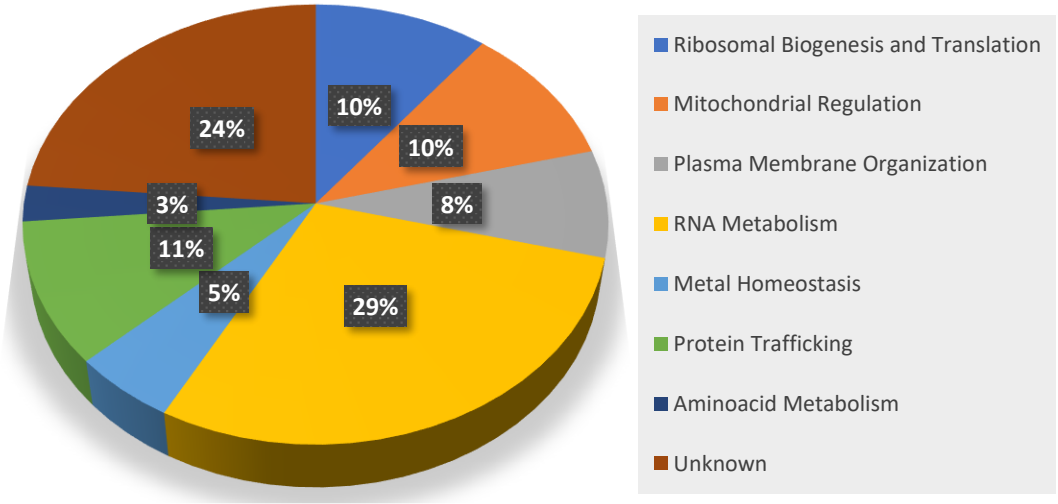

Figure 3. 9. | Major functional groups found to have significant expression changes in the *C. glabrata CgRPN4* deletion mutant relatively to the wild-type strain under mild fluconazole-induced stress conditions.

Significant expression changes in metal homeostasis, plasma membrane organization activity and mitochondrial regulation related ORFs, in both control and fluconazole-induced stress conditions, might be due to the stress induced by the absence of *CgRPN4*, since it is a predicted transcription factor involved in proteasomal genes activation its absence lead to protein degradation difficulties which might induce different stress in those mutant cells. Protein trafficking related ORFs presented significant expression changes specially in cells under drug exposure, 11% against 5% in cells under control conditions. ORFs with unknown function constitutes the second majority of genes with significant expression changes in both conditions tested. Those ORFs are uncharacterized and have no homolog in the closely related yeast *S. cerevisiae*.

To further analysed if the influence of CgRpn4 on the ORFs found to be downregulated in the *Δcgrpn4* mutant is through direct binding of the transcription factor to the ORFs promoter regions, those regions were analysed using bioinformatic tools. ORFs promoter regions were obtained using Pathoyeastract (http://www.pathoyeastract.org/) and RSAT: oligo-analysis (http://floresta.eead.csic.es/rsat/oligo-analysis_form.cgi) was used to search for binding motifs in those sequences.

Table 3. 5. | *S. cerevisiae* Rpn4 known binding motifs. The binding motif sequences were obtained in the Yeastract database (http://www.yeastract.com/index.php) and consensus sequences are represented according to the IUPAC frequency table (Table S3.).

***S. cerevisiae* Rpn4 binding motifs**
GGTGGCAAA
CGCCACc
aCGCCACCCtaatc
HccgCCaC
HGCCACHg
gHGCCACH

RSAT: oligo-analysis provides a series of modular computer programs specifically designed for the detection of regulatory signals in non-coding sequences. However, since little is known about *C. glabrata* regulatory network, the background model used to search for binding motifs in the input *C. glabrata* ORFs promoter regions was the closely related yeast *S. cerevisiae*. The software searched for oligomers lengths from 6 to 8 nucleotides in both DNA strands and combined the reverse complements together in the output. Purge removed redundant sequences from the *C. glabrata* ORFs FASTA file. This is recommended in order to prevent highly similar sequences distorting the search for motifs.

After analysing the promoter regions of the 6 CgRpn4 upregulated *C. glabrata* protein encoding ORFs, the software found a total 17 different enriched motifs with lengths from 6 to 8 nucleotides (Figure 3.12.). With 6, 7 and 8 nucleotides length, 2080, 8192 and 32896 possible oligomers, respectively, were tested for significance, with an E- value minor than 1. RSAT bioinformatic tool displayed the number of

observed occurrences for each binding motif, and the correspondent number of expected occurrences based on random nucleotide distribution in the promoter regions under study (Table S7.). The same motif can be found several times in the same promoter region, meaning that the number of occurrences does not necessarily demonstrate that a specific binding site is present in more sequences of the input than another. In Figure 3.12., the different binding motifs found using the software are displayed from the one which had the highest occurrence significance to the one which had the lowest.

Once having the transcription factor binding motifs predicted to exist in the upstream region of each CgRpn4 upregulated ORFs, a search for conserved consensus sequences of *S. cerevisiae* Rpn4 known binding motifs (Table 3.5.) was performed based on the predicted oligomers. GCCAC is the most significant part of the known ScRpn4 binding sites, being present in the consensus sequence of 5 of the 6 binding motifs known for this transcription factor. However, this oligomer sequence was not found in the predicted binding motifs of *C. glabrata* ORFs. The longest consensus sequence found in these predicted motifs that might correspond to a conserved part of known ScRpn4 binding motifs was CCAC (highlighted in grey in Figure 3.12.). This 4-nucleotide long sequence was found in 4 differently predicted binding motifs, although with different associated-significance. However, 4 nucleotide length consensus sequence has a high random nucleotide distribution associated.

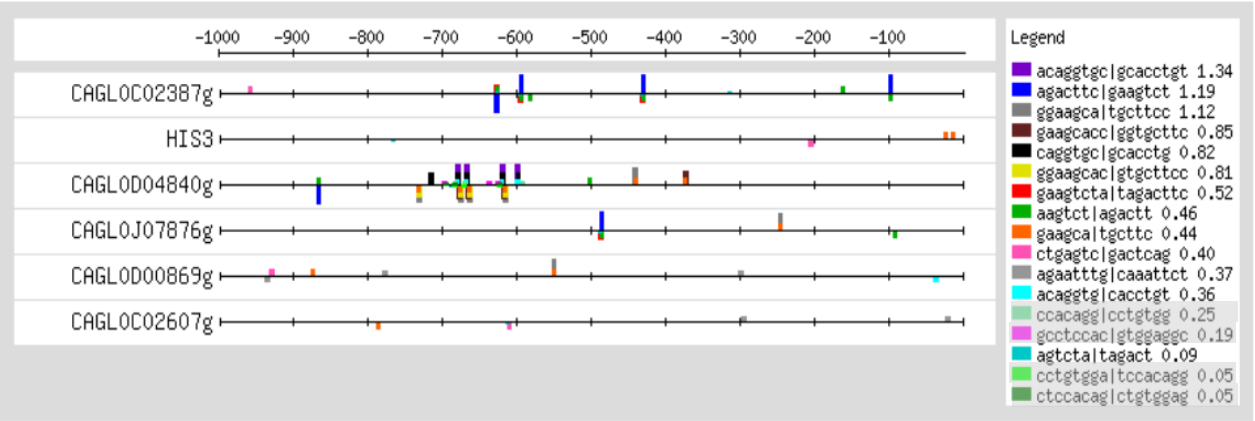

Figure 3. 10. | RSAT -feature-map. The map, obtained in RSAT: oligo-analysis, represents DNA sequences (oligomers) located upstream each CgRpn4 upregulated *C. glabrata* ORFs of the input. Each regulatory site constitutes a feature. The oligomers that have conserved parts of *S. cerevisiae* Rpn4 known binding motifs are highlighted in grey.

Within the 17 different binding motifs found to be enriched in CgRpn4 upregulated *C. glabrata* ORFs promoter regions, GAAGCA and AGTCTA were found in 5 of the 6 inputted upstream regions (Figure 3.13.), suggesting that these consensus sequences may be part of CgRpnp4 binding sites in *C. glabrata*. However, although there is no sequence similarity with known ScRpn4 binding motifs, *CgRPN4* gene expression was able to complement the absence of its *S. cerevisiae* homolog *ScRPN4* in BY4741_*Δrpn4* cells, suggesting that Rpn4 binding site cannot be completely different in both organisms.

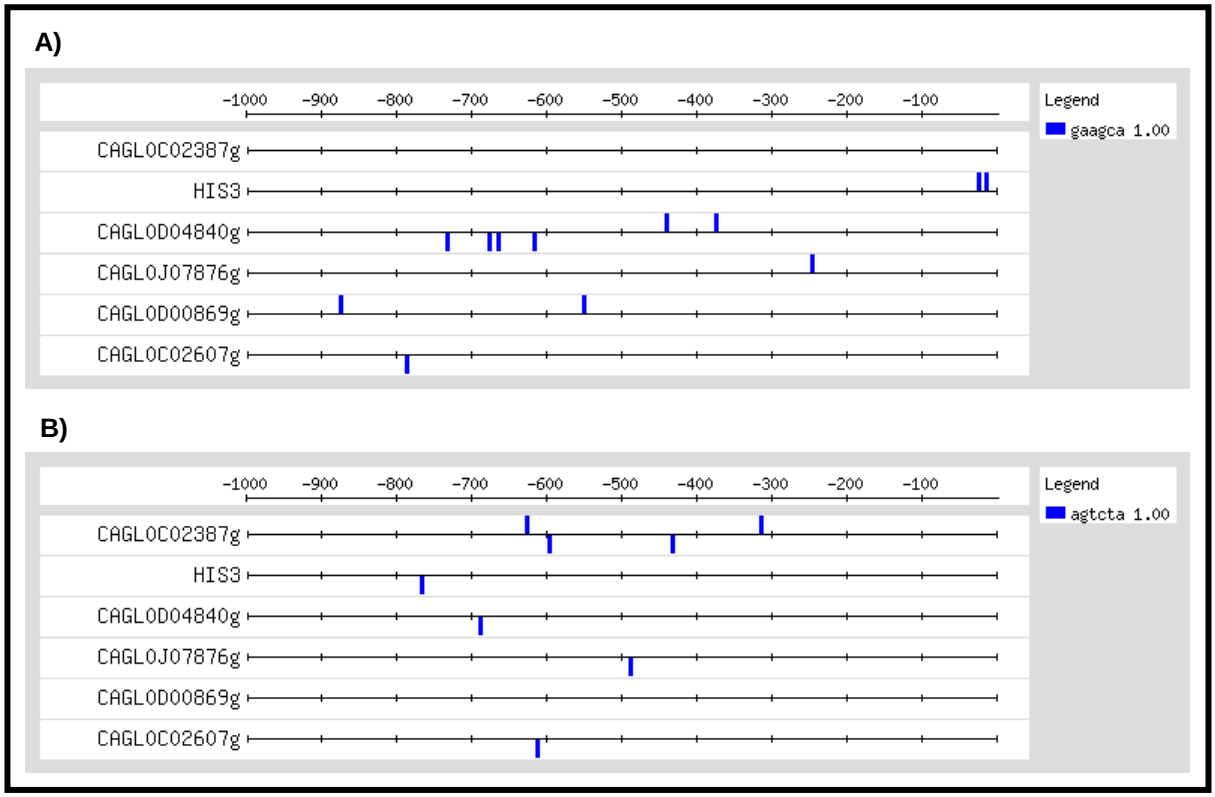

Figure 3. 11. | RSAT -feature-map. The map, obtained in RSAT: oligo-analysis, represents DNA sequences (oligomers) located upstream each CgRpn4 upregulated *C. glabrata* ORFs of the input. Each regulatory site constitutes a feature. GAAGCA **(A)** and AGTCTA **(B)** are present in all CgRpn4 upregulated *C. glabrata* ORFs upstream regions except for *CAGL0C02387g* and *CAGL0D00869g*, respectively.

4. Discussion

In this study, the first phenotypic screening on seventeen uncharacterized *C. glabrata* predicted transcription factors was undertaken in order to identify new players involved in pathogenesis related phenotypes. This analysis led to functional characterization of the *C. glabrata* CgRpn4 transcription factor, in the context of azole drug resistance.

The seventeen transcription factors were selected for their similarity to *C. albicans* transcription factors involved in multidrug resistance and biofilm formation, or their similarity to *S. cerevisiae* transcription factors involved in multidrug resistance and oxidative stress response.

Many *Candida* infections involve the formation of biofilms on implanted devices such as indwelling catheters or prosthetic heart valves. The major problem in treating these biofilm-associated infections is the increased resistance of the fungal population to most classes of antifungals. Therefore, the seventeen *C. glabrata* ORFs were screened for possible role in this pathogen biofilm formation.

CgRpn4 was demonstrated to play an important role in *C. glabrata* biofilm production under less nutritious conditions (SDB medium). This might occur due to the fact that when nutrients are exhausted, yeast cells enter stationary phase during which the synthesis of most proteins is attenuated and proliferation ceases. While biosynthetic processes are generally downregulated in stationary phase, prior studies have pointed to enhanced protein degradation during adaptation to nutrient deprivation in yeast [143]. Components of the ubiquitin-proteasome pathway are induced during this stage in order to degrade unneeded or damaged proteins. In fact, it was previously demonstrated that the impairment of proteasomal activity (using tea polyphenols) contributes to cellular metabolic and structural disruptions that expedite the inhibition of biofilm formation and maintenance by *C. albicans* [126]. However, relation with the growth media has not yet been reported. Therefore, since *CgRPN4* is a putative transcription factor for proteasomal genes, its absence in *C. glabrata* cells grown under less nutritious conditions impairs the proteasome pathway crucial for starving cells survival. Consequently, biofilm formation is probably also affected.

CgYAP1 was shown to be important for biofilm formation/maintenance in both rich and less nutritious medium. Several transcription factors involved in oxygen homeostasis and oxidative stress responses are targeted by *CgYAP1*, including *CgRPN4* [144]. This might suggest that, under less nutritious conditions, *CgRPN4* is the main target of *CgYAP1*. Reinforcing this idea, the biofilm production of KUE100_*Δcgrpn4* and KUE100_*Δcgyap1* mutants was found to be similar in SDB medium. Interestingly, KUE100_*Δcgskn7* (transcriptionally regulated by *CgYAP1*) and KUE100_*Δcgcad1* mutants also displayed great decrease in biofilm production. *CgYAP1*, *CgSKN7* and *CgCAD1* are involved in *C. glabrata* oxidative stress response and it was previously demonstrated that the elevated expression of anti-oxidant biomarkers is a likely cause of antifungal drug resistance commonly observed in biofilm mode *Candida* [145]. Additionally, it was demonstrated that *Candida* biofilms express a greater degree of antioxidant activity and contain significantly low ROS than their planktonic counterparts, meaning that anti-oxidants could contribute to the higher resistance to antifungals observed in *Candida* biofilms [145]. However, the importance of oxidative stress response-associated transcription factors in *C. glabrata* biofilm formation had not been elucidated until now.

Additionally, *CgHAP1* and *CgMRR1* were also shown to be involved in *C. glabrata* biofilm production. Although neither *CgMRR1* and *CgHAP1* or their *C. albicans* closest homologue *MRR1* have been reported to be induced in biofilm producing cells, *CgYAP1* was found to regulate these ORFs expression as well as *CgSKN7* and *CgRPN4*, according to the data gathered in the Pathoyeastract database (http://www.pathoyeastract.org/) (Figure 4.1.). These findings suggest, for the first time, that *CgYAP1*, the major known regulator of oxidative stress resistance in *C. glabrata*, plays an important role in *C. glabrata* biofilm formation and regulates other predicted transcription factors that demonstrated to be involved in this process as well.

Susceptibility assays were performed in single deletion mutant *C. glabrata* KUE100 cells for each selected ORF using specific concentrations of different antifungal classes. The effect of azole antifungals, polyene amphotericin B and pyrimidine flucytosine was assessed in the mutants through spot assays and, in the case of selected antifungal drugs, confirmed by MIC assays. On one hand, none of the *C. glabrata* predicted transcription factors demonstrated to be involved in the resistance towards amphotericin B or flucytosine. On the other hand, the absence of *CgMRR1* and specially *CgRPN4* and *CgPDR1* was found to increase *C. glabrata* susceptibility towards azole antifungals.

Previous studies reported that *C. glabrata* resistance toward azoles is largely mediated by the transcription factor *CgPDR1*, homologue of *S. cerevisiae PDR1,* resulting in the upregulation of ABC transporter proteins and drug efflux [123]. Single point mutations in *CgPDR1* have previously been shown to play a role in azole resistance development in clinical isolates [123]. In *S. cerevisiae,* Rpn4 is a transcription factor that stimulates expression of proteasome genes and is upregulated in strains harboring gain-of-function alleles of *PDR1* [123], and the same was reported to happen in *C. glabrata* by Caudle *et al.* (2011) [11]. These findings suggest that the proteasome may be influenced by *CgPDR1* via *CgRPN4* expression; however, the eventual role of *CgRPN4* in *C. glabrata* azole resistance had not yet been elucidated. Herein, CgRpn4 was shown to play an important role in *C. glabrata* resistance toward azole drugs and also against the echinocandin caspofungin. Nonetheless, the absence of *CgPDR1* was shown to exert a more detrimental effect on *C. glabrata* resistance to azoles than the absence of *CgRPN4*, suggesting that *CgPDR1* plays a major role in azole resistance, eventually in part through the regulation of *CgRPN4*. Using Pathoyeastract (http://www.pathoyeastract.org/), the interaction of CgPdr1p with *CgRPN4* was verified (Figure 4.1.). These results suggest that cross-regulation of *PDR1* and *RPN4* is conserved from *S. cerevisiae* to *C. glabrata*, with *CgPDR1* being the major azole drug-resistance regulator and *CgRPN4* an important azole-resistance player regulated by *CgPDR1*.

CAGL0B03421g ORF is the *C. glabrata* closest homolog to *C. albicans* multidrug resistance regulator transcription factor *MRR1*, thus being predicted to be a drug resistance transcriptional regulator in *C. glabrata*. In fact, susceptibility assays demonstrated that this ORF is important for this pathogen azole-resistance, since KUE100_*Δcgmrr1* mutant cells displayed growth impairment in the presence of inhibitory azoles. In *C. albicans*, *MRR1* controls the expression of *MDR1,* a MFS-MDR gene involved specifically in resistance to fluconazole rather than other azoles, and upregulated in drug-resistant clinical isolates. Expanding previous indications [146], it was demonstrated herein that *CgMRR1* confers resistance to all azole antifungal drug tested, mostly towards ketoconazole.

Interestingly, according to the data store at the Pathoyeastract database (http://www.pathoyeastract.org/) *CgMRR1* is also regulated by the major azole drug-resistance regulator *CgPDR1* (Figure 4.1.).

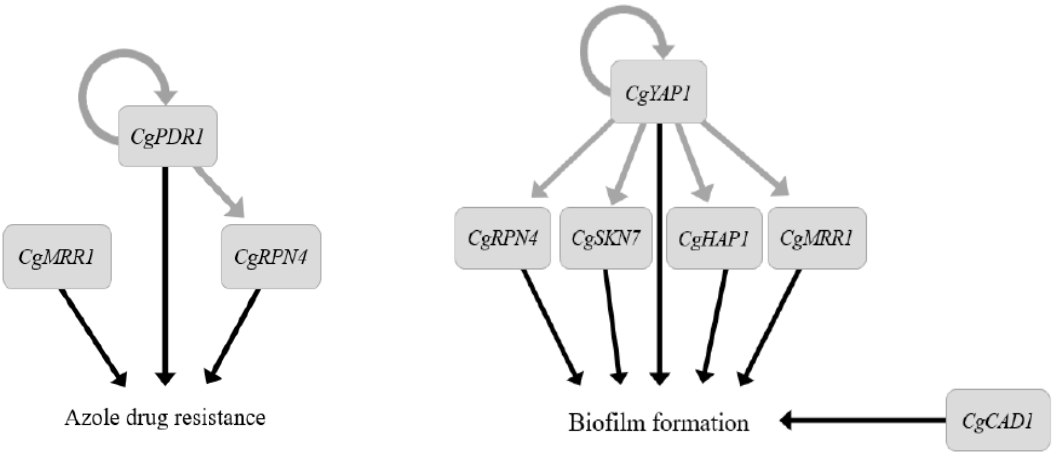

Figure 4. 1. | Transcriptional regulation of drug resistance and biofilm formation in *C. glabrata*. Relation between the predicted transcription factors were assessed through Pathoyeastract (http://www.pathoyeastract.org/). Associated phenotype based on the results obtained in this study.

Altogether, the screening results highlight the multifactorial nature of the drug resistance and biofilm formation control in *C. glabrata*. Nonetheless, *CgRPN4* demonstrated to be an important player in both drug resistance and biofilm formation in *C. glabrata*, two process that contributes to the high prevalence of this human pathogen. Therefore, to further assess the role of this predicted transcription factor in the control of *C. glabrata* drug resistance, its functional analysis was undertaken. The overexpression of *CgRPN4* was found to greatly increase *C. glabrata* resistance to fluconazole and ketoconazole. Moreover, *CgRPN4* gene expression was able to complement the absence of its *S. cerevisiae* homolog (*ScRPN4*) in BY4741_*Δrpn4* mutant cells, increasing those cells resistance toward fluconazole and ketoconazole, strongly suggesting that *ScRPN4* and *CgRPN4* are orthologous genes. Interestingly, the overexpression of *CgRPN4* in wild-type *S. cerevisiae* BY4741 cells demonstrated to has a detrimental effect on this organism resistance. BY4741 cells harboring the cloning vector demonstrated lower susceptibility toward inhibitory concentrations of both fluconazole and ketoconazole than those overexpressing *CgRPN4*. Altogether these results suggest, on one hand, that *ScRPN4* and *CgRPN4* are orthologous genes, since the presence of these transcription factors was shown to be crucial for *S. cerevisiae* and *C. glabrata* cells survival, respectively, resistance toward azole antifungals. On the other hand, interestingly and unexpectedly, the overexpression of *CgRPN4* in BY4741 *S. cerevisiae* wild-type cells does not seem to bring any advantage concerning this organism drug resistance. Actually, BY4741 cells harboring the cloning vector demonstrated a slightly lower susceptibility toward inhibitory concentrations of both fluconazole and ketoconazole when compared to those overexpressing *CgRPN4*, through the recombinant plasmid. These results suggest that, in *S.*

cerevisiae, the overexpression of Rpn4 has no positive effect in this organism resistance toward antifungals, as it has in *C. glabrata*. In fact, Wang *et al.* (2010) [121] demonstrated that inhibition of Rpn4p degradation dramatically sensitizes the cells to several genotoxic and proteotoxic stressors. These authors have shown that over-induction of Rpn4 is toxic if the protein cannot be removed rapidly by the proteasome. In this sense, a hypothesis is that CgRpn4 might not be controlled/degraded in *S. cerevisiae* in the same way as ScRpn4, leading to the apparent contradictory phenotypes observed. It was previously shown that degradation of ScRpn4 can be both ubiquitin-dependent and -independent [147]. The portable Ub-independent degron is located from 1 to 80 amino acid residues, and portable Ub-dependent degron of was mapped from 172 to 229 residues. Comparing *ScRPN4* and *CgRPN4* amino acid sequences, it is clear that these two domains are poorly conserved between these homologs proteins (Figure S8.), suggesting that CgRpn4 degradation in *S. cerevisiae* might not occur efficiently thus explaining the results obtained herein. On the other hand, *CgRPN4* overexpression levels are likely to be different in *S. cerevisiae* and *C. glabrata*, since different promoters were used to drive it. This difference in CgRpn4 expression may also justify the different effects of CgRpn4 overexpression in *C. glabrata* and *S. cerevisiae*. On the other hand, the possibility that Rpn4 target genes might not be exactly the same in both organisms, since the overexpressing of Rpn4 in *C. glabrata* constitutes an advantage concerning this pathogen survival under stress conditions whereas in *S. cerevisiae* its overexpression slightly impair cell growth under stress conditions, cannot be excluded.

To address the issue of CgRpn4 activation mechanisms, subcellular localization of CgRpn4p was assessed in different environmental conditions. Nuclear localization of the transcription factor was verified in both cells under control conditions and cells undergoing fluconazole or ketoconazole exposure. However, in exponential growing cells, nuclear localization was much less pronounced than in stationary phase cells. Actually, in *S. cerevisiae*, proteasome-dependent proteolysis was shown to be enhanced during early stationary phase and is then suppressed during late, or mature, stationary [148] . These results suggest that, although a large proportion of the population displays CgRpn4 accumulation in the nucleus even in unstressed exponential growth, there is a certain degree of increased nuclear accumulation of CgRpn4 under stress, both that induced by antifungal drugs or by reaching stationary phase of growth. Since CgRpn4 is a predicted transcription factor for proteasome genes, its target genes might be genes involved in cell survival at stationary phase, where increased oxidative stress and proteasome induction are verified [148]. When cells underwent azole drug exposure CgRpn4 concentrated even more in the cell nucleus, which suggest that ubiquitin-proteasome system may be controlled by transcriptional regulators of multidrug resistance via *RPN4* expression as it happens in closely related yeast *S. cerevisiae*. Additionally, besides proteasome-related genes, other genes related with multidrug resistance might be Rpn4 targets and susceptibility assays also suggest that. To further analyse this hypothesis, the effect of *CgRPN4* deletion in the transcriptome-wide response of *C. glabrata* cells toward mild fluconazole-induced stress conditions was assessed through RNA-sequencing.

Although the drug concentration used was not sufficiently inhibitory to induce a strong response in wild-type cells, the results obtained concerning the genes that are up or downregulated in both control and fluconazole-induced stress conditions, in the *Δcgrpn4* mutant compared to the wild-type strain, enabled the identification of a short list of genes whose expression was seen to depend on the CgRpn4

transcription factor. Interestingly, the *C. glabrata ScRPL29* homolog was found to be down-regulated via *CgRpn4* in cells under fluconazole-induced stress conditions, an observation that could partially explain the *Δcgrpn4* azole susceptibility phenotype, since *S. cerevisiae Δscrpl29* null mutant presents higher resistance toward miconazole [142].

Genes found to have significant expression changes in the *C. glabrata RPN4* deletion mutant relatively to the wild-type were grouped into predicted functional clusters. The majority of them were shown to be involved in RNA metabolism, in both control and fluconazole-induced stress conditions. Under stress conditions, several ribosomal biogenesis and translation- associated and protein trafficking- associated genes presented significant expression changes. In *S. cerevisiae*, it was previously shown that the repression of the ribosomal genes, along with a large set of genes involved in RNA metabolism, protein synthesis, and aspects of cell growth, is a general feature of the environmental stress response [149]. The inducible gene expression kinetics observed in response to stress is achieved by fine regulation of multiple steps of the mRNA biogenesis process. Although this is common to many stresses, the underlying mechanistic details of how such regulation is achieved are highly dependent on the particular stress and organism. Herein, all the four ribosomal biogenesis and translation-associated ORFs demonstrated to be downregulated by CgRpn4 under mild fluconazole-induced stress conditions. Nonetheless, concerning protein-trafficking and RNA metabolism-associated, both CgRpn4 up and downregulated ORFs were found.

Mitochondrial regulation-associated genes also demonstrated to be regulated by CgRpn4 in both control and fluconazole-induced stress conditions, being upregulated in its absence. In *S. cerevisiae*, mitochondrial respiratory functions were found to be overrepresented in H_2O_2 sensitive mutants [150]. Other studies demonstrated that, in *S. cerevisiae*, most of the energy generation gene products downregulated are mitochondrial electron transport proteins. It is speculated that these genes are downregulated in order to lessen the amount of endogenously generated reactive oxygen species (ROS) in the cell. This would be in response to generation of ROS due to the action of azoles on the cell membrane. Kobayashi and colleagues (2002) [151] demonstrated the production of ROS in *C. albicans* by miconazole and fluconazole, and there was a strong inverse correlation between the level of ROS production and the MIC. The authors hypothesize that resistant isolates may exhibit resistance mechanisms that involve scavenging ROS. On the other hand, François and colleagues (2006) [152] demonstrated that fluconazole inhibits neither catalase nor peroxidase and does not induce a significant increase of ROS levels in *C. albicans*. The authors speculate that these differences might have occurred due to the different *C. albicans* strains used. Therefore, since *C. glabrata* is a different species, phylogenetically closer to *S. cerevisiae*, fluconazole-induced endogenous ROS level can be a hypothesis.

In previous studies, iron homeostasis genes were found to be downregulated in fluconazole-resistant clinical *C. albicans* isolates [153]. Here, two ORF products predicted to be involved in metal homeostasis were found to be upregulated in *Δcgrpn4* mutant, suggesting that in *C. glabrata CgRPN4* indirectly downregulates genes involved in metal homeostasis in response to fluconazole.

Amino acid metabolism cluster were presented, under fluconazole-induced stress conditions, by a single CgRpn4 upregulated ORF homolog to *ScHIS3* which is involved in histidine biosynthesis. In

fact, Rogers *et al.* (2002) demonstrated that amino acid metabolism-associated genes were differently expressed in a *C. albicans* azole-resistant clinical isolate [153]. However, there is no evidence connecting *C. glabrata* azole-resistance with amino acid metabolism so far.

Moreover, several ORFs with still unknown function, with no *S. cerevisiae* or *C. albicans* homologs, demonstrated to be regulated by CgRpn4 in both control and fluconazole-induced stress conditions.

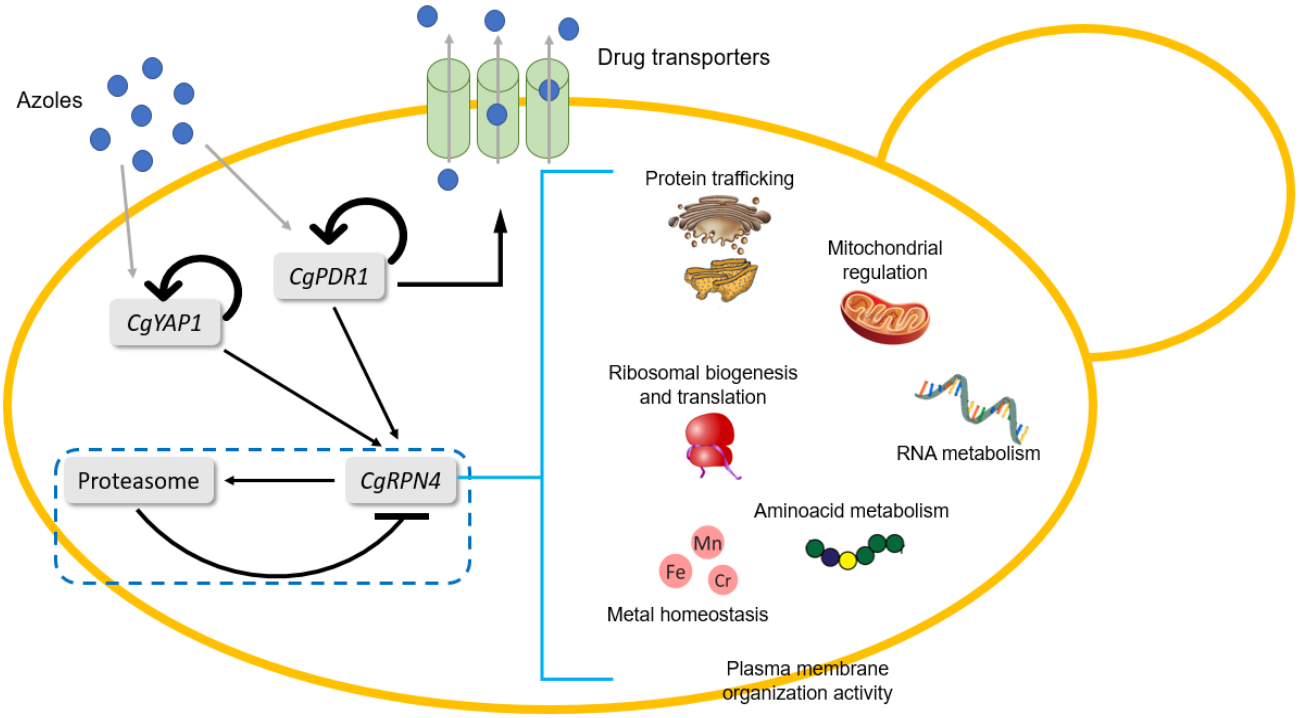

Figure 4. 2. | Model of *CgRPN4* regulation and action in *C. glabrata* under fluconazole exposure. Azole drug exposure activates the pleiotropic drug resistance regulator *CgPDR1*, which besides regulates its own expression induces the expression of drug transporters such as ABC transporters (black arrows). Recently, it was demonstrated that *CgYAP1* also induce the expression of multidrug transporters, besides being the major known oxidative stress response regulator in *C. glabrata*. These two drug responsive genes, activates the expression of the transcription factor *CgRPN4* (black arrows) which activates proteasomal genes, such as in *S. cerevisiae*. In turn, the assembled proteasome degrades CgRpn4, in order to maintain a negative feedback loop (dark blue dashed line) to control proteome homeostasis and expression of Rpn4 target genes. Herein, a screening to analyse CgRpn4 targets in response to fluconazole was performed for the first time, through RNA-seq approach, unveiling several genes belonging to different functional clusters involved in different cellular processes being regulated by CgRpn4 (light blue bracket) in response to fluconazole. For instance, mitochondrial regulator, plasma membrane organization activity and metal homeostasis-associated genes were found to be downregulated by CgRpn4. This represents the first step to unveil the mechanism through which CgRpn4 expression influences *C. glabrata* resistance toward azole antifungals.

Upstream regions of the ORFs found to be upregulated by CgRpn4 were analysed searching for a common motif that might correspond to the CgRpn4 binding site. The longest consensus sequence found in the predicted motifs that might correspond to a conserved part of known ScRpn4 binding motifs was CCAC. However, a 4-nucleotide length consensus sequence has a high random nucleotide distribution associated.

Within the 17 different binding motifs found to be enriched in CgRpn4 upregulated *C. glabrata* ORFs promoter regions, GAAGCA and AGTCTA were found in 5 of the 6 inputted upstream regions (Figure 3.13.), suggesting that these consensus sequences may be part of CgRpnp4 binding sites in *C. glabrata*. However, although there is no sequence similarity with known ScRpn4 binding motifs, *CgRPN4* gene expression was able to complement the absence of its *S. cerevisiae* homolog *ScRPN4* in BY4741_*Δrpn4* cells, suggesting that Rpn4 binding site cannot be completely different in both organisms. Gasch *et al.* (2004) [154] explored the evolution of the proteasome *cis*-regulatory element in *S. cerevisiae* and *C. albicans*, particularly the case of *RPN4*, and noticed that, in addition to the Rpn4p consensus site, a number of related hexameric sequences were also highly enriched in the orthologous upstream regions from *C. albicans*, hinting the possibility that a different set of regulatory sequences control the expression of the *C. albicans* proteasome genes. They demonstrated that *S. cerevisiae* and *C. albicans* use different sequences to control the expression of the proteasome genes. Additionally, ScRpn4p and its orthologue CaRpn4p were shown to have different DNA-binding specificities. Unlike the evolutionary rates of protein coding regions, for which essential proteins typically evolve at a slower rate, the same authors found no evidence for a retarded rate of evolution/loss of the *cis*-regulatory systems of essential genes. For example, the proteasome subunits and the ribosomal proteins are among the most highly conserved proteins, and the genes that encode them are expressed with similar patterns in *S. cerevisiae* and *C. albicans*. Nevertheless, they identified different upstream sequences for these groups in the different species, suggesting that the regulation of the genes' expression has evolved even though their expression patterns have not. These observations might suggest that, even though *C. glabrata* is phylogenetically closer to *S. cerevisiae* than *C. albicans*, the regulation underlying orthologous genes expression may have diverged at consensus sequence level leading to differences in these genes regulatory regions.

Interestingly, Ju *et al.* (2010) [155] demonstrated that, in *S. cerevisiae*, the nuclear localization signal of Rpn4 is located in the C-terminal half of Rpn4, from 206 to 531 residues, whereas the transactivation domain resides in the N-terminal region, from 11 to 210 residues. Comparing *ScRPN4* and *CgRPN4* amino acid sequences, it is clear that these two domains are poorly conserved among these yeasts (Figure S8.). In contrast, comparing the C_2H_2 DNA binding domain of *ScRNP4*, from 477 to 507 amino acid residues [155], with the correspondent amionacid residues sequence in *CgRPN4* a high conservation level is verified (Figure S8.). This observation supports the results of complementation assays, in which *CgRPN4* gene expression was able to complement the absence of its *S. cerevisiae* homolog *ScRPN4* in BY4741_*Δrpn4* cells, suggesting that *RPN4* binding site is not so different in both organisms. However, none of the ScRpn4 known binding motifs were found in the upstream region of CgRpn4 upregulated ORFs.

Altogether, the results described in this study testify the importance of orthology relationships studies as an effort to unveil regulatory mechanisms in non-studied human pathogens. The characterization of *CgRPN4* predicted transcription factor involved in proteasomal genes activation reinforce the need for study the mechanisms underlying the multidrug resistance phenomenon on *candida* species, specially *C. glabrata* due to its innate resistance to azole antimycotic therapy, as well as the mechanisms that lead to biofilm formation, which increases this human pathogen resistance to administrated antifungal drugs. This work also highlights the importance of genome/transcriptome-wide approaches in the study of possible resistance determinants like CgRpn4, as global approaches are very useful in identifying previously unforeseen or uncharacterized genes relevant for drug resistance phenotypes.

5. Future Trends

Given the increasingly appearance of multidrug resistance phenomenon, and the relative lack of information concerning azole resistance mechanisms in *C. glabrata*, it is imperative to understand how this pathogenic yeast is able to cope with azole drug treatment in clinical practice.

The attained results demonstrate a variety of predicted transcription factors involved in drug resistance and biofilm formation, highlighting the relevance for further studies focused on the mechanisms underlying these phenomena.

RNA-seq is a powerful technique to analyse a transcriptome-wide response toward different scenarios. Herein, the effect of the deletion of *CgRPN4* encoding gene in *C. glabrata* transcriptome-wide response to fluconazole was assessed using this approach. Although some genes were shown to have significant expression changes, the concentration of fluconazole used was too mild to induce a clear response to this drug. Therefore, a new experiment must be performed with a higher fluconazole concentration.

Afterwards, in order to further analyse which genes are regulated by *CgRPN4* through direct transcription factor binding, ChIP-seq approach should be applied. This technology combines chromatin immunoprecipitation ('ChIP') with NGS tools. ChIP-seq allows the identification of the cistrome, the sum of binding sites, for DNA-binding proteins on a genome-wide basis [156].

Another feature of *C. glabrata* is that this yeast is highly resistant to oxidative stress compared to *S. cerevisiae*, but its resistance mechanism is not well understood [137]. Nevertheless, the study of *C. glabrata* oxidative stress response-related genes is crucial to understand how this human pathogen resist to the reactive oxygen species (ROS) produced by the host as a defense mechanism. *CgYAP1*, the major known regulator of oxidative stress resistance in *C. glabrata*, has also been related to the control of multidrug resistance transporters. Additionally, the involvement of Rpn4 regulatory module in the oxidative stress response controlled by the Yap1 transcription factor and its conservation in the pathogenic yeast *C. glabrata* was previously demonstrated [125]. Thus, it would be interesting to culture single deletion mutants of *CgYAP1* and *CgRPN4* and a double deletion mutant *CgΔyap1Δrpn4* under oxidative conditions stress, for instance in the presence of H_2O_2, in order to assess phenotypic differences.

6. References

[1] Matsumoto, E., Boyken, L., Tendolkar, S., McDanel, J., Castanheira, M., Pfaller, M., & Diekema, D. (2014). Candidemia surveillance in Iowa: emergence of echinocandin resistance. Diagnostic microbiology and infectious disease, 79(2), 205-208;

[2] Fidel, P. L., Vazquez, J. A., & Sobel, J. D. (1999). *Candida glabrata*: review of epidemiology, pathogenesis, and clinical disease with comparison to *C. albicans*. Clinical microbiology reviews, 12(1), 80-96;

[3] Pankhurst, C. L. (2012). Candidiasis (oropharyngeal). BMJ clinical evidence, 2012;

[4] Calderone, R. A., & Clancy, C. J. (Eds.). (2011). *Candida* and candidiasis. American Society for Microbiology Press;

[5] Spence, D. (2010). Candidiasis (vulvovaginal). BMJ clinical evidence, 2010;

[6] Kauffman, C. A. (2014). Diagnosis and management of fungal urinary tract infection. Infectious disease clinics of North America, 28(1), 61-74;

[7] Morschhäuser, J. (2002). The genetic basis of fluconazole resistance development in *Candida albicans*. Biochimica et Biophysica Acta (BBA)-Molecular Basis of Disease, 1587(2), 240-248;

[8] Pappas, P. G., Alexander, B. D., Andes, D. R., Hadley, S., Kauffman, C. A., Freifeld, A., ... & Kontoyiannis, D. P. (2010). Invasive fungal infections among organ transplant recipients: results of the Transplant-Associated Infection Surveillance Network (TRANSNET). Clinical Infectious Diseases, 50(8), 1101-1111;

[9] Kojic, E. M., & Darouiche, R. O. (2004). Candida infections of medical devices. Clinical microbiology reviews, 17(2), 255-267;

[10] Pereira, C. A., Toledo, B. C., Santos, C. T., Costa, A. C. B. P., Back-Brito, G. N., Kaminagakura, E., & Jorge, A. O. C. (2013). Opportunistic microorganisms in individuals with lesions of denture stomatitis. Diagnostic microbiology and infectious disease, 76(4), 419-424;

[11] Anderson, H. W. (1917). Yeast-like fungi of the human intestinal tract. The Journal of Infectious Diseases, 341-386;

[12] Bolotin-Fukuhara, M., & Fairhead, C. (2014). *Candida glabrata*: a deadly companion?. Yeast, 31(8), 279-288;

[13] Plaut, A. (1950). Human Infection with *Cryptococcus glabratus*. Report of a Case involving Uterus and Fallopian Tube. American journal of clinical pathology, 20(4), 377-80;

[14] Grimley, P. M., Wright Jr, L. D., & Jennings, A. E. (1965). *Torulopsis glabrata* Infection in Man. American journal of clinical pathology, 43(3), 216-23;

[15] Hazen, K. C. (1995). New and emerging yeast pathogens. Clinical microbiology reviews, 8(4), 462-478;

[16] Wolfe, K. H., & Shields, D. C. (1997). Molecular evidence for an ancient duplication of the entire yeast genome. Nature, 387(6634), 708;

[17] Butler, G., Rasmussen, M. D., Lin, M. F., Santos, M. A., Sakthikumar, S., Munro, C. A., ... & Agrafioti, I. (2009). Evolution of pathogenicity and sexual reproduction in eight *Candida* genomes. Nature, 459(7247), 657;

[18] Hittinger, C. T., Rokas, A., & Carroll, S. B. (2004). Parallel inactivation of multiple *GAL* pathway genes and ecological diversification in yeasts. Proceedings of the National Academy of Sciences of the United States of America, 101(39), 14144-14149;

[19] Kaur, R., Domergue, R., Zupancic, M. L., & Cormack, B. P. (2005). A yeast by any other name: *Candida glabrata* and its interaction with the host. Current opinion in microbiology, 8(4), 378-384;

[20] Fitzpatrick, D. A., O'Gaora, P., Byrne, K. P., & Butler, G. (2010). Analysis of gene evolution and metabolic pathways using the *Candida* Gene Order Browser. BMC genomics, 11(1), 290;

[21] Yang, Y. L., Ho, Y. A., Cheng, H. H., Ho, M., & Lo, H. J. (2004). Susceptibilities of *Candida* species to amphotericin B and fluconazole: the emergence of fluconazole resistance in *Candida tropicalis*. Infection Control & Hospital Epidemiology, 25(01), 60-64;

[22] Mayer, F. L., Wilson, D., & Hube, B. (2013). *Candida albicans* pathogenicity mechanisms. Virulence, 4(2), 119-128;

[23] Roetzer, A., Gratz, N., Kovarik, P., & Schüller, C. (2010). Autophagy supports *Candida glabr*ata survival during phagocytosis. Cellular microbiology, 12(2), 199-216;

[24] Seider, K., Brunke, S., Schild, L., Jablonowski, N., Wilson, D., Majer, O., ... & Hube, B. (2011). The facultative intracellular pathogen *Candida glabrata* subverts macrophage cytokine production and phagolysosome maturation. The Journal of Immunology, 187(6), 3072-3086;

[25] Weig, M., Jänsch, L., Groß, U., De Koster, C. G., Klis, F. M., & De Groot, P. W. (2004). Systematic identification in silico of covalently bound cell wall proteins and analysis of protein–polysaccharide linkages of the human pathogen *Candida glabrata*. Microbiology, 150(10), 3129-3144;

[26] Pryszcz, L. P., Huerta-Cepas, J., & Gabaldón, T. (2010). MetaPhOrs: orthology and paralogy predictions from multiple phylogenetic evidence using a consistency-based confidence score. Nucleic acids research, 39(5), e32-e32;

[27] Rodrigues, C. F., Silva, S., & Henriques, M. (2014). *Candida glabrata*: a review of its features and resistance. European journal of clinical microbiology & infectious diseases, 33(5), 673-688;

[28] Kelly, M. T., MacCallum, D. M., Clancy, S. D., Odds, F. C., Brown, A. J., & Butler, G. (2004). The *Candida albicans CaACE2* gene affects morphogenesis, adherence and virulence. Molecular microbiology, 53(3), 969-983;

[29] MacCallum, D. M., Findon, H., Kenny, C. C., Butler, G., Haynes, K., & Odds, F. C. (2006). Different consequences of *ACE2* and *SWI5* gene disruptions for virulence of pathogenic and nonpathogenic yeasts. Infection and immunity, 74(9), 5244-5248;

[30] Gabaldón, T., & Carreté, L. (2016). The birth of a deadly yeast: tracing the evolutionary emergence of virulence traits in *Candida glabrata*. FEMS yeast research, 16(2);

[31] Ehrlich, G. D., Hiller, N. L., & Hu, F. Z. (2008). What makes pathogens pathogenic. Genome biology, 9(6), 225;

[32] Marichal, P., Koymans, L., Willemsens, S., Bellens, D., Verhasselt, P., Luyten, W., ... & Bossche, H. V. (1999). Contribution of mutations in the cytochrome P450 14α-demethylase (Erg11p, Cyp51p) to azole resistance in *Candida albicans*. *Microbiology*, *145*(10), 2701-2713;

[33] Sanglard, D. (2002). Resistance of human fungal pathogens to antifungal drugs. Current opinion in microbiology, 5(4), 379-385;

[34] Pfaller, M. A., Castanheira, M., Messer, S. A., & Jones, R. N. (2015). In vitro antifungal susceptibilities of isolates of *Candida spp*. and *Aspergillus spp*. from China to nine systemically active antifungal agents: data from the SENTRY antifungal surveillance program, 2010 through 2012. Mycoses, 58(4), 209-214;

[35] Katragkou, A., Roilides, E., & Walsh, T. J. (2015). Role of echinocandins in fungal biofilm–related disease: vascular catheter–related infections, immunomodulation, and mucosal surfaces. Clinical Infectious Diseases, 61(suppl 6), S622-S629;

[36] Bano, S. (2013). *Candida albicans* Pathogenesis. Advances in Life Sciences, 2(2), 9-11;

[37] Hawser, S., & Islam, K. (1999). Comparisons of the effects of fungicidal and fungistatic antifungal agents on the morphogenetic transformation of *Candida albicans*. Journal of Antimicrobial Chemotherapy, 43(3), 411-413;

[38] Chen, S. C., & Sorrell, T. C. (2007). Antifungal agents. Medical Journal of Australia, 187(7), 404;

[39] Kanafani, Z. A., & Perfect, J. R. (2008). Resistance to antifungal agents: mechanisms and clinical impact. *Clinical Infectious Diseases*, *46*(1), 120-128;

[40] Niimi, M., Firth, N. A., & Cannon, R. D. (2010). Antifungal drug resistance of oral fungi. Odontology, 98(1), 15-25;

[41] Borst, A., Raimer, M. T., Warnock, D. W., Morrison, C. J., & Arthington-Skaggs, B. A. (2005). Rapid acquisition of stable azole resistance by *Candida glabrata* isolates obtained before the clinical introduction of fluconazole. Antimicrobial agents and chemotherapy, 49(2), 783-787;

[42] Van Bambeke, F., Balzi, E., & Tulkens, P. M. (2000). Antibiotic efflux pumps. Biochemical pharmacology, 60(4), 457-470;

[43] Eicher, T., Hauptmann, S., & Speicher, A. (2013). The Chemistry of Heterocycles: Structures, Reactions, Synthesis, and Applications 3rd. John Wiley & Sons;

[44] Jandric, Z., & Schüller, C. (2011). Stress response in *Candida glabrata*: pieces of a fragmented picture. Future microbiology, 6(12), 1475-1484;

[45] Bard, M., Sturm, A. M., Pierson, C. A., Brown, S., Rogers, K. M., Nabinger, S., ... & Hazen, K. C. (2005). Sterol uptake in *Candida glabrata*: rescue of sterol auxotrophic strains. Diagnostic microbiology and infectious disease, 52(4), 285-293;

[46] Xiao, L., Madison, V., Chau, A. S., Loebenberg, D., Palermo, R. E., & McNicholas, P. M. (2004). Three-dimensional models of wild-type and mutated forms of cytochrome P450 14α-sterol demethylases from *Aspergillus fumigatus* and *Candida albicans* provide insights into posaconazole binding. Antimicrobial agents and chemotherapy, 48(2), 568-574;

[47] Shapiro, R. S., Robbins, N., & Cowen, L. E. (2011). Regulatory circuitry governing fungal development, drug resistance, and disease. Microbiology and Molecular Biology Reviews, 75(2), 213-267;

[48] Anderson, J. B. (2005). Evolution of antifungal-drug resistance: mechanisms and pathogen fitness. Nature Reviews Microbiology, 3(7), 547-556;

[49] Ji, H., Zhang, W., Zhou, Y., Zhang, M., Zhu, J., Song, Y., ... & Zhu, J. (2000). A three-dimensional model of lanosterol 14α-demethylase of *Candida albicans* and its interaction with azole antifungals. Journal of medicinal chemistry, 43(13), 2493-2505;

[50] Sanglard, D., Ischer, F., Koymans, L., & Bille, J. (1998). Amino acid substitutions in the cytochrome P-450 lanosterol 14α-demethylase (CYP51A1) from azole-resistant *Candida albicans* clinical isolates contribute to resistance to azole antifungal agents. Antimicrobial Agents and Chemotherapy, 42(2), 241-253;

[51] White, T. C., Marr, K. A., & Bowden, R. A. (1998). Clinical, cellular, and molecular factors that contribute to antifungal drug resistance. Clinical microbiology reviews, 11(2), 382-402;

[52] Cowen, L. E., Sanglard, D., Calabrese, D., Sirlundgrensingh, C., Anderson, J. B., & Kohn, L. M. (2000). Evolution of drug resistance in experimental populations of *Candida albicans*. Journal of Bacteriology, 182(6), 1515-1522;

[53] Silver, P. M., Oliver, B. G., & White, T. C. (2004). Role of *Candida albicans* transcription factor Upc2p in drug resistance and sterol metabolism. Eukaryotic Cell, 3(6), 1391-1397;

[54] Oliver, B. G., Song, J. L., Choiniere, J. H., & White, T. C. (2007). cis-Acting elements within the *Candida albicans* ERG11 promoter mediate the azole response through transcription factor Upc2p. Eukaryotic cell, 6(12), 2231-2239;

[55] Hoot, S. J., Brown, R. P., Oliver, B. G., & White, T. C. (2010). The UPC2 promoter in *Candida albicans* contains two cis-acting elements that bind directly to Upc2p, resulting in transcriptional autoregulation. Eukaryotic cell, 9(9), 1354-1362;

[56] Heilmann, C. J., Schneider, S., Barker, K. S., Rogers, P. D., & Morschhäuser, J. (2010). An A643T mutation in the transcription factor Upc2p causes constitutive ERG11 upregulation and increased fluconazole resistance in *Candida albicans*. Antimicrobial agents and chemotherapy, 54(1), 353-359;

[57] Morschhäuser, J. (2010). Regulation of multidrug resistance in pathogenic fungi. Fungal Genetics and Biology, 47(2), 94-106;

[58] Sanglard, D., Ischer, F., Monod, M., & Bille, J. (1997). Cloning of *Candida albicans* genes conferring resistance to azole antifungal agents: characterization of CDR2, a new multidrug ABC transporter gene. Microbiology, 143(2), 405-416;

[59] Sanglard, D., Ischer, F., Monod, M., & Bille, J. (1996). Susceptibilities of *Candida albicans* multidrug transporter mutants to various antifungal agents and other metabolic inhibitors. Antimicrobial agents and chemotherapy, 40(10), 2300-2305;

[60] Sanglard, D., Kuchler, K., Ischer, F., Pagani, J. L., Monod, M., & Bille, J. (1995). Mechanisms of resistance to azole antifungal agents in Candida albicans isolates from AIDS patients involve specific multidrug transporters. Antimicrobial agents and chemotherapy, 39(11), 2378-2386;

[61] Micheli, M. D., Bille, J., Schueller, C., & Sanglard, D. (2002). A common drug-responsive element mediates the upregulation of the *Candida albicans* ABC transporters CDR1 and CDR2, two genes involved in antifungal drug resistance. Molecular microbiology, 43(5), 1197-1214;

[62] Coste, A., Turner, V., Ischer, F., Morschhäuser, J., Forche, A., Selmecki, A., ... & Sanglard, D. (2006). A mutation in Tac1p, a transcription factor regulating CDR1 and CDR2, is coupled with loss of heterozygosity at chromosome 5 to mediate antifungal resistance in *Candida albicans*. Genetics, 172(4), 2139-2156;

[63] Coste, A., Selmecki, A., Forche, A., Diogo, D., Bougnoux, M. E., d'Enfert, C., ... & Sanglard, D. (2007). Genotypic evolution of azole resistance mechanisms in sequential *Candida albicans* isolates. Eukaryotic cell, 6(10), 1889-1904;

[64] Liu, Teresa T., Sadri Znaidi, Katherine S. Barker, Lijing Xu, Ramin Homayouni, Saloua Saidane, Joachim Morschhäuser, André Nantel, Martine Raymond, and P. David Rogers. "Genome-wide expression and location analyses of the *Candida albicans* Tac1p regulon." Eukaryotic cell 6, no. 11 (2007): 2122-2138;

[65] Morschhäuser, J., Barker, K. S., Liu, T. T., Blaß-Warmuth, J., Homayouni, R., & Rogers, P. D. (2007). The transcription factor Mrr1p controls expression of the MDR1 efflux pump and mediates multidrug resistance in *Candida albicans*. PLoS Pathog, 3(11), e164;

[66] DUNKEL, Nico et al. Mutations in the multi-drug resistance regulator MRR1, followed by loss of heterozygosity, are the main cause of MDR1 overexpression in fluconazole-resistant *Candida albicans* strains. Molecular microbiology, v. 69, n. 4, p. 827-840, 2008;

[67] Vermitsky, J. P., & Edlind, T. D. (2004). Azole resistance in *Candida glabrata*: coordinate upregulation of multidrug transporters and evidence for a Pdr1-like transcription factor. Antimicrobial Agents and Chemotherapy, 48(10), 3773-3781;

[68] Sanglard, D., Ischer, F., & Bille, J. (2001). Role of ATP-binding-cassette transporter genes in high-frequency acquisition of resistance to azole antifungals in *Candida glabrata*. Antimicrobial Agents and Chemotherapy, 45(4), 1174-1183;

[69] Torelli, R., Posteraro, B., Ferrari, S., La Sorda, M., Fadda, G., Sanglard, D., & Sanguinetti, M. (2008). The ATP-binding cassette transporter–encoding gene CgSNQ2 is contributing to the CgPDR1-dependent azole resistance of *Candida glabrata*. Molecular microbiology, 68(1), 186-201;

[70] Balzi, E., & Goffeau, A. (1995). Yeast multidrug resistance: the PDR network. Journal of bioenergetics and biomembranes, 27(1), 71-76;

[71] Paul, S., Schmidt, J. A., & Moye-Rowley, W. S. (2011). Regulation of the CgPdr1 transcription factor from the pathogen *Candida glabrata*. Eukaryotic cell, 10(2), 187-197;

[72] Ferrari, S., Ischer, F., Calabrese, D., Posteraro, B., Sanguinetti, M., Fadda, G., ... & Sanglard, D. (2009). Gain of function mutations in CgPDR1 of *Candida glabrata* not only mediate antifungal resistance but also enhance virulence. PLoS Pathog, 5(1), e1000268;

[73] Costa, C., Pires, C., Cabrito, T. R., Renaudin, A., Ohno, M., Chibana, H., ... & Teixeira, M. C. (2013). *Candida glabrata* drug: H+ antiporter CgQdr2 confers imidazole drug resistance, being activated by transcription factor CgPdr1. Antimicrobial agents and chemotherapy, 57(7), 3159-3167;

[74] Costa, C., Nunes, J., Henriques, A., Mira, N. P., Nakayama, H., Chibana, H., & Teixeira, M. C. (2014). *Candida glabrata* drug: H+ antiporter CgTpo3 (ORF CAGL0I10384g): role in azole drug resistance and polyamine homeostasis. Journal of Antimicrobial Chemotherapy, 69(7), 1767-1776;

[75] Pais, P., Costa, C., Pires, C., Shimizu, K., Chibana, H., & Teixeira, M. C. (2016). Membrane proteome-wide response to the antifungal drug clotrimazole in *Candida glabrata*: role of the transcription factor CgPdr1 and the Drug: H+ Antiporters CgTpo1_1 and CgTpo1_2. Molecular & Cellular Proteomics, 15(1), 57-72.

[76] Costa, C., Ribeiro, J., Miranda, I. M., Silva-Dias, A., Cavalheiro, M., Costa-de-Oliveira, S., ... & Teixeira, M. C. (2016). Clotrimazole Drug Resistance in *Candida glabrata* Clinical Isolates Correlates with Increased Expression of the Drug: H+ Antiporters CgAqr1, CgTpo1_1, CgTpo3, and CgQdr2. Frontiers in microbiology, 7;

[77] Chen, K. H., Miyazaki, T., Tsai, H. F., & Bennett, J. E. (2007). The bZip transcription factor Cgap1p is involved in multidrug resistance and required for activation of multidrug transporter gene *CgFLR1* in *Candida glabrata*. Gene, 386(1), 63-72;

[78] Gbelska, Y., Krijger, J. J., & Breunig, K. D. (2006). Evolution of gene families: the multidrug resistance transporter genes in five related yeast species. FEMS yeast research, 6(3), 345-355;

[79] COSTA, Catarina et al. MFS multidrug transporters in pathogenic fungi: do they have real clinical impact?. Frontiers in physiology, v. 5, p. 197, 2014;

[80] PAIS, Pedro et al. Membrane proteomics analysis of the *Candida glabrata* response to 5-flucytosine: unveiling the role and regulation of the drug efflux transporters CgFlr1 and CgFlr2. Frontiers in Microbiology, v. 7, 2016;

[81] Hull, C. M., Parker, J. E., Bader, O., Weig, M., Gross, U., Warrilow, A. G., ... & Kelly, S. L. (2012). Facultative sterol uptake in an ergosterol-deficient clinical isolate of *Candida glabrata* harboring a missense mutation in *ERG11* and exhibiting cross-resistance to azoles and amphotericin B. Antimicrobial agents and chemotherapy, 56(8), 4223-4232;

[82] Nakayama, H., Tanabe, K., Bard, M., Hodgson, W., Wu, S., Takemori, D., ... & Chibana, H. (2007). The *Candida glabrata* putative sterol transporter gene *CgAUS1* protects cells against azoles in the presence of serum. Journal of antimicrobial chemotherapy, 60(6), 1264-1272;

[83] Brun, S., Bergès, T., Poupard, P., Vauzelle-Moreau, C., Renier, G., Chabasse, D., & Bouchara, J. P. (2004). Mechanisms of azole resistance in petite mutants of *Candida glabrata*. Antimicrobial agents and chemotherapy, 48(5), 1788-1796;

[84] DEFONTAINE, A., BOUCHARA, J. P., DECLERK, P., PLANCHENAULT, C., CHABASSE, D., & HALLET, J. N. (1999). In-vitro resistance to azoles associated with mitochondrial DNA deficiency in *Candida glabrata*. Journal of medical microbiology, 48(7), 663-670;

[85] Sanguinetti, M., Posteraro, B., Fiori, B., Ranno, S., Torelli, R., & Fadda, G. (2005). Mechanisms of azole resistance in clinical isolates of *Candida glabrata* collected during a hospital survey of antifungal resistance. Antimicrobial agents and chemotherapy, 49(2), 668-679;

[86] Denning, D. W. (2003). Echinocandin antifungal drugs. The Lancet, 362(9390), 1142-1151;

[87] Ibrahim, A. S., Bowman, J. C., Avanessian, V., Brown, K., Spellberg, B., Edwards, J. E., & Douglas, C. M. (2005). Caspofungin inhibits *Rhizopus oryzae* 1, 3-β-D-glucan synthase, lowers burden in brain measured by quantitative PCR, and improves survival at a low but not a high dose during murine disseminated zygomycosis. Antimicrobial agents and chemotherapy, 49(2), 721-727;

[88] Peman, J., E. Canton, and A. Espinel-Ingroff, Antifungal drug resistance mechanisms. (2009). Expert Rev Anti Infect Ther, 2009. 7(4): p. 453-60;

[89] Alexander, B. D., Johnson, M. D., Pfeiffer, C. D., Jiménez-Ortigosa, C., Catania, J., Booker, R., ... & Pfaller, M. A. (2013). Increasing echinocandin resistance in *Candida glabrata*: clinical failure correlates with presence of FKS mutations and elevated minimum inhibitory concentrations. Clinical infectious diseases, 56(12), 1724-1732;

[90] Balashov, S. V., Park, S., & Perlin, D. S. (2006). Assessing resistance to the echinocandin antifungal drug caspofungin in *Candida albicans* by profiling mutations in FKS1. Antimicrobial agents and chemotherapy, 50(6), 2058-2063;

[91] Park, S., Kelly, R., Kahn, J. N., Robles, J., Hsu, M. J., Register, E., ... & Flattery, A. (2005). Specific substitutions in the echinocandin target Fks1p account for reduced susceptibility of rare laboratory and clinical *Candida sp.* isolates. Antimicrobial Agents and Chemotherapy, 49(8), 3264-3273;

[92] Laverdière, M., Lalonde, R. G., Baril, J. G., Sheppard, D. C., Park, S., & Perlin, D. S. (2006). Progressive loss of echinocandin activity following prolonged use for treatment of *Candida albicans* oesophagitis. Journal of Antimicrobial Chemotherapy, 57(4), 705-708;

[93] Zimbeck, A. J., Iqbal, N., Ahlquist, A. M., Farley, M. M., Harrison, L. H., Chiller, T., & Lockhart, S. R. (2010). FKS mutations and elevated echinocandin MIC values among *Candida glabrata* isolates from US population-based surveillance. Antimicrobial Agents and Chemotherapy, 54(12), 5042-5047;

[94] Arendrup, M. C., Perlin, D. S., Jensen, R. H., Howard, S. J., Goodwin, J., & Hope, W. (2012). Differential in vivo activities of anidulafungin, caspofungin, and micafungin against *Candida glabrata* isolates with and without *FKS* resistance mutations. Antimicrobial agents and chemotherapy, 56(5), 2435-2442;

[95] Shields, R. K., Nguyen, M. H., Press, E. G., Kwa, A. L., Cheng, S., Du, C., & Clancy, C. J. (2012). The presence of an *FKS* mutation rather than MIC is an independent risk factor for failure of echinocandin therapy among patients with invasive candidiasis due to *Candida glabrata*. Antimicrobial agents and chemotherapy, 56(9), 4862-4869;

[96] Singh, S. D., Robbins, N., Zaas, A. K., Schell, W. A., Perfect, J. R., & Cowen, L. E. (2009). Hsp90 governs echinocandin resistance in the pathogenic yeast *Candida albicans* via calcineurin. PLoS Pathog, 5(7), e1000532;

[97] Stevens, D. A., Ichinomiya, M., Koshi, Y., & Horiuchi, H. (2006). Escape of *Candida* from caspofungin inhibition at concentrations above the MIC (paradoxical effect) accomplished by increased cell wall chitin; evidence for β-1, 6-glucan synthesis inhibition by caspofungin. Antimicrobial agents and chemotherapy, 50(9), 3160-3161;

[98] Eisman, B., Alonso-Monge, R., Roman, E., Arana, D., Nombela, C., & Pla, J. (2006). The Cek1 and Hog1 mitogen-activated protein kinases play complementary roles in cell wall biogenesis and chlamydospore formation in the fungal pathogen *Candida albicans*. Eukaryotic Cell, 5(2), 347-358;

[99] Munro, C. A., Selvaggini, S., De Bruijn, I., Walker, L., Lenardon, M. D., Gerssen, B., ... & Gow, N. A. (2007). The PKC, HOG and Ca2+ signalling pathways co-ordinately regulate chitin synthesis in *Candida albicans*. Molecular microbiology, 63(5), 1399-1413;

[100] Singh-Babak, S. D., Babak, T., Diezmann, S., Hill, J. A., Xie, J. L., Chen, Y. L., ... & Cowen, L. E. (2012). Global analysis of the evolution and mechanism of echinocandin resistance in *Candida glabrata*. PLoS Pathog, 8(5), e1002718;

[101] Pfaller, M. A., Messer, S. A., Boyken, L., Rice, C., Tendolkar, S., Hollis, R. J., & Diekema, D. J. (2003). Caspofungin activity against clinical isolates of fluconazole-resistant Candida. Journal of clinical microbiology, 41(12), 5729-5731;

[102] Uppuluri, P., Chaturvedi, A. K., Srinivasan, A., Banerjee, M., Ramasubramaniam, A. K., Köhler, J. R., ... & Lopez-Ribot, J. L. (2010). Dispersion as an important step in the *Candida albicans* biofilm developmental cycle. PLoS pathogens, 6(3), e1000828;

[103] Ramage, G., Rajendran, R., Sherry, L., & Williams, C. (2012). Fungal biofilm resistance. International journal of microbiology, 2012;

[104] Kuhn, D. M., George, T., Chandra, J., Mukherjee, P. K., & Ghannoum, M. A. (2002). Antifungal susceptibility of *Candida* biofilms: unique efficacy of amphotericin B lipid formulations and echinocandins. Antimicrobial agents and chemotherapy, 46(6), 1773-1780;

[105] Odds, F. C., Cockayne, A., Hayward, J., & Abbott, A. B. (1985). Effects of imidazole-and triazole-derivative antifungal compounds on the growth and morphological development of *Candida albicans* hyphae. Microbiology, 131(10), 2581-2589;

[106] Iraqui, I., Garcia-Sanchez, S., Aubert, S., Dromer, F., Ghigo, J. M., d'Enfert, C., & Janbon, G. (2005). The Yak1p kinase controls expression of adhesins and biofilm formation in *Candida glabrata* in a Sir4p-dependent pathway. Molecular microbiology, 55(4), 1259-1271;

[107] Roetzer, A., Gabaldón, T., & Schüller, C. (2010). From *Saccharomyces cerevisiae* to *Candida glabrata* in a few easy steps: important adaptations for an opportunistic pathogen. FEMS microbiology letters, 314(1), 1-9;

[108] Silva, S., Henriques, M., Oliveira, R., Williams, D., & Azeredo, J. (2010). In vitro biofilm activity of non-*Candida albicans* *Candida* species. Current microbiology, 61(6), 534-540;

[109] Nobile, C. J., Fox, E. P., Nett, J. E., Sorrells, T. R., Mitrovich, Q. M., Hernday, A. D., ... & Johnson, A. D. (2012). A recently evolved transcriptional network controls biofilm development in Candida albicans. Cell, 148(1), 126-138;

[110] Caudle, K. E., Barker, K. S., Wiederhold, N. P., Xu, L., Homayouni, R., & Rogers, P. D. (2011). Genomewide expression profile analysis of the *Candida glabrata Pdr1* regulon. Eukaryotic cell, 10(3), 373-383;

[111] Kraneveld, E. A., de Soet, J. J., Deng, D. M., Dekker, H. L., de Koster, C. G., Klis, F. M., ... & de Groot, P. W. (2011). Identification and differential gene expression of adhesin-like wall proteins in *Candida glabrata* biofilms. Mycopathologia, 172(6), 415-427;

[112] Castaño, I., Pan, S. J., Zupancic, M., Hennequin, C., Dujon, B., & Cormack, B. P. (2005). Telomere length control and transcriptional regulation of subtelomeric adhesins in *Candida glabrata*. Molecular microbiology, 55(4), 1246-1258;

[113] Palladino, F., Laroche, T., Gilson, E., Axelrod, A., Pillus, L., & Gasser, S. M. (1993). SIR3 and SIR4 proteins are required for the positioning and integrity of yeast telomeres. Cell, 75(3), 543-555;

[114] Riera, M., Mogensen, E., d'Enfert, C., & Janbon, G. (2012). New regulators of biofilm development in *Candida glabrata.* Research in microbiology, 163(4), 297-307;

[115] Mao, X., Cao, F., Nie, X., Liu, H., & Chen, J. (2006). The Swi/Snf chromatin remodeling complex is essential for hyphal development in *Candida albicans*. FEBS letters, 580(11), 2615-2622;

[116] Octavio, L. M., Gedeon, K., & Maheshri, N. (2009). Epigenetic and conventional regulation is distributed among activators of FLO11 allowing tuning of population-level heterogeneity in its expression. PLoS Genet, 5(10), e1000673;

[117] Mundy, R. D., & Cormack, B. (2009). Expression of *Candida glabrata* adhesins after exposure to chemical preservatives. Journal of Infectious Diseases, 199(12), 1891-1898;

[118] Wang, X., Xu, H., Ju, D., & Xie, Y. (2008). Disruption of Rpn4-induced proteasome expression in *Saccharomyces cerevisiae* reduces cell viability under stressed conditions. Genetics, 180(4), 1945-1953;

[119] Ju, D., Wang, L., Mao, X., & Xie, Y. (2004). Homeostatic regulation of the proteasome via an Rpn4-dependent feedback circuit. Biochemical and biophysical research communications, 321(1), 51-57;

[120] Owsianik, G., Balzi, L., & Ghislain, M. (2002). Control of 26S proteasome expression by transcription factors regulating multidrug resistance in *Saccharomyces cerevisiae*. Molecular microbiology, 43(5), 1295-1308;

[121] Wang, X., Xu, H., Ha, S. W., Ju, D., & Xie, Y. (2010). Proteasomal degradation of Rpn4 in *Saccharomyces cerevisiae* is critical for cell viability under stressed conditions. Genetics, 184(2), 335-342;

[122] Cherry, J. M., Hong, E. L., Amundsen, C., Balakrishnan, R., Binkley, G., Chan, E. T., ... & Fisk, D. G. (2011). *Saccharomyces* Genome Database: the genomics resource of budding yeast. Nucleic acids research, 40(D1), D700-D705;

[123] Vermitsky, J. P., Earhart, K. D., Smith, W. L., Homayouni, R., Edlind, T. D., & Rogers, P. D. (2006). Pdr1 regulates multidrug resistance in *Candida glabrata*: gene disruption and genome-wide expression studies. *Molecular microbiology*, *61*(3), 704-722;

[124] Tsai, H. F., Sammons, L. R., Zhang, X., Suffis, S. D., Su, Q., Myers, T. G., ... & Bennett, J. E. (2010). Microarray and molecular analyses of the azole resistance mechanism in *Candida glabrata* oropharyngeal isolates. Antimicrobial agents and chemotherapy, 54(8), 3308-3317;

[125] Salin, H., Fardeau, V., Piccini, E., Lelandais, G., Tanty, V., Lemoine, S., ... & Devaux, F. (2008). Structure and properties of transcriptional networks driving selenite stress response in yeasts. BMC genomics, 9(1), 333;

[126] Evensen, N. A., & Braun, P. C. (2009). The effects of tea polyphenols on *Candida albicans*: inhibition of biofilm formation and proteasome inactivation. Canadian journal of microbiology, 55(9), 1033-1039;

[127] Jansen, G., Wu, C., Schade, B., Thomas, D. Y., & Whiteway, M. (2005). Drag&Drop cloning in yeast. Gene, 344, 43-51;

[128] Rodríguez-Tudela, J. L., Barchiesi, F., Bille, J., Chryssanthou, E., Cuenca-Estrella, M., Denning, D., ... & Richardson, M. (2003). Method for the determination of minimum inhibitory concentration (MIC) by broth dilution of fermentative yeasts. Clinical Microbiology and Infection, 9(8), i-viii;

[129] Pathak, A. K., Sharma, S., & Shrivastva, P. (2012). Multi-species biofilm of *Candida albicans* and non-*Candida albicans Candida* species on acrylic substrate. Journal of Applied Oral Science, 20(1), 70-75;

[130] Cabrito, T. R., Teixeira, M. C., Duarte, A. A., Duque, P., & Sá-Correia, I. (2009). Heterologous expression of a Tpo1 homolog from Arabidopsis thaliana confers resistance to the herbicide 2, 4-D and other chemical stresses in yeast. Applied microbiology and biotechnology, 84(5), 927-936;

[131] Garber, M., Grabherr, M. G., Guttman, M., & Trapnell, C. (2011). Computational methods for transcriptome annotation and quantification using RNA-seq. Nature methods, 8(6), 469-477.

[132] Jiang H, Lei R, Ding S-W, Zhu S. Skewer: a fast and accurate adapter trimmer for next-generation sequencing paired-end reads. BMC Bioinformatics. 2014;15: 182. doi:10.1186/1471-2105-15-182;

[133] Trapnell C, Pachter L, Salzberg SL. TopHat: Discovering splice junctions with RNA-Seq. Bioinformatics. 2009;25: 1105–1111. doi:10.1093/bioinformatics/btp120;

[134] Anders S, Huber W. Differential expression analysis for sequence count data. Genome Biol. 2010;11: R106. doi:10.1186/gb-2010-11-10-r106;

[135] Love MI, Huber W, Anders S. Moderated estimation of fold change and dispersion for RNA-seq data with DESeq2. Genome Biol. 2014;15: 550. doi:10.1186/s13059-014-0550-8;

[136] Inglis DO, Arnaud MB, Binkley J, Shah P, Skrzypek MS, et al. (2012) The *Candida* genome database incorporates multiple *Candida* species: multispecies search and analysis tools with curated gene and protein information for *Candida albicans* and *Candida glabrata*. Nucleic Acids Res 40: D667–674;

[137] Noble, J. A., Tsai, H. F., Suffis, S. D., Su, Q., Myers, T. G., & Bennett, J. E. (2013). *STB5* is a negative regulator of azole resistance in *Candida glabrata*. Antimicrobial agents and chemotherapy, 57(2), 959-967;

[138] Kucharíková, S., Tournu, H., Lagrou, K., Van Dijck, P., & Bujdakova, H. (2011). Detailed comparison of *Candida albicans* and *Candida glabrata* biofilms under different conditions and their susceptibility to caspofungin and anidulafungin. *Journal of medical microbiology*, *60*(9), 1261-1269;

[139] Schmidt, P., Walker, J., Selway, L., Stead, D., Yin, Z., Enjalbert, B., ... & Brown, A. J. (2008). Proteomic analysis of the pH response in the fungal pathogen *Candida glabrata*. Proteomics, 8(3), 534-544;

[140] Chandra, J., Zhou, G., & Ghannoum, M. A. (2005). Fungal biofilms and antimycotics. Current drug targets, 6(8), 887-894;

[141] Kapitzky, L., Beltrao, P., Berens, T. J., Gassner, N., Zhou, C., Wüster, A., ... & Lokey, R. S. (2010). Cross-species chemogenomic profiling reveals evolutionarily conserved drug mode of action. Molecular systems biology, 6(1), 451;

[142] Vandenbosch, D., De Canck, E., Dhondt, I., Rigole, P., Nelis, H. J., & Coenye, T. (2013). Genomewide screening for genes involved in biofilm formation and miconazole susceptibility in *Saccharomyces cerevisiae*. FEMS yeast research, 13(8), 720-730;

[143] Bajorek, M., Finley, D., & Glickman, M. H. (2003). Proteasome disassembly and downregulation is correlated with viability during stationary phase. Current Biology, 13(13), 1140-1144;

[144] Merhej, J., Thiebaut, A., Blugeon, C., Pouch, J., Chaouche, M. E. A. A., Camadro, J. M., ... & Devaux, F. (2016). A Network of Paralogous Stress Response Transcription Factors in the Human Pathogen *Candida glabrata*. Frontiers in microbiology, 7;

[145] Seneviratne, C. J., Wang, Y., Jin, L., Abiko, Y., & Samaranayake, L. P. (2008). *Candida albicans* biofilm formation is associated with increased anti-oxidative capacities. Proteomics, 8(14), 2936-2947;

[146] Singh, R. P., Prasad, H. K., Sinha, I., Agarwal, N., & Natarajan, K. (2011). Cap2-HAP complex is a critical transcriptional regulator that has dual but contrasting roles in regulation of iron homeostasis in *Candida albicans*. Journal of Biological Chemistry, 286(28), 25154-25170;

[147] Ju, D., & Xie, Y. (2004). Proteasomal degradation of *RPN4* via two distinct mechanisms, ubiquitin-dependent and-independent. Journal of Biological Chemistry, 279(23), 23851-23854;

[148] Fujimuro, M., Takada, H., Saeki, Y., Toh-e, A., Tanaka, K., & Yokosawa, H. (1998). Growth-dependent change of the 26S proteasome in budding yeast. Biochemical and biophysical research communications, 251(3), 818-823;

[149] Gasch, A. P., Spellman, P. T., Kao, C. M., Carmel-Harel, O., Eisen, M. B., Storz, G., ... & Brown, P. O. (2000). Genomic expression programs in the response of yeast cells to environmental changes. Molecular biology of the cell, 11(12), 4241-4257;

[150] Thorpe, G. W., Fong, C. S., Alic, N., Higgins, V. J., & Dawes, I. W. (2004). Cells have distinct mechanisms to maintain protection against different reactive oxygen species: oxidative-stress-response genes. Proceedings of the National Academy of Sciences of the United States of America, 101(17), 6564-6569;

[151] Kobayashi, D., Kondo, K., Uehara, N., Otokozawa, S., Tsuji, N., Yagihashi, A., & Watanabe, N. (2002). Endogenous reactive oxygen species is an important mediator of miconazole antifungal effect. Antimicrobial Agents and Chemotherapy, 46(10), 3113-3117;

[152] Francois, I. E., Cammue, B., Borgers, M., Ausma, J., Dispersyn, G. D., & Thevissen, K. (2006). Azoles: mode of antifungal action and resistance development. Effect of miconazole on endogenous reactive oxygen species production in *Candida albicans*. Anti-Infective Agents in Medicinal Chemistry (Formerly Current Medicinal Chemistry-Anti-Infective Agents), 5(1), 3-13;

[153] Rogers, P. D., & Barker, K. S. (2002). Evaluation of differential gene expression in fluconazole-susceptible and-resistant isolates of *Candida albicans* by cDNA microarray analysis. Antimicrobial agents and chemotherapy, 46(11), 3412-3417;

[154] Gasch, A. P., Moses, A. M., Chiang, D. Y., Fraser, H. B., Berardini, M., & Eisen, M. B. (2004). Conservation and evolution of *cis*-regulatory systems in ascomycete fungi. PLoS biology, 2(12), e398;

[155] Ju, D., Xu, H., Wang, X., & Xie, Y. (2010). The transcription activation domain of Rpn4 is separate from its degrons. The international journal of biochemistry & cell biology, 42(2), 282-286;

[156] Aparicio, O., Geisberg, J. V., Sekinger, E., Yang, A., Moqtaderi, Z., & Struhl, K. (2005). Chromatin immunoprecipitation for determining the association of proteins with specific genomic sequences in vivo. Current protocols in molecular biology, 21-3;

7. Annexe

Table S 1. | *Candida glabrata* predicted transcription factors. ORFs were grouped according to their predicted function based on the function of their *S. cerevisiae* closest homolog. Some of the ORFs are verified (named *Cg*) others are uncharacterized. The description of the predicted function of each ORF was retrieved from SGD https://www.yeastgenome.org/.

***C. glabrata* protein ORF**	***S. cerevisiae* homologue**	**Description of the predicted function of the *C. glabrata* ORF or its *S. cerevisiae* homologue**
Predicted Multidrug Resistance-Related Transcription Factors		
CgRPN4 (*CAGL0K01727g*)	*ScRPN4*	Uncharacterized. Putative transcription factor for proteasome genes; upregulated in azole-resistant strain.
CgSTB5 (*CAGL0I02552g*)	*ScSTB5*	Predicted sequence-specific DNA binding transcription factor, negative regulator of azole resistance; acts as transcriptional repressor of ATP-binding cassette (ABC) transporter genes.
CgPDR1 (*CAGL0A00451g*)	*ScPDR1*	Zinc finger transcription factor, activator of drug resistance genes via pleiotropic drug response elements (PDRE); regulates drug efflux pumps and controls multidrug resistance; upregulated and/or mutated in azole-resistant strains.
CAGL0L04576g and CAGL0L04400g	*ScYRM1*	Uncharacterized. *S. cerevisiae* homologue encodes a zinc finger transcription factor that activates genes involved in multidrug resistance.
Predicted Oxidative Stress Response-Related Transcription Factors		
CgYAP1 (*CAGL0H04631g*)	*ScYAP1*	Protein with a basic leucine zipper (bZip) domain involved in drug resistance and the response to oxidative stress; activates multidrug transporter *FLR1*.
CAGL0F09229g	*ScTOG1*	Uncharacterized. *S. cerevisiae* homologue encodes a transcriptional activator of oleate genes and regulates genes involved in fatty acid utilization; deletion confers sensitivity to calcofluor white, and prevents growth on glycerol or lactate as sole carbon source.
CgCAD1 (*CAGL0F03069g*)	*ScCAD1*	Uncharacterized. *S. cerevisiae* homologue encodes an AP-1-like basic leucine zipper (bZip) transcriptional activator; involved in stress responses, iron metabolism, and pleiotropic drug resistance.
CgSKN7 (*CAGL0F09097g*)	*ScSKN7*	Predicted transcription factor, involved in oxidative stress response; required for induction of *TRX2*, *TRR1* and *TSA1* transcription under oxidative stress.

Table S 2. | *Candida glabrata* predicted transcription factors. ORFs were grouped according to their predicted function based on the function of their *C. albicans* closest homolog. All the ORFs are uncharacterized. The description of the predicted function of each ORF was retrieved from CGD http://www.candidagenome.org/.

***C. glabrata* protein ORF**	***C. albicans* homologue**	**Description of the predicted function of the *C. glabrata* ORF or its *C. albicans* homologue**
Predicted Multidrug Resistance-Related Transcription Factors		
CgHAP1 (*CAGL0K05841g*) and *CAGL0B03421g*	*CaMRR1*	Uncharacterized. *C. albicans* homologue encodes a putative Zn(II)2Cys6 transcription factor regulator of *MDR1* transcription; gain-of-function mutations cause upregulation of *MDR1* and increases multidrug resistance; orthologous to *S. cerevisiae HAP1*.
CAGL0F07909g	*CaTAC1*	Uncharacterized. *C. albicans* homologue encodes a Zn(II)2Cys6 transcriptional activator of drug-responsive genes (*CDR1* and *CDR2*); spider biofilm induced.
CgHAL9 (*CAGL0I07755g*)	*CaTAC1*	Uncharacterized. Encodes a transcription factor that regulates pH homeostasis in *C. glabrata*; confers the tolerance to acid stress; deletion of *CgHAL9* resulted in the inability to survive in an acidic environment.
Predicted Oxidative Stress Response-Related Transcription Factors		
CAGL0M01716g and *CAGL0F04081g*	*CaTEC1*	Uncharacterized. *C. albicans* homologue encodes a TEA/ATTS transcription factor; hyphal gene regulation required for spider and RPMI biofilm formation; regulates *BCR1*.
CAGL0L00583g	*CaBCR1*	Uncharacterized. *C. albicans* homologue encodes a transcription factor that regulates alpha biofilm formation, matrix, cell-surface-associated genes; confers adherence, impermeability, impenetrability, fluconazole resistance; *TUP1*/*TEC1*/*MNL1*-regulated.
CAGL0L13090g	*CaNDT80*	Uncharacterized. *C. albicans* homologue encodes a meiosis-specific transcription factor; activator of *CDR1* induction by antifungal drugs; required for wild-type drug resistance and for spider biofilm formation.

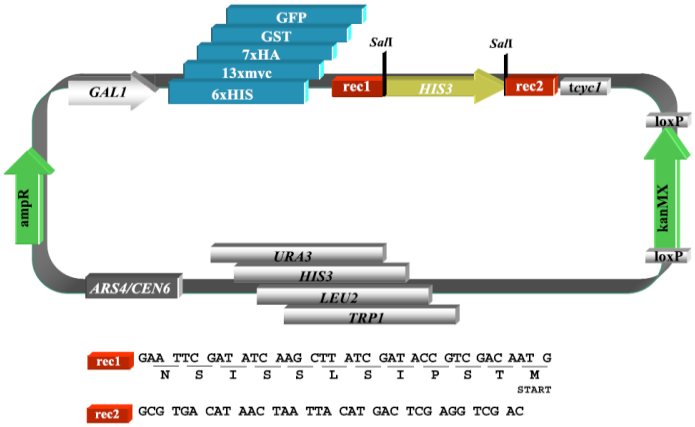

Figure S 1. | Schema representation of the basic pGREG vector system. The inducible *GAL1* promoter controls the expression of tags or generated fusion proteins. Downstream of the tags a *HIS3* stuffer fragment is located flanked by specific sites for recombination, rec1 and rec2. The vectors contain one of the selectable yeast markers *URA3*, *LEU2*, *TRP1* and *HIS3* as well as an additional KanMX cassette flanked by loxP sites. Sequences of rec1 and rec2 used for the targeted in vivo recombination of DNA fragments into the vector, including the translated sequence encoded by the rec1 linker between tag and protein of interest [127].

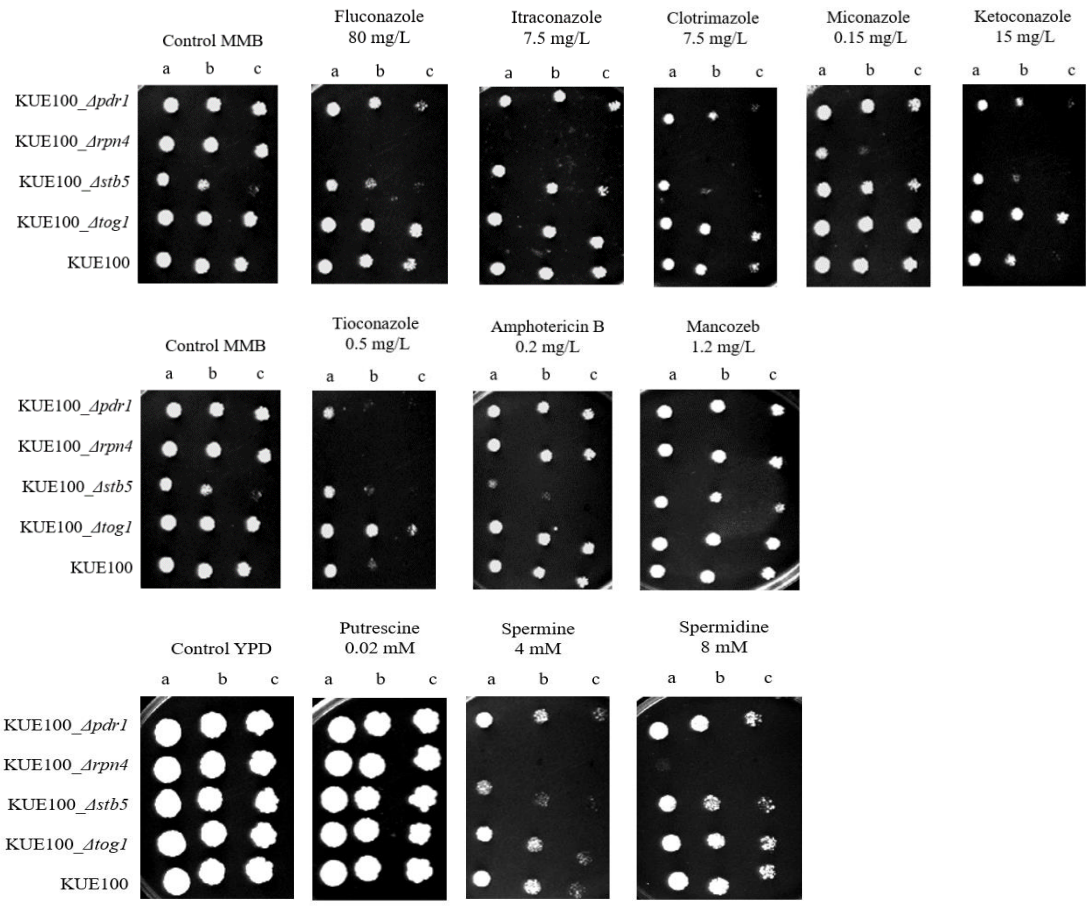

Figure S 2. | Comparison of the susceptibility to inhibitory concentrations of several chemical stress inducers, at the indicated concentrations, of the *C. glabrata* wild-type KUE100, KUE100_*Δcgpdr1*, KUE100_*Δcgrpn4*, KUE100_*Δcgstb5*, KUE100_*Δcgtog1* strains, in MMB plates by spot assays. The inocula were prepared as described in Section 2.2.1. Cell suspensions used to prepare the spots were 1:5 (b) and 1:25 (c) dilutions of the cell suspension used in (a). The displayed images are representative of at least three independent experiments.

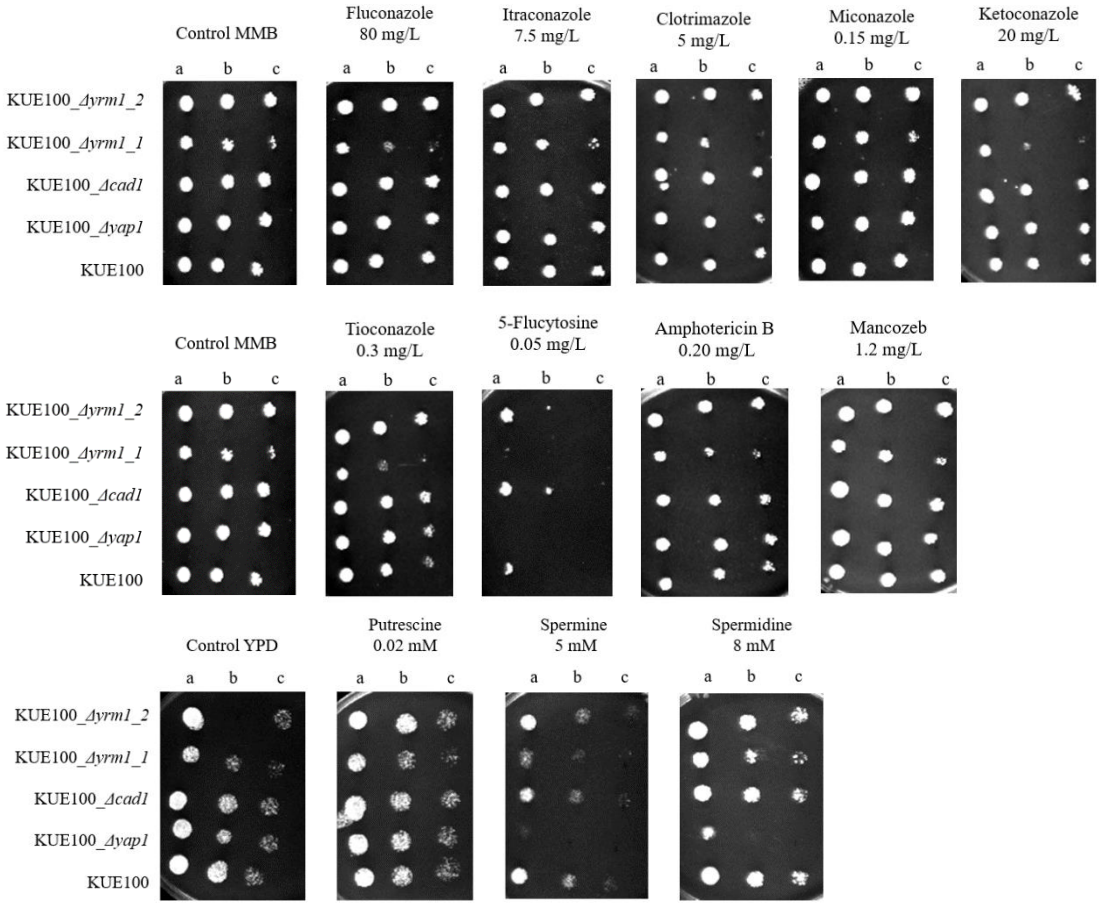

Figure S 3. | Comparison of the susceptibility to inhibitory concentrations of several chemical stress inducers, at the indicated concentrations, of the *C. glabrata* wild-type KUE100, KUE100_*Δcgyap1*, KUE100_*Δcgcad1*, KUE100_*Δcgyrm1_1*, KUE100_*Δcgyrm1_2* strains, in MMB plates by spot assays. The inocula were prepared as described in Section 2.2.1. Cell suspensions used to prepare the spots were 1:5 (b) and 1:25 (c) dilutions of the cell suspension used in (a). The displayed images are representative of at least three independent experiments.

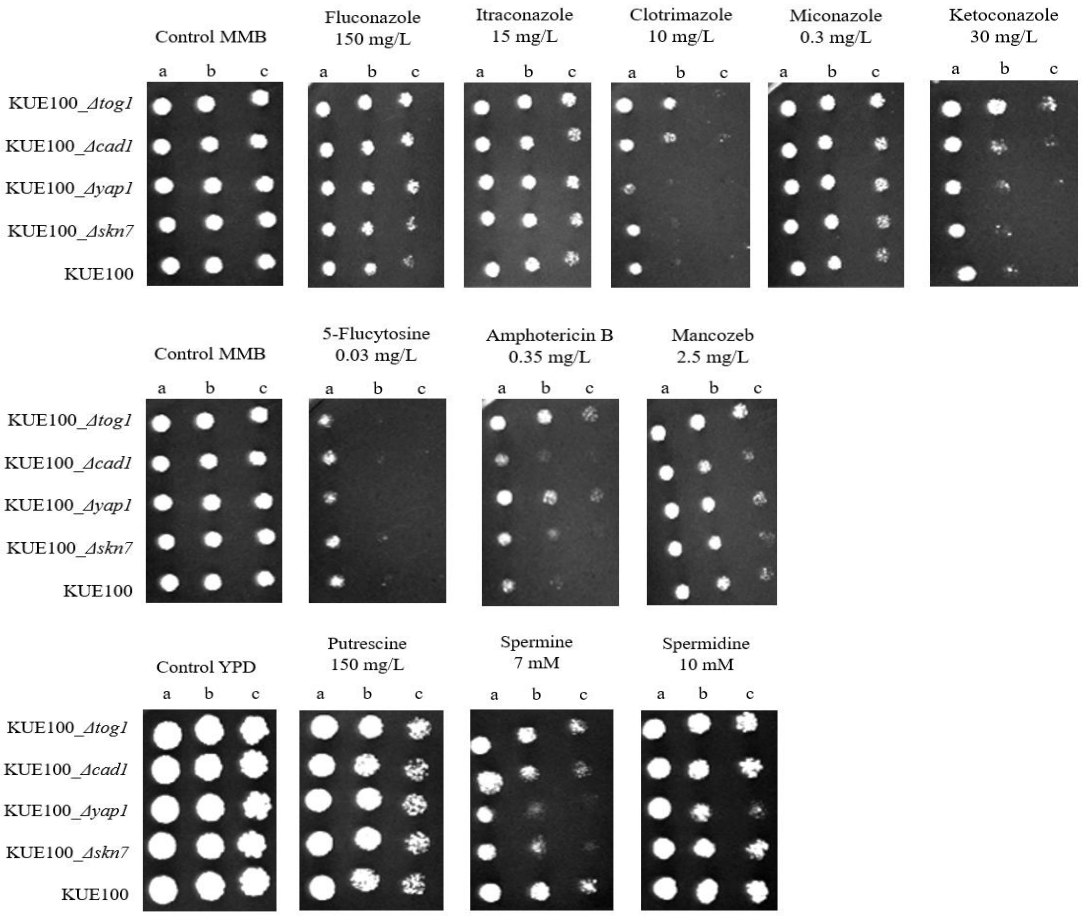

Figure S 4. | Comparison of the susceptibility to inhibitory concentrations of several chemical stress inducers, at the indicated concentrations, of the *C. glabrata* wild-type KUE100, KUE100_*Δcgskn7*, KUE100_*Δcgyap1*, KUE100_*Δcgcad1*, KUE100_*Δcgtog1* strains, in MMB plates by spot assays. The inocula were prepared as described in Section 2.2.1. Cell suspensions used to prepare the spots were 1:5 (b) and 1:25 (c) dilutions of the cell suspension used in (a). The displayed images are representative of at least three independent experiments.

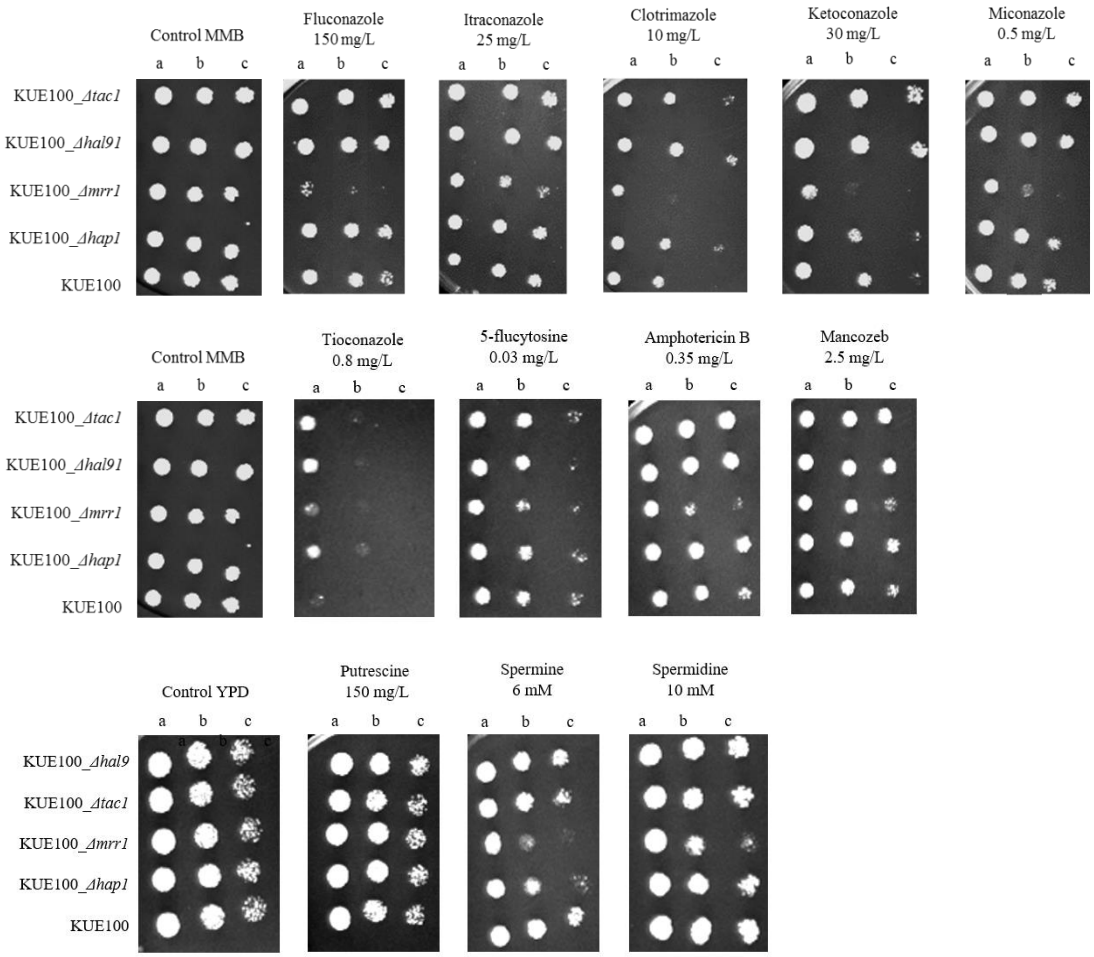

Figure S 5. | Comparison of the susceptibility to inhibitory concentrations of several chemical stress inducers, at the indicated concentrations, of the *C. glabrata* wild-type KUE100, KUE100_*Δcghap1*, KUE100_*Δcgmrr1*, KUE100_*Δcgtac1*, KUE100_*Δcghal9* strains, in MMB plates by spot assays. The inocula were prepared as described in Section 2.2.1. Cell suspensions used to prepare the spots were 1:5 (b) and 1:25 (c) dilutions of the cell suspension used in (a). The displayed images are representative of at least three independent experiments.

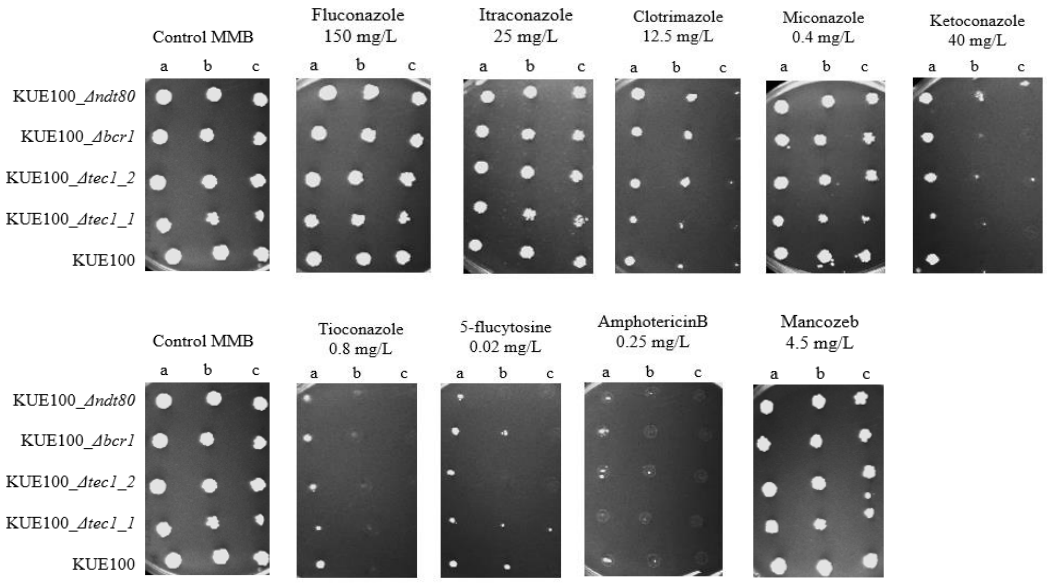

Figure S 6. | Comparison of the susceptibility to inhibitory concentrations of several chemical stress inducers, at the indicated concentrations, of the *C. glabrata* wild-type KUE100, KUE100_*Δcgtec1_1*, KUE100_*Δcgtec1_2*, KUE100_*Δcgbcr1*, KUE100_*Δcgndt80* strains, in MMB plates by spot assays. The inocula were prepared as described in Section 2.2.1. Cell suspensions used to prepare the spots were 1:5 (b) and 1:25 (c) dilutions of the cell suspension used in (a). The displayed images are representative of at least three independent experiments.

Table S 3. | IUPAC frequency table. Consensus sequences *of ScRpn4* binding sites were obtained in SGD https://www.yeastgenome.org/ and were represented according to the following IUPAC frequency table.

IUPAC frequency table				
	A	C	G	T
A	1	0	0	0
C	0	1	0	0
G	0	0	1	0
T	0	0	0	1
W	1/2	0	0	1/2
S	0	1/2	1/2	0
R	1/2	0	1/2	0
Y	0	1/2	0	1/2
M	1/2	1/2	0	0
K	0	0	1/2	1/2
B	0	1/3	1/3	1/3
D	1/3	0	1/3	1/3
H	1/3	1/3	0	1/3
V	1/3	1/3	1/3	0
N	1/4	1/4	1/4	1/4
x	1/4	1/4	1/4	1/4
a	1/2	1/6	1/6	1/6
c	1/6	1/2	1/6	1/6
g	1/6	1/6	1/2	1/6
t	1/6	1/6	1/6	1/2

seq	id	exp_freq	occ	exp_occ	occ_P	occ_E	occ_sig	rank	ovl_occ	forbocc
aagtct	aagtct|agactt	0.0003926297516	10	2.34	0.00017	3.5e-01	0.46	1	0	50
gaagca	gaagca|tgcttc	0.0005537250684	12	3.31	0.00017	3.6e-01	0.44	2	0	60
agtcta	agtcta|tagact	0.0002849014017	8	1.70	0.00039	8.1e-01	0.09	3	0	40

seq	id	exp_freq	occ	exp_occ	occ_P	occ_E	occ_sig	rank	ovl_occ	forbocc
agacttc	agacttc|gaagtct	0.0000754171852	6	0.45	7.8e-06	6.4e-02	1.19	1	0	36
ggaagca	ggaagca|tgcttcc	0.0001183380201	7	0.71	9.3e-06	7.6e-02	1.12	2	0	42
caggtgc	caggtgc|gcacctg	0.0000521268096	5	0.31	1.9e-05	1.5e-01	0.82	3	0	30
ctgagtc	ctgagtc|gactcag	0.0000321636306	4	0.19	4.8e-05	4.0e-01	0.40	4	0	24
acaggtg	acaggtg|cacctgt	0.0000651028761	5	0.39	5.3e-05	4.4e-01	0.36	5	0	30
ccacagg	ccacagg|cctgtgg	0.0000351581075	4	0.21	6.8e-05	5.6e-01	0.25	6	0	24

seq	id	exp_freq	occ	exp_occ	occ_P	occ_E	occ_sig	rank	ovl_occ	forbocc
acaggtgc	acaggtgc|gcacctgt	0.0000129629189	4	0.08	1.4e-06	4.6e-02	1.34	1	0	28
gaagcacc	gaagcacc|ggtgcttc	0.0000172936058	4	0.10	4.3e-06	1.4e-01	0.85	2	0	28
ggaagcac	ggaagcac|gtgcttcc	0.0000176267356	4	0.11	4.7e-06	1.5e-01	0.81	3	0	28
gaagtcta	gaagtcta|tagacttc	0.0000209580331	4	0.12	9.2e-06	3.0e-01	0.52	4	0	28
agaatttg	agaatttg|caaattct	0.0000482746730	5	0.29	1.3e-05	4.2e-01	0.37	5	0	35
gcctccac	gcctccac|gtggaggc	0.0000082991024	3	0.05	1.9e-05	6.4e-01	0.19	6	0	21
cctgtgga	cctgtgga|tccacagg	0.0000092984917	3	0.06	2.7e-05	8.9e-01	0.05	7	0	21
ctccacag	ctccacag|ctgtggag	0.0000092984917	3	0.06	2.7e-05	8.9e-01	0.05	8	0	21

Figure S 7. | RSAT: oligo-analysis. seq: oligomer sequence; **id:** oligomer identifier; **exp_freq:** expected relative frequency; **occ:** observed occurrences; **occ_P:** occurrence probability (binomial); **occ_E:** E-value for occurrences (binomial); **occ_sig:** occurrence significance (binomial); **rank:** rank; **ovl_oc3c:** number of overlapping occurrences (discarded from the count); **forbocc:** forbidden positions (to avoid self-overlap).

Figure S8. | ScRpn4p and CgRpn4p multiple sequence alignment. EMBL-EBI (https://www.ebi.ac.uk/) bioinformatic tool was used to compare ScRpn4p (EDV08304.1) amino acid sequence to that of CgRpn4p (XP_4483001). Portable ubiquitin-independent (yellow) and -dependent (green) degrons, and C_2H_2 DNA binding domain (blue) of ScRpn4 were compared to the correspondent CgRpn4 amino acid sequence.